CONTRIBUTIONS TO THE THEORY OF NONLINEAR OSCILLATIONS

BY

YOSHIKAZU NISHIKAWA

JANUARY, 1962

CONTRIBUTIONS TO THE THEORY OF NONLINEAR OSCILLATIONS

CONTRIBUTIONS TO THE THEORY OF NONLINEAR OSCILLATIONS

BY

YOSHIKAZU NISHIKAWA

JANUARY, 1962

INTRODUCTION

This paper is devoted to the study of nonlinear oscillations in certain types of physical systems. The systems under consideration are concerned with electric circuits and are described by nonlinear differential equations. The method of analysis presented in the paper may also be applicable to other physical systems which are described by differential equations of the like form. The subject of investigation is mostly limited to the field of forced oscillations.

The text consists of five chapters. Analytical methods and graphical procedures for solving nonlinear differential equations are described in the first two chapters. The three chapters that follow are concerned with the analysis of certain phenomena in nonlinear systems. Complementary remarks are provided in four appendices to the text.

Chapter I is concerned with the analytical methods of widest utility, i.e., the perturbation method, the iteration method, and the method of harmonic balance. The argument in this chapter is confined to the analysis of the harmonic solutions of nonautonomous equations. There is usually considerable advantage in obtaining an analytical solution for a differential equation when this is possible. It is recognized that an exact solution probably cannot be found for a nonlinear differential equation, and that an approximate solution of sufficient accuracy may be possible.

According to the principle of the perturbation method for solving a nonlinear differential equation, we develop unknown quantities in powers of a small parameter of the equation and determine the coefficients of the developments stepwise. The author describes a method in which the amplitude and phase of the desired solution are sought in powers of the small parameter. This method may be natural and practical as compared with the method in which the amplitude of the solution is first prescribed and the frequency of the external force is obtained as a function of that amplitude [29, 32].

A method of solving nonlinear differential equations based on the process of successive iteration is called the iteration method. Iteration may be performed in a number of ways. We present a method in which the amplitude and phase of the oscillation are determined by the process of successive iteration.

A periodic solution may be developed in a Fourier series. According to the principle of harmonic balance, the term of the fundamental frequency and one or two additional components of predominant amplitudes are assumed to a first approximation. In Chapter I a method is described where we start with a first approximation of very simple form and then improve the accuracy of the approximation by adding correction terms stepwise.

The analytical methods described in Chapter I are legitimate mathematically only for equations of small nonlinearity. However, they may still be applicable even to the solution of equations with large nonlinearity to some extent. We examine the applicability of the methods by solving numerical examples where large nonlinearity is associated with them. The accuracy of the numerical solution is estimated by inserting the solution into the original equation and evaluating the residual produced.

Chapter II describes graphical methods for solving certain types of nonlinear differential equations. An analytical method, though it has considerable advantage, is restricted to the solution of rather simple equation. A graphical method is usually simple to utilize and may be effective as an exploratory tool when a nonlinear characteristic is known in the form of a curve. We are particularly concerned with the investigation of the following graphical methods, i.e., the slopeline method and the delta method. Both of them are based on the step-by- step integration procedure and are useful to find a single solution curve with a given initial condition.

No claim is made as to the originality of the principles of the methods, inasmuch as the basic notions have been in use for some time. The author systematizes the use of the methods and clarify the possible range of their applicability. Various modifications and extensions of the basic methods are described in the present investigation. Namely, a modification of the slopeline method enables its application to the graphical solution of nonautonomous equations. A modification of the delta method improves the accuracy of the solution. The double-delta method, an extension of the delta method, is presented. It is applicable to the solution of differential equations of a complicated type. Errors produced in each procedure of the graphical constructions are evaluated by making use of Taylor's expansion. The results of the graphical solutions for several numerical examples, including van der Pol's equation and Duffing's equation, prove the excellency of the methods.

Chapter III deals with subharmonic oscillations which occur in nonlinear systems under the action of a periodic force. A subharmonic oscillation is an oscillation whose fundamental frequency is a fraction of that of the applied force. In this chapter is studied the subharmonic oscillations of order one half in the system represented by Duffing's equation. The 1/2-harmonic oscillations have been discussed by Prof. C. Hayashi [11, 30] and the present author [8]. A more detailed investigation is described in this chapter. The phase-space analysis is used for the investigation of the oscillations. The phase-space analysis is based on an approach through the methods of harmonic balance and variation of parameters. The response of the system is developed in a Fourier series in which the coefficients are assumed to be slowly-varying functions of time. These coefficients constitute the coordinates of a representative point in the phase space. The periodic solutions in the steady state, which are correlated with singular points in the phase space, are first sought for various combinations of the system parameters. The stability of the periodic solutions is investigated by making use of the Routh-Hurwitz' criterion. The transient state of the oscillations is discussed by illustrating the geometrical configuration of the integral curves in the phase space.

Particular attention is directed toward obtaining the relationship between the initial conditions and the resulting subharmonic responses. It is a distinctive feature of nonlinear systems that various types of steady-state responses may take place even in the same system depending upon different values of the initial conditions. Several patterns of initial conditions leading to different types of subharmonic responses are shown on the phase plane. Theoretrical results are compared with the solutions obtained by analog-computer analysis and found to be in satisfactory agreement with them.

Chapter IV is concerned with the relationship between the initial conditions and the resulting periodic responses in the system governed by Duffing's equation. A different method of analysis from that used in Chapter III is developed. The phase-space (or phase-plane) method, as described in Chapter III, has been used extensively for the study of oscillations in the transient state [11, 30]. However, it has the following drawbacks. First, if the initial conditions are prescribed at values which are far different from those of the steady state, the assumption that the amplitude and phase of the oscillation vary slowly does not hold. The second drawback is that, if a number of steady state responses are to be expected, this method is practically inapplicable, since the analysis is compelled to resort to the graphical solution in a higher-dimensional phase-space.

Chapter IV describes the method of analysis which is applicable under such situations [12]. The phase-plane analysis, where the coordinates are the dependent variable v and the first derivative of v with respect to the independent variable τ, is used. The mapping, which transfers a representative point on the phase plane at $\tau = \tau_0$ to a representative point at $\tau = \tau_0 + T$ (T refers to the period of the applied force), plays an essential role in the analysis. Then a periodic solution will be correlated with a fixed point of the mapping. We may determine the location of a directly unstable fixed point by using the method of harmonic balance. Through the directly unstable fixed point there is a invariant curve of the mapping, which is the locus of the images that approach the unstable fixed point with increasing time. This invariant curve is a boundary between domains of attraction, in each of them any initial conditions leading to a particular stable fixed point with increasing time [4]. In the neighborhood of the unstable fixed point, we may locate the small segment of the invariant curve by making use of the solution of the variational equation from the unstable periodic solution. Then the whole configuration of the boundary curve is obtained by integrating the original equation from a point on the segment for decreasing time.

Two examples of the domains of attraction are illustrated. The first deals with the domains of attraction leading to the harmonic and subharmonic oscillation of order 1/3 in a symmetrical system. The second example is concerned with the domains of attraction for the harmonic oscillation, the subharmonic oscillations of order 1/2 and of order 1/3 in an unsymmetrical system.

Chapter V deals with the so-called quasi-periodic oscillation where the amplitude and phase of the oscillation vary slowly but periodically even in the steady state [18]. Since the waveform of the oscillation is not usually repeated, the quasi-periodic oscillation is in general nonperiodic. The phase-space analysis such as used in Chapter III is also applicable to the analysis of the oscillation of this type. A periodic oscillation is correlated with a singular point in the phase space; while a quasi-periodic oscillation is represented by a limit cycle. Since the quasi-periodic oscillation is affected by amplitude and phase modulation, the representative point does not tend to a singular point but keeps on moving along the limit cycle with increasing time. The period required for the representative point to complete one revolution along the limit cycle is not an integral multiple of the period of the external force; the ratio of these periods is in general irrational.

Two representative cases of the quasi-periodic oscillation are studied in Chapter V. The first is the case in which a harmonic oscillation in a resonant nonlinear circuit becomes unstable and changes into a quasi-periodic oscillation. The second case deals with the quasi-periodic oscillation which develops from a subharmonic oscillation of order 1/2 in a parametric excitation circuit. The numerical analysis is carried out for these cases; thus two distinctive types of the limit cycle as well as the location of the singular points in the phase space are determined for particular sets of the system parameters. The theoretical results are compared with the solutions obtained by analog-computer analysis and found to be in satisfactory agreement with them.

As has been mentioned earlier, four appendices are annexed to the text. Appendix I describes one of the iteration method, which is somewhat different from that of Chapter I. Appendix II is concerned with error analysis of the graphical construction procedures. Appendix III shows the regions of the parameters of Duffing's equation in which the oscillations of different types are sustained. Appendix IV describes the solutions of the variational equations associated with the unstable fixed points of the numerical examples in Chapter IV.

ACKNOWLEDGMENTS

The author owes lasting debt of gratitude to Professor Dr. C. Hayashi, who has suggested the field of research of the present thesis and has given him constant and generous guidance and encouragement in promoting this work.

In the preparation of the present paper the author has been given many aids and useful advices by the staffs of Dr. Hayashi's Labaratory.

The author is also grateful to Messrs. M. Nagasaki, M. Terada, Y. Ueda, S. Miyagawa, S. Okamura, J. Tsuji, Y. Tsuji, S. Hiraoka, and M. Tsuchida for carrying out a great deal of tedious computations.

The author wishes to express his thanks to the KDC-1 Computer Labaratory of Kyoto University for making time available to him.

CONTENTS

Introduction iii

Chapter I. Analytical Methods for solving Nonlinear Differential Equations

1.1 Introduction 1

1.2 Perturbation method 2

1.3 Iteration method 10

1.4 Method of harmonic balance 15

1.5 Comparison of the three methods 18

1.6 Numerical examples 20

1.6.1 Equation without term for dissipation 21

1.6.2 Equation with a term for dissipation 25

1.7 Conclusion 29

Chapter II. Graphical Methods for solving Nonlinear Differential Equations

2.1 Introduction 30

2.2 Slopeline method 31

2.2.1 Development of method 31

2.2.2 Second-order equations of the autonomous type 34

2.2.3 Second-order equations of the nonautonomous type 37

2.3 Delta method 40

2.3.1 Development of method 41

2.3.2 Modification of method 43

2.3.3 Double-delta method 45

2.4 Conclusion 47

Chapter III. Subharmonic Oscillations of Order One Half

3.1 Introduction 65

3.2 The fundamental equations 66

3.3 Subharmonic oscillations of order 1/2 in the steady state 69

3.3.1 Periodic solutions 69

3.3.2 Stability investigation 70

3.3.3 Numerical examples 73

3.4 Subharmonic oscillations of order 1/2 in the transient state 74

3.4.1 Phase-plane analysis 74

3.4.2 Numerical examples 77

3.5 Analog-computer analysis 85

3.5.1 The fundamental equation and the computer block diagram 85

3.5.2 Computer solutions 86

3.6 Conclusion 87

Chapter IV. Initial Conditions leading to Different Types of Periodic Solutions

4.1 Introduction 107

4.2 Symmetrical system 111

4.2.1 Determination of the coefficients of the periodic solutions 112

4.2.2 Stability investigation of the periodic solutions 113

4.2.3 Domains of attraction leading to harmonic and 1/3-harmonic responses 116

4.3 Unsymmetrical system 120

4.3.1 Periodic solutions and conditions for stability 121

4.3.2 Domains of attraction leading to harmonic, 1/2-harmonic, and 1/3-harmonic responses 125

4.4 Conclusion 127

Chapter V. Quasi-Periodic Oscillations

5.1 Introduction 134

5.2 Quasi-periodic oscillations in a resonant circuit with d-c superposed 134

5.2.1 The circuit equations 134

5.2.2 Periodic solutions and conditions for stability 137

5.2.3 Quasi-periodic oscillations 142

5.2.4 Numerical examples 144

5.2.5 Analog-computer analysis 144

5.3 Quasi-periodic oscillations in a parametric excitation circuit 145

5.3.1 The circuit equations 145

5.3.2 Periodic solutions and conditions for stability 147

5.3.3 Quasi-periodic oscillations 149

5.3.4 Numerical examples 150

5.3.5 Analog-computer analysis 151

5.4 Conclusion 151

Appendix I. Complementary Remarks to Iteration Method 165

Appendix II. Analysis of Errors of Graphical Integration Methods 168

Appendix III. Regions of Parameters of Duffing's Equation in which the Oscillations of Different Types are sustained 171

Appendix IV. Solutions of the Variational Equations associated with the Unstable Fixed Points 177

References 185

CHAPTER I

ANALYTICAL METHODS FOR SOLVING NONLINEAR DIFFERENTIAL EQUATIONS

1.1 Introduction

There is usually considerable advantage in obtaining an analytical solution for a differential equation when this is possible. The analytical solution is obtained in algebraic form without the necessity of introducing numerical values for parameters. Once the solution is obtained, any desired numerical values can be inserted. Because of this flexibility, it is often worth while expending considerable effort to find a solution in analytical form.

It is recognized that an exact solution probably cannot be found for a nonlinear differential equation, but an approximate solution of sufficient accuracy may be possible. In this chapter we are concerned with the analytical methods, i.e., the perturbation method, the iteration method, and the method of harmonic balance, which are of general widest utility. The argument will be confined to the analysis of nonautonomous equations.

According to the principle of the perturbation method for solving a nonlinear differential equation, we develop unknown quantities in powers of a small parameter of the equation and determine the coefficients of the developments stepwise. The author describes a method in which the amplitude and phase of the desired solution are sought in powers of the small parameter. This method may be natural and practical as compared with the method in which the amplitude of the solution is first prescribed and the frequency of the external force is obtained as a function of that amplitude [29, 32].

A method of solving nonlinear differential equations based on the process of successive iteration is called the iteration method. In earlier days, G. Duffing applied this method to the solution of the equation named after himself [33]. Prof. J. J. Stoker has also referred to this method [32]. In his description, however, the frequency of the external force is not considered to be prescribed in advance, but rather to be determined depending upon the value of the amplitude of the solution. The author will present a method in which the amplitude and phase of the solution are determined by the process of successive iteration.

A periodic solution can be developed in a Fourier series of sine and cosine components. According to the principle of harmonic balance, the component of the fundamental frequency and one or two additional components of predominant amplitudes are assumed to a first approximation. Coefficients of the Fourier series are adjusted to satisfy the equation so far as terms of the considered frequencies are concerned. In this chapter we shall describe a method where we start with a first approximation of very simple form and then improve the accuracy of the approximation by adding correction terms stepwise.

The analytical methods described in the present chapter are legitimate mathematically only for equations in which the degree of nonlinearity is sufficiently small. However, they may still be applicable even to the solution of equations with large nonlinearity to some extent. We shall examine the applicability of them by solving numerical examples where large nonlinearity is associated with them. The accuracy of the numerical solution will be estimated by inserting the solution to the original equation and evaluating the residual produced.

1.2 Perturbation Method

One of the well-known methods for solving nonlinear equations is the perturbation method. This method is applicable to the solution of equations where a small parameter is associated with the nonlinear terms. We develop the desired quantities in powers of the small parameter and determine the coefficients of the developments stepwise, usually by solving a sequence of linear equations.

We shall explain the use of the method for obtaining the harmonic solution, which has the same frequency as the external force, of second-order differential equations of the type

$$\frac{d^2x}{dt^2}+x=\mu f(x,\frac{dx}{dt},t), \tag{1.1}$$

where μ is a small parameter and f is a periodic function in time t with period 2π. If the period of the function f is different from 2π only in order of μ, it may be reduced to 2π by changing the scale of the time appropriately. For example, let us consider the equation of the form

$$\frac{d^2x}{dt^2}+x=\mu f(x,\frac{dx}{dt},\omega t), \tag{1.2}$$

where f is a periodic function in ωt with the period 2π, and ω is different from unity in order of μ. Introducing the variable defined by $\tau = \omega t$, this equation is transformed into a equation of the form (1.1). Therefore the period of time functions is always set to be 2π in what follows.

Equation (1.1) may be rewritten as

$$\left.\begin{aligned} &\frac{d^2x}{d\tau^2}+x=\mu f(x,\frac{dx}{d\tau},\tau+\delta), \\ \text{where}\quad &\tau=t-\delta. \end{aligned}\right\} \tag{1.3}$$

The unknown phase angle δ is introduced to permit choice of the initial condition such that*

$$\dot{x}(\tau) = 0 \qquad \text{at} \qquad \tau = 0. \tag{1.4}$$

The perturbation method consists in developing the desired solution $x(\tau)$ in a power series with respect to small parameter μ. In addition to x it is also necessary to develop the unknown quantity δ with respect to μ. Thus a solution for (1.3) is sought in the series

$$\left.\begin{aligned} x(\tau) &= x_0(\tau) + \mu x_1(\tau) + \mu^2 x_2(\tau) + \cdots, \\ \delta &= \delta_0 + \mu\delta_1 + \mu^2\delta_2 + \cdots. \end{aligned}\right\} \tag{1.5}$$

The functions $x_0(\tau)$, $x_1(\tau)$,... and the coefficients δ_0, δ_1,... are to be determined stepwise.

Substituting Eqs. (1.5) into (1.3), we obtain a power series in μ which must vanish identically in μ; hence the coefficients of the successive powers of μ must vanish. Equating these coefficients separately to zero, we obtain a set of second-order differential equations:

$$\mu^0: \qquad \ddot{x}_0 + x_0 = 0, \tag{1.6}$$

$$\mu^1: \qquad \ddot{x}_1 + x_1 = [f], \tag{1.7}$$

$$\mu^2: \qquad \ddot{x}_2 + x_2 = [f_x]x_1 + [f_{\dot{x}}]\dot{x}_1 + [f_\tau]\delta_1, \tag{1.8}$$

$$\begin{aligned} \mu^3: \qquad \ddot{x}_3 + x_3 = {} & [f_x]x_2 + [f_{\dot{x}}]\dot{x}_2 + [f_\tau]\delta_2 \\ & + \tfrac{1}{2}[f_{xx}]x_1^2 + \tfrac{1}{2}[f_{\dot{x}\dot{x}}]\dot{x}_1^2 + \tfrac{1}{2}[f_{\tau\tau}]\delta_1^2 \\ & + [f_{x\dot{x}}]x_1\dot{x}_1 + [f_{x\tau}]x_1\delta_1 + [f_{\dot{x}\tau}]\dot{x}_1\delta_1, \end{aligned} \tag{1.9}$$

---

* Here and throughout this chapter dots over a quantity refer to differentiations with respect to τ.

etc., where

$$\left.\begin{aligned} [f] &= f(x_0,\, \dot{x}_0,\, \tau+\delta_0), \\ [f_x] &= \frac{\partial f}{\partial x}(x_0,\, \dot{x}_0,\, \tau+\delta_0), \\ [f_{xx}] &= \frac{\partial^2 f}{\partial x^2}(x_0,\, \dot{x}_0,\, \tau+\delta_0), \\ &\text{etc.} \end{aligned}\right\}$$

The solution of (1.6), i.e., so-called the generating solution, is found to be

$$x_0(\tau) = A_0 \cos\tau, \tag{1.10}$$

with the initial condition

$$x_0(0) = A_0, \quad \text{and} \quad \dot{x}_0(0) = 0.$$

Substituting (1.10) into (1.7) leads to

$$\ddot{x}_1 + x_1 = f(A_0 \cos\tau, -A_0 \sin\tau,\, \tau+\delta_0). \tag{1.11}$$

The right-hand side of (1.11) may be developed in a Fourier series. If the terms containing $\cos\tau$ and $\sin\tau$ were not zero in the Fourier series, the solution of (1.11) would contain terms of the type $\tau\cos\tau$ and $\tau\sin\tau$, i.e., the secular terms. The condition for periodicity of x_1 requires that these coefficients vanish, i.e., the following relation hold:

$$\left.\begin{aligned} P_1(A_0, \delta_0) &= 0, \\ Q_1(A_0, \delta_0) &= 0, \end{aligned}\right\} \tag{1.12}$$

where

$$\left.\begin{aligned} P_1(A_0, \delta_0) &= \frac{1}{\pi}\int_0^{2\pi} [f] \cos\tau\, d\tau, \\ Q_1(A_0, \delta_0) &= \frac{1}{\pi}\int_0^{2\pi} [f] \sin\tau\, d\tau. \end{aligned}\right\}$$

The values of A_0 and δ_0 are to be determined from (1.12).

The general solution $x_1(\tau)$ of (1.11) may now be obtained with the initial condition $\dot{x}_1(0) = 0$. The solution contains one arbitrary constant A_1 of integration. It is determined so as to satisfy the condition for periodicity of the second order term $x_2(\tau)$.

As an example of differential equations of the form (1.1), let us consider Duffing's equation without terms for dissipation:

$$\frac{d^2x}{dt^2} + (1+\mu\alpha)x + \mu\beta x^3 = \mu F \cos t. \tag{1.13}$$

Introducing the unknown phase angle δ, equation (1.13) is rewritten as

$$\left.\begin{aligned} &\frac{d^2x}{d\tau^2} + x = \mu[-\alpha x - \beta x^3 + F\cos(\tau+\delta)], \\ \text{with}\quad &\tau = t - \delta, \qquad \dot{x}(0) = 0. \end{aligned}\right\} \tag{1.14}$$

A solution of (1.14) is sought in the form

$$\left.\begin{aligned} x(\tau) &= x_0(\tau) + \mu x_1(\tau) + \mu^2 x_2(\tau) + \cdots, \\ \delta &= \delta_0 + \mu\delta_1 + \mu^2\delta_2 + \cdots. \end{aligned}\right\} \tag{1.15}$$

Substitution of (1.15) into (1.14) and collection of like powers of μ give a set of simultaneous equations:

$$\mu^0: \quad \ddot{x}_0 + x_0 = 0, \tag{1.16}$$

$$\mu^1: \quad \ddot{x}_1 + x_1 = -\alpha x_0 - \beta x_0^3 + F\cos(\tau+\delta_0), \tag{1.17}$$

$$\mu^2: \quad \ddot{x}_2 + x_2 = -\alpha x_1 - 3\beta x_0^2 x_1 - F\delta_1 \sin(\tau+\delta_0), \tag{1.18}$$

etc. Terms of order zero in μ yields

$$\frac{d^2x_0}{d\tau^2} + x_0 = 0. \tag{1.19}$$

Solving (1.19) with the initial condition $\dot{x}_0(0) = 0$, we obtain

$$x_0(\tau) = A_0 \cos\tau. \tag{1.20}$$

Substitution of (1.20) into (1.17) gives the differential equation

$$\frac{d^2x_1}{d\tau^2} + x_1 = -(\alpha A_0 + \frac{3}{4}\beta A_0^3 - F\cos\delta_0)\cos\tau - F\sin\delta_0 \sin\tau$$
$$-\frac{1}{4}\beta A_0^3 \cos 3\tau. \tag{1.21}$$

If the coefficients of $\cos\tau$ and $\sin\tau$ were not zero in the right-hand side of (1.21), secular terms would appear in the solution $x_1(\tau)$. The periodicity condition for $x_1(\tau)$ requires that these coefficients vanish, namely

$$\left.\begin{aligned} &\alpha A_0 + \frac{3}{4}\beta A_0^3 - F\cos\delta_0 = 0, \\ &\sin\delta_0 = 0. \end{aligned}\right\}$$

Hence we obtain $\delta_0 = 0$ and

$$\alpha A_0 + \frac{3}{4}\beta A_0^3 - F = 0. \tag{1.22}$$

Equation (1.22) determines the amplitude A_0. Then, with the initial condition $x_1(0) = 0$, the general solution of (1.21) may be written as

$$x_1(\tau) = A_1\cos\tau + \frac{1}{32}\beta A_0^3 \cos 3\tau. \tag{1.23}$$

Substitution of (1.20) and (1.23) into (1.18) gives

$$\frac{d^2x_2}{d\tau^2} + x_2 = -(\alpha A_1 + \frac{9}{4}\beta A_0^2 A_1 + \frac{3}{128}\beta^2 A_0^5)\cos\tau - F\delta_1 \sin\tau$$
$$-\frac{1}{4}\beta A_0^2 (3A_1 + \frac{1}{8}\alpha A_0 + \frac{3}{16}\beta A_0^3)\cos 3\tau - \frac{3}{128}\beta^2 A_0^5 \cos 5\tau. \tag{1.24}$$

The periodicity condition for $x_2(\tau)$ requires that the coefficients of $\cos\tau$ and $\sin\tau$ in the right-hand side of (1.24) be zero. Thus we obtain $\delta_1 = 0$ and

$$A_1 = \frac{-3\beta^2 A_0^5}{128(\alpha + \frac{9}{4}\beta A_0^2)} \quad . \tag{1.25}$$

Using (1.25) the general solution of (1.24) may be written as

$$x_2(\tau) = A_2 \cos\tau + \frac{1}{32}\beta A_0^2 (3A_1 + \frac{1}{8}\alpha A_0 + \frac{3}{16}\beta A_0^3)\cos 3\tau$$
$$+ \frac{3}{3072}\beta^2 A_0^5 \cos 5\tau . \tag{1.26}$$

The condition for periodicity of $x_3(\tau)$ will lead to

$$\left. \begin{aligned} A_2 &= \frac{-3\beta A_0(\alpha\beta A_0^4 + 2\beta^2 A_0^6 + 40\beta A_0^3 A_1 + 768 A_1^2)}{1024(\alpha + \frac{9}{4}\beta A_0^2)} , \\ \delta_2 &= 0. \end{aligned} \right\} \tag{1.27}$$

Proceeding analogously, one may determine $x_3(\tau)$, $x_4(\tau)$,... and δ_3, δ_4, ... successively.

Summarizing the above results the solution $x(t)$ of (1.13), up to terms of order μ^2, is

$$x(t) = (A_0 + \mu A_1 + \mu^2 A_2)\cos t + \frac{1}{32}\mu\beta A_0^2 (A_0 + 3\mu A_1 + \frac{1}{8}\mu\alpha A_0 + \frac{3}{16}\mu\beta A_0^3)\cos 3t$$
$$+ \frac{3}{3072}\mu^2\beta^2 A_0^5 \cos 5t , \tag{1.28}$$

where the amplitudes A_0, A_1, and A_2 are determined from (1.22), (1.25), and (1.27), respectively. The phase angle δ is known to be zero in this case.

The harmonic solution of Duffing's equation with term for dissipation

$$\frac{d^2x}{dt^2} + \mu k \frac{dx}{dt} + (1+\mu\alpha)x + \mu\beta x^3 = \mu F \cos t \tag{1.29}$$

may be determined in much the same way. Equation (1.29) is rewritten in the form

$$\left.\begin{aligned}&\frac{d^2x}{d\tau^2}+x=\mu\left[-\alpha x-\beta x^3-k\frac{dx}{d\tau}+F\cos(\tau+\delta)\right],\\ \text{with}\qquad &\tau=t-\delta,\qquad \dot{x}(0)=0.\end{aligned}\right\}\tag{1.30}$$

A solution of (1.30) is sought in the series

$$\left.\begin{aligned}x(\tau)&=x_0(\tau)+\mu x_1(\tau)+\mu^2x_2(\tau)+\cdots,\\ \delta&=\delta_0+\mu\delta_1+\mu^2\delta_2+\cdots.\end{aligned}\right\}\tag{1.31}$$

The first approximation is found to be

$$x_0(\tau)=A_0\cos\tau.\tag{1.32}$$

The amplitude A_0 and the phase angle δ_0 are to be determined by the periodicity condition for $x_1(\tau)$, namely

$$\left.\begin{aligned}&\alpha A_0+\frac{3}{4}\beta A_0^3-F\cos\delta_0=0,\\ &kA_0-F\sin\delta_0=0.\end{aligned}\right\}\tag{1.33}$$

From (1.33) we may derive the equations

$$\left.\begin{aligned}&\left[\left(\alpha+\tfrac{3}{4}\beta A_0^2\right)^2+k^2\right]A_0^2=F^2,\\ &\cos\delta_0=\left(\alpha+\tfrac{3}{4}\beta A_0^2\right)\frac{A_0}{F},\qquad \sin\delta_0=k\frac{A_0}{F}.\end{aligned}\right\}\tag{1.34}$$

which are more useful to determine A_0 and δ_0 than (1.33).

It is worth while noting that the first approximation $x_0(\tau)$ may be written in terms of the original variable t, by virtue of (1.34), as follows:

$$x_0(t)=A_0\cos(t-\delta_0)$$

$$= A_0' \cos t + B_0' \sin t\,,$$

where

$$A_0' = (\alpha + \tfrac{3}{4}\beta A_0^2)\frac{A_0^2}{F}, \qquad B_0' = k\frac{A_0^2}{F}. \tag{1.35}$$

The solution $x_1(\tau)$, i.e., the correction term of order μ is found to be

$$x_1(\tau) = A_1 \cos\tau + \frac{1}{32}\beta A_0^3 \cos 3\tau. \tag{1.36}$$

The amplitude A_1 and the phase angle δ_1 are determined by the periodicity condition for $x_2(\tau)$, namely

$$\left.\begin{aligned} A_1 &= \frac{-3\beta^2 A_0^5}{128\,[\alpha + \frac{9}{4}\beta A_0^2 + k \tan\delta_0]}\,, \\ \delta_1 &= \frac{-3\beta^2 A_0^5 k}{128 F \cos\delta_0 [\alpha + \frac{9}{4}\beta A_0^2 + k \tan\delta_0]}. \end{aligned}\right\} \tag{1.37}$$

Summarizing the above results the solution $x(t)$ of (1.29), up to terms of order μ, is

$$x(t) = (A_0 + \mu A_1)\cos(t - \delta_0 - \mu\delta_1) + \frac{1}{32}\mu\beta A_0^3 \cos 3(t - \delta_0 - \mu\delta_1), \tag{1.38}$$

where the amplitudes and phase angles A_0, δ_0 and A_1, δ_1 are determined from (1.34) and (1.37), respectively.

1.3 Iteration Method

This is a method which is based on the process of successive approximation. In earlier days, G. Duffing applied this method to the solution of the equation named after himself [33]. Iteration may be performed in a number of ways. Here we describe one of them for obtaining the harmonic solution of Duffing's equation. Another way will be presented in Appendix I. These are somewhat different from each other. In our methods the amplitude and phase of the solution are determined in the process of successive iteration.

We consider Duffing's equation of the form

$$\frac{d^2x}{dt^2}+(1+\mu\alpha)x+\mu\beta x^3=\mu F\cos t.$$

This equation may be rewritten as

$$\frac{d^2x}{dt^2}=-x-\mu(\alpha x+\beta x^3-F\cos t). \tag{1.39}$$

First we explain the basic notion of the method. Let x_{a0} be an approximate solution of (1.39). Inserting x_{a0} into (1.39) we obtain

$$\frac{d^2x_{a0}}{dt^2}+r_{a0}=-x_{a0}-\mu(\alpha x_{a0}+\beta x_{a0}^3-F\cos t), \tag{1.40}$$

where the term r_{a0} arises from the inaccuracy of x_{a0}. Upon integrating (1.40) twice with respect to t, we have

$$\begin{aligned} x_{a1} &= x_{a0}+\iint r_{a0}\,dt\,dt \\ &= -\iint[x_{a0}+\mu(\alpha x_{a0}+\beta x_{a0}^3-F\cos t)]\,dt\,dt. \end{aligned} \tag{1.41}$$

Constants of integration are set to be zero in order to ensure the periodicity of x_{a1}. Insertion of x_{a1} into (1.39) yields

$$\begin{aligned} r_{a1} &= -x_{a1}-\mu[\alpha x_{a1}+\beta x_{a1}^3-F\cos t]-\frac{d^2x_{a1}}{dt^2} \\ &= -\iint r_{a0}\,dt\,dt+\text{(small terms of higher order in } \mu) \end{aligned} \tag{1.42}$$

The quantity r_{a1} arises from the inaccuracy of x_{a1}.

If x_{a0} is chosen such that r_{a0} contains only terms of higher harmonic frequency, r_{a1} must be, by virtue of (1.42), a smaller quantity than r_{a0}. That is to say, x_{a1} must be a closer approximation than x_{a0}. By equating the harmonic components of x_{a0} and x_{a1}, r_{a0} is let to contain no harmonic component.

We shall explain this process concretely in what follows. For the solution of (1.39) we start with the first approximation*

$$x_0(t) = A_0 \cos t. \tag{1.43}$$

Substituting (1.43) into the right hand-side of (1.39) we obtain

$$\frac{d^2x}{dt^2} = -[A_0 + \mu(\alpha A_0 + \tfrac{3}{4}\beta A_0^3 - F)]\cos t - \tfrac{1}{4}\mu\beta A_0^3 \cos 3t. \tag{1.44}$$

Upon integrating twice (1.44) we have

$$x(t) = +[A_0 + \mu(\alpha A_0 + \tfrac{3}{4}\beta A_0^3 - F)]\cos t + \tfrac{1}{36}\mu\beta A_0^3 \cos 3t. \tag{1.45}$$

Constants of integration are set to zero in order to ensure the periodicity of the solution. The coefficients of $\cos t$ in (1.45) is taken equal to A_0:

$$\alpha A_0 + \frac{3}{4}\beta A_0^3 - F = 0. \tag{1.46}$$

The value of A_0 is determined from this equation.

The solution x as given by (1.45) or

$$x(t) = A_0 \cos t + \frac{1}{36}\mu\beta A_0^3 \cos 3t, \tag{1.47}$$

itself, may be considered as the second approximation. It is, however, more

---

* A term $B_0 \sin t$ should be added, but B_0 would turn out to be zero in the next step of the iteration procedure.

reasonable to reassume the second approximation of the form

$$x_1(t) = A_1 \cos t + \frac{1}{36}\mu\beta A_1^3 \cos 3t, \tag{1.48}$$

where the amplitude A_1 is to be determined in the next step. Substituting (1.48) into the right-hand side of (1.39) and integrating it twice leads*

$$x(t) = \left[A_1 + \mu(\alpha A_1 + \tfrac{3}{4}\beta A_1^3 - F) + \tfrac{1}{48}\mu^2\beta^2 A_1^5 + \tfrac{1}{864}\mu^3\beta^3 A_1^7\right]\cos t$$
$$+ \frac{1}{36}\mu\beta A_1^3\left[\frac{10}{9} + \frac{1}{18}\mu(2\alpha + 3\beta A_1^2) + \frac{1}{15552}\mu^3\beta^3 A_1^6\right]\cos 3t$$
$$+ \frac{1}{1200}\mu^2\beta^2 A_1^5\left[1 + \frac{1}{36}\mu\beta A_1^2\right]\cos 5t. \tag{1.49}$$

Integration constants are again set to be zero in order to ensure the periodicity of the solution. The coefficients of $\cos t$ in (1.49) is taken equal to A_1:

$$\alpha A_1 + \frac{3}{4}\beta A_1^3 - F + \frac{1}{48}\mu\beta^2 A_1^5 + \frac{1}{864}\mu^2\beta^3 A_1^7 = 0. \tag{1.50}$$

This determines the value of A_1. Equation (1.50) is similar to (1.46), except for the last two additive terms.

Further iteration of the procedure may allow a more accurate solution to be found, but it is rather troublesome for actual computaion. Therefore we may regard x of (1.49) with A_1 furnished by (1.50) as the third approximation.

In like manner, the harmonic solution of Duffing's equation with term for dissipation

$$\frac{d^2x}{dt^2} + \mu k\frac{dx}{dt} + (1+\mu\alpha)x + \mu\beta x^3 = \mu F \cos t \tag{1.51}$$

---

* Terms of frequency 7 and 9 are omitted in this equation, since they are sufficiently small.

may be obtained. It is reasonable to start the iteration process with the first approximation

$$x_0(t) = A_0 \cos t + B_0 \sin t. \tag{1.52}$$

Substituting (1.52) into the right-hand side of (1.51) and integrating it twice leads to

$$\begin{aligned} x(t) = &\left[A_0 + \mu\left(\alpha A_0 + k B_0 + \tfrac{3}{4}\beta A_0^3 + \tfrac{3}{4}\beta A_0 B_0^2 - F\right)\right]\cos t \\ &+ \left[B_0 + \mu\left(-k A_0 + \alpha B_0 + \tfrac{3}{4}\beta A_0^2 B_0 + \tfrac{3}{4}\beta B_0^3\right)\right]\sin t \\ &+ \tfrac{1}{36}\mu\beta A_0\left(A_0^2 - 3B_0^2\right)\cos 3t + \tfrac{1}{36}\mu\beta B_0\left(3A_0^2 - B_0^2\right)\sin 3t \end{aligned} \tag{1.53}$$

Integration constants are set to zero. Equating the coefficients of $\cos t$ and $\sin t$ to A_0 and B_0 respectively, we obtain

$$\left.\begin{aligned} A_0 &= \left(\alpha + \tfrac{3}{4}\beta R_0^2\right)\frac{R_0^2}{F}, \\ B_0 &= k\,\frac{R_0^2}{F}, \end{aligned}\right\} \tag{1.54}$$

where $R_0^2 = A_0^2 + B_0^2$ is determined from

$$\left[\left(\alpha + \tfrac{3}{4}\beta R_0^2\right)^2 + k^2\right] R_0^2 = F^2. \tag{1.55}$$

The solution

$$\begin{aligned} x(t) = &A_0 \cos t + B_0 \sin t \\ &+ \tfrac{1}{36}\mu\beta A_0\left(A_0^2 - 3B_0^2\right)\cos 3t + \tfrac{1}{36}\mu\beta B_0\left(3A_0^2 - B_0^2\right)\sin 3t \end{aligned} \tag{1.56}$$

is a closer approximation than (1.52).

1.4 Method of Harmonic Balance

The periodic solution may be developed in a Fourier series of sine and cosine components. In many cases, the component of the fundamental frequency and one or two additional components are of predominant amplitudes. According to the method of harmonic balance, such few terms are assumed to a first approximation. Coefficients of the Fourier series are determined to satisfy the equation so far as terms of the considered frequencies are concerned. Terms of frequency other than those considered are certain to be present also but are ignored to this order of approximation. In theory, the more terms are taken into consideration, the closer approximation may be obtained. However, numerical computations will be cumbersome too much. In the following description, we shall start with a first approximation of very simple form and then improve the accuracy of the approximation by adding correction terms step-by-step.

Let us consider the same equation as in the preceding sections:

$$\frac{d^2x}{dt^2}+(1+\mu\alpha)x+\mu\beta x^3=\mu F\cos t. \tag{1.57}$$

First we assume the approximation of the form

$$x_0(t)=A_{10}\cos t. \tag{1.58}$$

Substitution of (1.58) into (1.57) leads to

$$\mu(\alpha A_{10}+\tfrac{3}{4}\beta A_{10}^3-F)\cos t+\tfrac{1}{4}\mu\beta A_{10}^3\cos 3t=0. \tag{1.59}$$

Equating the amplitude of the fundamental component to zero we obtain

$$\alpha A_{10}+\tfrac{3}{4}\beta A_{10}^3-F=0. \tag{1.60}$$

Equation (1.60) takes the same form as (1.22) obtained by the perturbation method or (1.46) obtained by the iteration procedure. That is to say, any of the methods gives the same solution of the first approximation.

Next we assume the second approximation of the form

$$x_1(t) = (A_{10} + \varepsilon A_{11})\cos t + \varepsilon A_{31}\cos 3t \tag{1.61}$$

taking into consideration the third-harmonic component. Correction terms associated with εA_{11} and εA_{31} are considered to be relatively small, i.e., the first-order quantities in a small parameter ε. The use of ε is not indispensable, but make it convenient to clarify the orders of small quantities. We substitute (1.61) into (1.57) and equate the coefficients of $\cos t$ and $\sin t$ separately to zero. Ignoring terms of order higher than the first in ε, we have

$$\left.\begin{aligned} &\mu(\alpha + 3a)(\varepsilon A_{11}) + \mu a(\varepsilon A_{31}) = 0, \\ &-\mu a(\varepsilon A_{11}) + (8 - \mu\alpha - 2\mu a)(\varepsilon A_{31}) = \frac{1}{3}\mu a A_{10}, \\ &a = \frac{3}{4}\beta A_{10}^2 . \end{aligned}\right\} \tag{1.62}$$

where

The amplitudes εA_{11} and εA_{31} are readily determined by solving these linear simultaneous equations.

The third approximation is assumed in the form

$$x_2(t) = (A_{10} + \varepsilon A_{11} + \varepsilon^2 A_{12})\cos t + (\varepsilon A_{31} + \varepsilon^2 A_{32})\cos 3t + \varepsilon^2 A_{52}\cos 5t. \tag{1.63}$$

Correction terms associated with $\varepsilon^2 A_{12}$, $\varepsilon^2 A_{32}$, and $\varepsilon^2 A_{52}$ are considered to be still smaller than those associated with εA_{11} and εA_{31}. Substituting (1.63) into (1.57) and equating the coefficients of $\cos t$, $\cos 3t$, and $\cos 5t$ separately to zero, we obtain the linear simultaneous equations in $\varepsilon^2 A_{12}$, $\varepsilon^2 A_{32}$, and $\varepsilon^2 A_{52}$:

$$\left.\begin{aligned}
&-\mu(\alpha+3a)(\varepsilon^2A_{12})-\mu a(\varepsilon^2A_{32}) = \tfrac{3}{4}\mu\beta A_{10}\left[3(\varepsilon A_{11})^2+2(\varepsilon A_{11})(\varepsilon A_{31})+2(\varepsilon A_{31})^2\right],\\
&-\mu a(\varepsilon^2A_{12})+(8-\mu\alpha-2\mu a)(\varepsilon^2A_{32})-\mu a(\varepsilon^2A_{52}) = \tfrac{3}{4}\mu\beta A_{10}\left[(\varepsilon A_{11})^2+4(\varepsilon A_{11})(\varepsilon A_{31})\right],\\
&-\mu a(\varepsilon^2A_{32})+(24-\mu\alpha-2\mu a)(\varepsilon^2A_{52}) = \tfrac{3}{4}\mu\beta A_{10}\left[A_{10}(\varepsilon A_{31})+2(\varepsilon A_{11})(\varepsilon A_{31})+(\varepsilon A_{31})^2\right],\\
&\text{where} \qquad a=\tfrac{3}{4}\beta A_{10}^2 .
\end{aligned}\right\} \tag{1.64}$$

Terms of order higher than the second in ε are discarded in this step.

In like manner, we can obtain the harmonic solution of Duffing's equation with a term for dissipation

$$\frac{d^2x}{dt^2}+\mu k\frac{dx}{dt}+(1+\mu\alpha)x+\mu\beta x^3=\mu F\cos t. \tag{1.65}$$

We start with the first approximation

$$x_0(t)=A_{10}\cos t+B_{10}\sin t. \tag{1.66}$$

The amplitudes A_{10} and B_{10} are determined to satisfy (1.65) so far as terms containing $\cos t$ and $\sin t$ are concerned. Thus we obtain

$$\left.\begin{aligned}
A_{10}&=(\alpha+\tfrac{3}{4}\beta R_{10}^2)\frac{R_{10}^2}{F},\\
B_{10}&=k\frac{R_{10}^2}{F},
\end{aligned}\right\} \tag{1.67}$$

where $R_{10}^2=A_{10}^2+B_{10}^2$ is to be determined from

$$\left[(\alpha+\tfrac{3}{4}\beta R_{10}^2)^2+k^2\right]R_{10}^2=F^2. \tag{1.68}$$

We readily see from (1.35), (1.54), and (1.67) that any methods give the same solution of the first approximation for Duffing's equation (1.29).

The second approximation is assumed in the form

$$x_1(t) = (A_{10} + \varepsilon A_{11})\cos t + (B_{10} + \varepsilon B_{11})\sin t + \varepsilon A_{31}\cos 3t + \varepsilon B_{31}\sin 3t. \tag{1.69}$$

We substitute (1.69) into (1.65) and equate the coefficients of $\cos t$, $\sin t$, $\cos 3t$, and $\sin 3t$ separately to zero. Ignoring terms of order higher than the first in ε, we obtain

$$\left.\begin{array}{l}
\mu(\alpha+2a+c)(\varepsilon A_{11})+\mu(k+b)(\varepsilon B_{11})+\mu c(\varepsilon A_{31})+\mu b(\varepsilon B_{31}) = 0, \\
\mu(k-b)(\varepsilon A_{11})-\mu(\alpha+2a-c)(\varepsilon B_{11})+\mu b(\varepsilon A_{31})-\mu c(\varepsilon B_{31}) = 0, \\
-\mu c(\varepsilon A_{11})+\mu b(\varepsilon B_{11})+(8-\mu\alpha-2\mu a)(\varepsilon A_{31})-3\mu k(\varepsilon B_{31}) = \frac{1}{2}\mu A_{10}(2c-\beta A_{10}^2), \\
-\mu b(\varepsilon A_{11})-\mu c(\varepsilon B_{11})+3\mu k(\varepsilon A_{31})+(8-\mu\alpha-2\mu a)(\varepsilon B_{31}) = \frac{1}{2}\mu B_{10}(2c+\beta B_{10}^2), \\
\text{where} \quad a = \frac{3}{4}\beta(A_{10}^2+B_{10}^2), \quad b = \frac{3}{2}\beta A_{10}B_{10}, \quad c = \frac{3}{4}\beta(A_{10}^2-B_{10}^2).
\end{array}\right\} \tag{1.70}$$

The amplitudes εA_{11}, εB_{11}, εA_{31}, and εB_{31} of the correction terms are determined by solving the linear simultaneous equations (1.70).

The method of improving the approximation described in this section is particularly useful when the amplitude of each harmonic component decreases with increasing order of the harmonics.

1.5 Comparison of the Three Methods

As mentioned in Section 1.4, any of the three methods give the same approximate solution of the first order. Higher-approximate solutions are not exactly the same. For example, we consider the second approximations for Duffing's equation

$$\frac{d^2x}{dt^2} + (1+\mu\alpha)x + \mu\beta x^3 = \mu F \cos t.$$

The first approximation takes the form

$$x_0(t) = A_0 \cos t.$$

The second approximations yielded are as follows:

$$\left.\begin{aligned} &\textbf{Perturbation :} \quad x_{1P}(t) = A_{1P}\cos t + A_{3P}\cos 3t, \\ &\qquad \textbf{where} \quad A_{1P} = A_0 - \frac{\frac{3}{128}\mu\beta^2 A_0^5}{\alpha + \frac{9}{4}\beta A_0^2}, \\ &\qquad\qquad\quad A_{3P} = \frac{1}{32}\mu\beta A_0^3. \end{aligned}\right\} \tag{1.71}$$

$$\left.\begin{aligned} &\textbf{Iteration :} \quad x_{1I}(t) = A_{1I}\cos t + A_{3I}\cos 3t, \\ &\qquad \textbf{where} \quad A_{1I} = A_0 - \frac{\frac{1}{48}\mu\beta^2 A_0^5}{\alpha + \frac{9}{4}\beta A_0^2} + O_2(\mu),^* \\ &\qquad\qquad\quad A_{3I} = \frac{1}{36}\mu\beta A_0^3 + O_2(\mu). \end{aligned}\right\} \tag{1.72}$$

Harmonic Balance : $x_{1H}(t) = A_{1H}\cos t + A_{3H}\cos 3t,$

---

* $O_2(\mu)$ refers to terms of order higher than the first in μ.

where

$$\left.\begin{aligned} A_{1H} &= A_0 - \frac{\frac{3}{128}\mu\beta^2 A_0^5}{\alpha+\frac{9}{4}\beta A_0^2} + O_2(\mu), \\ A_{3H} &= \frac{1}{32}\mu\beta A_0^3 + O_2(\mu). \end{aligned}\right\} \tag{1.73}$$

Thus, we obtain

$$\left.\begin{aligned} A_{1I} - A_{1P} &= \frac{\mu\beta^2 A_0^5}{384(\alpha+\frac{9}{4}\beta A_0^2)} + O_2(\mu), \\ A_{3I} - A_{3P} &= -\frac{1}{288}\mu\beta A_0^3 + O_2(\mu), \end{aligned}\right\} \tag{1.74}$$

and

$$\left.\begin{aligned} A_{1H} - A_{1P} &= O_2(\mu), \\ A_{3H} - A_{3P} &= O_2(\mu). \end{aligned}\right\} \tag{1.75}$$

That is to say, the perturbation method and the method of harmonic balance give the same second approximation up to terms of order μ, while the result of the iteration method slightly differs from that in terms of order μ.

Further we can see that the perturbation method and the method of harmonic balance give the same third approximation up to terms of order μ, while the third approximate solution of the iteration method differs from that in terms of order μ.

The same is also true in the case of the solution of the equation with a term for dissipation. From the above results, we may conclude that the iteration method is somewhat inferior to the other methods.

1.6 Numerical Examples

Analytical methods described in the preceding three sections are legitimat mathematically only for equations in which the degree of nonlinearity is suffic ly small. However, they may still be applicable even to the solution of equations with large nonlinearity to some extent. We have not seen much of numerical examples of large nonlinearity.

In this section we shall deal with the numerical examples of Duffing's equation

$$\frac{d^2x}{dt^2} + x^3 = 0.2\cos t, \tag{1.76}$$

and

$$\frac{d^2x}{dt^2} + 0.2\frac{dx}{dt} + x^3 = 0.3\cos t,$$

where the restoring terms are of cubic characteristic.

1.6.1 Equation without Term for Dissipation

(a) Perturbation Method

Equation (1.76), i.e.,

$$\frac{d^2x}{dt^2} + x^3 = 0.2\cos t \tag{1.77}$$

is obtained by setting the parameters of (1.13) as

$$\mu = 1, \quad \alpha = -1, \quad \beta = 1, \quad \text{and} \quad F = 0.2. \tag{1.78}$$

The first approximate solution (1.20) is obtained by using (1.22). Equation (1.22) has three real roots for the numerical parameters of (1.78); there are three harmonic solutions having different amplitudes. For each of them, the correction terms (1.23) and (1.26) are determined by using (1.25) and (1.27). The numerical values of the approximations up to the third order are listed in Table 1.1.

Table 1.1 Harmonic Solutions for Eq. (1.76) obtained by the Perturbation Method

Harmonic Solution	Order of Approximation	Approximate Solution $x(t) = a_1 \cos t + a_3 \cos 3t + a_5 \cos 5t$		
		a_1	a_3	a_5
1	1	-0.207	——	——
	2	-0.207	-0.000	——
	3	-0.207	-0.000	0.000
2	1	1.244	——	——
	2	1.216	0.060	——
	3	1.211	0.066	0.003
3	1	-1.037	——	——
	2	-1.017	-0.035	——
	3	-1.016	-0.036	-0.001

(b) Iteration Method

Equations (1.43), (1.48), and (1.49) give approximate solutions of the ord first, second, and third, respectively. Numerical values of the system parameters are given by (1.78). The amplitudes A_0 and A_1 are determined from (1.46) and (1.50) respectively. The solutions are listed in Table 1.2.

Table 1.2 Harmonic Solutions for Eq. (1.76) obtained by the Iteration Method

Harmonic Solution	Order of Approximation	Approximate Solution $x(t) = a_1 \cos t + a_3 \cos 3t + a_5 \cos 5t$		
		a_1	a_3	a_5
1	1	-0.207	——	——
	2	-0.207	-0.000	——
	3	-0.207	-0.000	0.000
2	1	1.244	——	——
	2	1.219	0.050	——
	3	1.219	0.063	0.002
3	1	-1.037	——	——
	2	-1.020	-0.029	——
	3	-1.020	-0.035	-0.001

(c) Method of Harmonic Balance

Equations (1.58), (1.61), and (1.63) give approximate solutions of the order first, second, and third, respectively. The amplitudes of the solutions are determined from (1.60), (1.62), and (1.64). The solutions are listed in Table 1.3.

Table 1.3 Harmonic Solutions for Eq. (1.76) obtained by the Method of Harmonic Balance

Harmonic Solution	Order of Approximation	Approximate Solution $x(t) = a_1 \cos t + a_3 \cos 3t + a_5 \cos 5t$		
		a_1	a_3	a_5

1	1	-0.207	——	——
	2	-0.207	-0.000	——
	3	-0.207	-0.000	0.000
2	1	1.244	——	——
	2	1.213	0.067	——
	3	1.212	0.066	0.003
3	1	-1.037	——	——
	2	-1.017	-0.036	——
	3	-1.016	-0.035	-0.001

(d) Accuracy of the Solutions

Unless we know the exact solution of (1.76), it is impossible to evaluate the errors of the approximate solutions shown in Table 1.1 through 1.3. Here we consider a practical way for estimating accuracy of the approximate solutions.

Let $x_a(t)$ be an approximate solution of the equation

$$\frac{d^2x}{dt^2} + (1+\mu\alpha)x + \mu\beta x^3 = \mu F \cos t.$$

Insertion of $x_a(t)$ into the equation yields

$$\frac{d^2x_a}{dt^2} + (1+\mu\alpha)x_a + \mu\beta x_a^3 - \mu F \cos t = r(t)$$

The function $r(t)$ may be called the residual function. It is, in general, found in the form

$$r(t) = \sum_n (a_{rn} \cos nt + b_{rn} \sin nt).$$

We make the quantity

$$\varepsilon = \sqrt{\sum_n (a_{rn}^2 + b_{rn}^2)} \quad . \tag{1.79}$$

This will give a measure of the inaccuracy of $x_a(t)$.

The numerical values of ε for the approximate solutions of (1.76) are listed in Table 1.4.

Table 1.4 Values of ε for the Approximate Solutions of (1.76)

Harmonic Solution	Order of Approximation	Method		
		Perturbation	Iteration	Harm. Bal.
1	1	0.002	0.002	0.002
	2	0.000	0.000	0.000
	3	0.000	0.000	0.000
2	1	0.481	0.481	0.481
	2	0.082	0.129	0.078
	3	0.010	0.042	0.011
3	1	0.279	0.279	0.279
	2	0.028	0.055	0.029
	3	0.007	0.009	0.004

1.6.2 Equation with a Term for Dissipation

(a) Perturbation Method

Equation (1.77), i.e.,

$$\frac{d^2x}{dt^2} + 0.2\frac{dx}{dt} + x^3 = 0.3\cos t$$

is obtained by setting the parameters of (1.29) as

$$\mu = 1, \quad k = 0.2, \quad \alpha = -1, \quad \beta = 1, \quad \text{and} \quad F = 0.3. \tag{1.80}$$

There are three harmonic solutions having different amplitudes and phases for these particular values of the parameters. By making use of Eqs. (1.32) through (1.37) found in Section 1.2, approximate solutions are calculated up to the second order. The numerical values are listed in Table 1.5.

Table 1.5 Harmonic Solutions for Eq. (1.77) obtained by the Perturbation Method

Harmonic Solution	Order of Approximation	Approximate Solution $x(t) = a_1\cos t + b_1\sin t + a_3\cos 3t + b_3\sin 3t$			
		a_1	b_1	a_3	b_3
1	1	-0.310	0.067	—	—
	2	-0.310	0.067	-0.001	0.001
2	1	0.703	1.012	—	—
	2	0.717	0.972	-0.055	0.019
3	1	-0.748	0.699	—	—
	2	-0.745	0.669	0.020	0.027

(b) Iteration Method

By making use of Eqs. (1.52) through (1.56), approximate solutions are calculated up to the second order. The numerical values are listed in Table 1.6.

Table 1.6 Harmonic Solutions for Eq. (1.77) obtained by the Iteration Method

Harmonic Solution	Order of Approximation	Approximate Solution $x(t) = a_1 \cos t + b_1 \sin t + a_3 \cos 3t + b_3 \sin 3t$			
		a_1	b_1	a_3	b_3
1	1	-0.310	0.067	——	——
	2	-0.310	0.067	-0.001	0.001
2	1	0.703	1.012	——	——
	2	0.703	1.012	-0.050	0.013
3	1	-0.748	0.699	——	——
	2	-0.748	0.699	0.019	0.023

(c) Method of Harmonic Balance

By making use of Eqs. (1.66) through (1.70), approximate solutions are calculated up to the second order. The numerical values are listed in Table 1.7.

Table 1.7 Harmonic Solutions for Eq. (1.77) obtained by the Method of Harmonic Balance

Harmonic Solution	Order of Approximation	Approximate Solution $x(t) = a_1 \cos t + b_1 \sin t + a_3 \cos 3t + b_3 \sin 3t$			
		a_1	b_1	a_3	b_3
1	1	-0.310	0.067	——	——
	2	-0.310	0.067	-0.001	0.001
2	1	0.703	1.012	——	——
	2	0.684	0.988	-0.061	0.021
3	1	-0.748	0.699	——	——
	2	-0.744	0.671	0.022	0.026

(d) Accuracy of the Solutions

In the like manner as in the preceding section, the value of ε as defined by (1.79) is calculated for each solution. Refer to Table 1.8.

Table 1.8 Values of ε for the Approximate Solutions of (1.77)

Harmonic Solution	Order of Approximation	Method		
		Perturbation	Iteration	Harm. Bal.
1	1	0.008	0.008	0.008
	2	0.001	0.001	0.001
2	1	0.468	0.468	0.468
	2	0.087	0.152	0.082

3	1	0.268	0.268	0.268
	2	0.032	0.051	0.033

1.7 Conclusion

The methods described in this chapter are useful tools for finding an analytical solution of a nonlinear nonautonomous differential equation. The amplitude and phase of the solution have been found as functions of the system parameters. For Duffing's equation without term for dissipation, the approximate solutions have been calculated up to the third order; for the equation with a term for dissipation, up to the second order. If the degree of nonlinearity is sufficiently small, these approximations are of sufficient accuracy and the three methods yield almost the same results. Even if the degree of nonlinearity is rather large, the methods may be useful to some extent. The results of the numerical examples in Section 1.6 have shown the practical applicability of the methods to equations of extremely large nonlinearity. The iteration procedure seems to be somewhat inferior to the other methods.

CHAPTER II

GRAPHICAL METHODS FOR SOLVING NONLINEAR DIFFERENTIAL EQUATIONS

2.1 Introduction

An analytical method, though it has considerable advantage, is only applicable to the solution of rather simple equations. A graphical method applies to much more varieties of nonlinear differential equations. A graphical method is usually simple to utilize and may be particularly effective as an exploratory tool when nonlinear characteristic is known only in the form of a curve, e.g., a experimentally determined curve. Such a curve can be incorporated directly into a graphical solution, and this may be a matter of considerable convenience.

There are many kinds of graphical methods developed. In this chapter we are particularly concerned with the following methods, i.e., the slopeline method and the delta method. Both of them are based on the step-by-step integration procedure and are useful to find a single solution curve with a given initial condition.

No claim is made as to the originality of the principles of the methods, inasmuch as the basic notions have been in use for some time [21, 23]. The author systematize the use of the methods and clarify the possible range of their applicability. Various modifications and extensions of the basic methods will be described in this chapter. Namely, a modification of the slopeline method enables its application to the graphical solution of nonautonomous equations. A modification of the delta method improves the accuracy of the solution. The double-delta method, a extension of the delta method, will be developed which is applicable to the solution of differential equations of a complicated type. Errors produced by each procedure of the graphical constructions are evaluated by making use of Taylor's expansion formula. The results of the solutions for several numerical examples, including van der Pol's equation and Duffing's equation and Duffing's equation, prove the excellency of the methods.

2.2 Slopeline Method

This section describes the slopeline method of graphical construction for solving certain types of nonlinear differential equations including van der Pol's equation and Duffing's equation. The basic notions have been in use for some time by several investigators [1, 2 , 25, 26]. The author is particularly indebted to H. M. Paynter for his contribution to this method and its application to the hydraulic transient studies [23]. A modification of the basic method enables its application to the solution of nonautonomous equations. The subharmonic oscillations of order 1/2 will be studied by this modified method.

2.2.1 Development of Method

As a preliminary example, let it be desired to determine the solution of the first-order differential equation

$$\frac{dx}{dt} = f(t), \tag{2.1}$$

with the initial condition that $x = x_0$ at $t = t_0$. The incremental relation of the variables may be written as

$$\Delta x = [f(t)]_{ave} \cdot \Delta t,$$

where
$$\left.\begin{aligned}&[f(t)]_{ave} = \frac{1}{\Delta t}\int_{t_0}^{t_1} f(t)\,dt,\\ &\Delta t = t_1 - t_0 \text{: small change in } t,\\ &\Delta x = x_1 - x_0 \text{: small change in } x \text{ during the increment } \Delta t.\end{aligned}\right| \tag{2.2}$$

The basic assumption of the slopeline method lies in the use of the arithmetic mean for $[f(t)]_{ave}$, i.e.,

$$\left.\begin{aligned}&[f(t)]_{ave} = \frac{1}{2}(f_0 + f_1),\\ \text{where}\quad & \\ &f_0 = f(t_0), \quad \text{and} \quad f_1 = f(t_1).\end{aligned}\right\} \tag{2.3}$$

Then an approximation Δx_s for Δx is given by

$$\Delta x_s = [f(t_0) + f(t_0 + \Delta t)]\frac{\Delta t}{2}. \tag{2.4}$$

This implies that the trapezoidal method of integration has been employed.

The approximate increment Δx_s is graphically determined as shown in Fig. 2.1. It shows the x, $f(t)$ plane, where the initial points $P_0(x_0, f(t_0))$ and $Q_0(x_0, 0)$ are first located. Starting from the point P_0, make the angle θ with the vertical line and draw the straight line, i.e., the slopeline to intersect the x axis at the point M. The angle θ is chosen such that

$$\tan\theta = \frac{\Delta t}{2} \tag{2.5}$$

for a predetermined value of Δt. From M draw another slopeline, making the same angle θ with the vertical line, to the point P_1 whose ordinate P_1Q_1 is $f(t_1)$. Then

$$\begin{aligned}Q_0Q_1 &= Q_0M + MQ_1 = f(t_0)\tan\theta + f(t_1)\tan\theta\\ &= (f_0 + f_1)\frac{\Delta t}{2}.\end{aligned}$$

This gives the increment Δx_s of (2.4).

A practical arrangement for carrying out this procedure is illustrated in Fig. 2.2. The function $f(t)$ is first plotted on the right-half plane, the coordinates being t and $f(t)$. The left-half of the figure shows x , $f(t)$ plane. The straight line with the inclination of 45° (chain line) plotted in the left-half plane merely serves to permit the graphical transfer of the x -values from the horizontal to the vertical scale and vice versa. The procedure of graphical work is as follows:

1. Locate the point $P_0(t_0, x_0)$, the initial point, in the right-half plane.
2. From P_0 draw the lines shown dotted in parallel with the coordinate axes, and locate the point $Q_0(x_0, f_0)$.
3. Starting from the point Q_0, make the angle θ with the vertical line and draw the slopeline Q_0M to intersect the x axis at the point M .
4. Draw the second slopeline from M to Q_1 whose ordinate is $f_1 = f(t_0+\Delta t)$.
5. From Q_1 draw the lines shown dotted in parallel with the coordinate axes, and locate $P_1(t_1, x_1)$ which is the point on the solution curve at $t_1 = t_0 + \Delta t$.
6. Find the successive points P_2 , P_3 ,... on the solution curve by repeating the above procedure.

The accuracy of this method corresponds to the precision of the trapezoidal approximation. The errors may be not so small if the curvature of $f(t)$ is large and the increment Δt is inappropriately chosen. By making use of Taylor's expansion of the increments, we obtain the general expression for the local error, i.e., the error committed at each step by

$$\varepsilon_s = \Delta x_s - \Delta x = \frac{1}{12} f_0'' \cdot (\Delta t)^3 + O_4(\Delta t), \tag{2.6}$$

where the prime refers to differentiation with respect to t and $O_4(\Delta t)$ represents the terms of order higher than the third in Δt . Equation (2.6) gives a measure of the appropriate increment in the independent variable t . If an allowable error ε_a is given in advance, the interval Δt may preferably be chosen as

$$\Delta t < \left(\frac{12\,\varepsilon_a}{f_0''}\right)^{\frac{1}{3}}$$

The details of error analysis will be described in Appendix II.

2.2.2 Second-Order Equations of the Autonomous Type

We can obtain graphical solutions for the simultaneous equations of the form

$$\left.\begin{aligned} &\frac{dx}{dt} + g(x) - y = 0, \\ &\frac{dy}{dt} + h(y) + x = 0. \end{aligned}\right\} \tag{2.7}$$

Equations (2.7) may be transformed into the second-order equation

$$\frac{d^2x}{dt^2} + \frac{dg}{dx}\frac{dx}{dt} + h\left(\frac{dx}{dt} + g\right) + x = 0. \tag{2.8}$$

Some of the well-known types of differential equations may be represented by Eq. (2.8); namely:

1. Linear equation of the second order

$$\left.\begin{aligned} &\frac{d^2x}{dt^2} + k\frac{dx}{dt} + x + kc = 0, \\ &\text{for} \\ &g(x) = c \text{ (: constant)},\ h(y) = ky \text{ (} k \text{ : constant)}. \end{aligned}\right\} \tag{2.9}$$

2. Van der Pol's equation

$$\left.\begin{aligned} &\frac{d^2x}{dt^2} - \mu(1-x^2)\frac{dx}{dt} + x = 0, \\ \text{for} \quad & \\ &g(x) = -\mu x + \frac{1}{3}\mu x^3 \ (\mu \text{ : constant}), \quad h(y) = 0. \end{aligned}\right\} \tag{2.10}$$

3. Rayleigh's equation

$$\left.\begin{aligned} &\frac{d^2x}{dt^2} - [\alpha - \beta(\frac{dx}{dt})^2]\frac{dx}{dt} + x = 0, \\ \text{for} \quad & \\ &g(x) = 0, \quad h(y) = -\alpha y + \beta y^3 (\alpha, \beta \text{ : constants}). \end{aligned}\right\} \tag{2.11}$$

4. Nonlinear equation of the second order

$$\left.\begin{aligned} &\frac{d^2x}{dt^2} + \frac{dG}{dx}\frac{dx}{dt} + G(x) = 0, \\ \text{for} \quad & \\ &G(x) = g(x) + x, \quad h(y) = y. \end{aligned}\right\} \tag{2.12}$$

Figure 2.3 shows the method of graphical construction of the solution curve in the x, y plane for (2.7). The curves $g(x)$ along the x axis and $-h(y)$ along the y axis are to be plotted beforehand. The procedure of graphical construction is as follows:

1. Locate the initial point $P_0(x_0, y_0)$ at $t = t_0$.
2. Starting from P_0, make the angle $\theta = \tan^{-1}\frac{\Delta t}{2}$ with the vertical line and draw the slopeline SL_1 to intersect the curve $g(x)$ at the point M. From M draw the slopeline SL_2.
3. Starting again from P_0, make the angle θ with the horizontal line and draw the slopeline SL_3 to intersect the curve $-h(y)$ at the point N. From N draw the slopeline SL_4. The intersection $P_1(x_1, y_1)$ of SL_4 with SL_2

gives the point P_1 on the solution curve at $t_1 = t_0 + \Delta t$.

4. Repeat the above procedure to find the successive points P_2 , P_3 ,....

It is clear, from the figure, that

$$\left.\begin{aligned} \Delta x_s &= x_1 - x_0 = (x_1 - x_m) + (x_m - x_0) \\ &= [y_0 - g(x_m)]\frac{\Delta t}{2} + [y_1 - g(x_m)]\frac{\Delta t}{2}, \\ \text{and} \quad \Delta y_s &= -[x_0 + h(y_n)]\frac{\Delta t}{2} - [x_1 + h(y_n)]\frac{\Delta t}{2}. \end{aligned}\right\} \tag{2.13}$$

These values give a good approximation for the increments Δx and Δy , since $2g(x_m) \cong g(x_0) + g(x_1)$ and $2h(y_n) \cong h(y_0) + h(y_1)$.

The local errors in this procedure are estimated to be

$$\left.\begin{aligned} \varepsilon_x &= \frac{1}{12}\Big\{[g(x_0) - y_0] + \left(\frac{dh}{dy}\right)_{y=y_0}[h(y_0) + x_0] + \frac{1}{2}\left(\frac{d^2g}{dx^2}\right)_{x=x_0}[g(x_0) - y_0]^2 \\ &\quad -2\left(\frac{dg}{dx}\right)_{x=x_0}[h(y_0) + x_0] - \left[\left(\frac{dg}{dx}\right)_{x=x_0}\right]^2[g(x_0) - y_0]\Big\}(\Delta t)^3 \\ &\quad + O_4(\Delta t), \\ \varepsilon_y &= \frac{1}{12}\Big\{[h(y_0) + x_0] - \left(\frac{dg}{dx}\right)_{x=x_0}[g(x_0) - y_0] + \frac{1}{2}\left(\frac{d^2h}{dy^2}\right)_{y=y_0}[h(y_0) + x_0]^2 \\ &\quad +2\left(\frac{dh}{dy}\right)_{y=y_0}[g(x_0) - y_0] - \left[\left(\frac{dh}{dy}\right)_{y=y_0}\right]^2[h(y_0) + x_0]\Big\}(\Delta t)^3 \\ &\quad + O_4(\Delta t), \end{aligned}\right\} \tag{2.14}$$

where ε_x and ε_y are the local errors of the increments Δx and Δy respectively.

Numerical Example

Let us consider van der Pol's equation as a typical example. Taking the parameter $\mu = 1.0$ in Eq. (2.10), we have

$$\frac{d^2x}{dt^2} - (1-x^2)\frac{dx}{dt} + x = 0, \tag{2.15}$$

or

$$\left.\begin{aligned} \frac{dx}{dt} &= x - \frac{1}{3}x^3 + y, \\ \frac{dy}{dt} &= -x. \end{aligned}\right\} \tag{2.16}$$

The curve $g(x) = -x + x^3/3$ is plotted along the x axis in Fig. 2.4. An initial point is prescribed at $x = 0$, $y = 0.05$ near the origin of the x, y plane. Construction then proceeds from this point with $\theta = \tan^{-1}\frac{\Delta t}{2} = \tan^{-1}\frac{0.2}{2}$. Few slopelines, from the point 1 to 4, are shown by fine lines in a part of the figure. The integral curve, on account of the negative damping for small values of x, spirals outward and finally moves onto the limit cycle trajectory. Similarly, an initial point outside the limit cycle would lead to a curve spiraling inward until it would coalesce with the same limit cycle. As the points graphically determined are equally spaced in time t, data from these points are readily transferred to the axes of t and x of Fig. 2.5. The time required for the representative point to complete one revolution along the limit cycle is 6.64, and the amplitude of x is 2.01. These values agree well with the values 6.687 and 2.009 which were correctly calculated to three decimal places by M. Urabe [28].

2.2.3 Second-Order Equations of the Nonautonomous Type [7]

A modification of the method for autonomous systems enables its extended application to the graphical solution of nonautonomous systems such as

$$\frac{dx}{dt} + g_1(x) - y = 0,$$

$$\left.\frac{dy}{dt} + h(y) + g_2(x) = f(t),\quad\right\} \tag{2.17}$$

or

$$\frac{d^2x}{dt^2} + \frac{dg_1}{dx}\frac{dx}{dt} + h\left[\frac{dx}{dt} + g_1(x)\right] + g_2(x) = f(t). \tag{2.18}$$

Among equations of this type, we have, for example:

1. Equation with nonlinear damping

$$\left.\begin{aligned} &\frac{d^2x}{dt^2} + g_3(x)\frac{dx}{dt} + g_2(x) = f(t),\\ \text{for}\qquad &g_3(x) = \frac{dg_1}{dx}, \qquad h(y) = 0. \end{aligned}\right\} \tag{2.19}$$

2. Duffing's equation

$$\left.\begin{aligned} &\frac{d^2x}{dt^2} + k\frac{dx}{dt} + g_2(x) = f(t),\\ \text{for}\qquad &g_1(x) = kx\ (k: \text{constant}), \quad h(y) = 0. \end{aligned}\right\} \tag{2.20}$$

Figure 2.6 shows the graphical construction of the solution curve in the x, y plane for (2.17). The functions $g_1(x)$ along the x axis and $-h(y)$ along the y axis are to be plotted beforehand. The procedure is as follows:

1. Starting from the initial point P_0, draw the slopeline SL_1 to intersect the curve $g_1(x)$. From the intersection draw the slopeline SL_2.

2. Calculate the value of $g_2(x)$ for the abscissa x of each point on the slopeline SL_2. Plot the curve $g_2(x)$ on which the abscissa of each point is $g_2(x)$ calculated above.

3. On one hand, locate the point $Q_0(g_2(x_0), y_0)$. Shift it to the left by $f(t_0)$ to locate the point R_0.

4. Starting from R_0 draw the line SL_3 to intersect the curve $-h(y)$ at the point N. From N draw the line SL_4.

5. Shift SL_4 to the right by $f(t_1)$ to obtain the line SL_4'. It intersects the curve $g_2(x)$ at Q_1.*

6. Passing through Q_1 draw the horizontal line as shown dotted. Its intersection with SL_2 locates the point P_1 on the solution curve at $t_1 = t_0 + \Delta t$.

7. Repeat the above procedure to find the successive points on the solution curve.

The construction yields the approximate increments in x and y as given by

$$\left.\begin{aligned} \Delta x_s &= [y_0 - g_1(x_m)]\frac{\Delta t}{2} + [y_1 - g_1(x_m)]\frac{\Delta t}{2}, \\ \Delta y_s &= [f(t_0) - g_2(x_0) - h(y_n)]\frac{\Delta t}{2} + [f(t_1) - g_2(x_1) - h(y_n)]\frac{\Delta t}{2}, \end{aligned}\right\} \qquad (2.21)$$

for the change Δt in t. The local errors are of order higher than the second in Δt.

Numerical Example

We deal with Duffing's equation**

---

* For practical purpose, reproduce the slopeline SL_2 and the curve $g_2(x)$ on another sheet of paper as illustrated in Fig. 2.6 (b). Putting the y axis and the line SL_2 in (b) of the figure upon those lines in (a), we can locate the intersection Q_1 of the line SL_4' with the curve $g_2(x)$.

** We shall deal with Duffing's equation in the following two chapters. Particularly as for the subharmonic oscillations of order 1/2, refer to Chapter III.

$$\left.\begin{aligned} &\frac{d^2x}{dt^2} + k\frac{dx}{dt} + |x|x = B\cos 2t + B_0, \\ \text{with} \\ &k = 0.20, \quad B = 1.50, \quad \text{and} \quad B_0 = 0.50, \end{aligned}\right\} \tag{2.22}$$

or in the equivalent simultaneous form of equations

$$\left.\begin{aligned} &\frac{dx}{dt} = y, \\ &\frac{dy}{dt} = -ky - |x|x + B\cos 2t + B_0. \end{aligned}\right\} \tag{2.23}$$

Figure 2.7 shows the integral curve with the initial condition $x = 0$, $\frac{dx}{dt} = y = 0$ at $t = 0$. The time interval Δt is $\pi/12$. Also plotted in the figure the curve obtained by using an analog computer for the sake of comparison. After a sufficiently long period of time, the integral curve ultimately tends to the closed curve shown in Fig. 2.8. Since the time required for the representative point to complete one revolution along the closed curve is 2π or equal to twice the period of the external force, a subharmonic oscillation of order 1/2 occurs. The time response curves are shown in Fig. 2.9. These curves graphically obtained agree well with the curves shown dotted which are the results of analog-computer analysis.

2.3 Delta Method

The delta method or δ-method for solving second-order differential equations is described in this section. This method was formulated by L. S. Jacobsen and is a generalization of Liénard's method. The double-delta method, a extension of the basic method, devised to deal with equations of a more complicated type will be described also.

2.3.1 Development of Method [5, 21]

The delta method applies to the solution of differential equations of the type

$$\frac{d^2x}{dt^2} + f\left(\frac{dx}{dt}, x, t\right) = 0, \tag{2.24}$$

where the function $f\left(\frac{dx}{dt}, x, t\right)$ is continuous and single-valued but may be non-linear. In applying the method, the equation is rewritten by adding and subtracting a term $\omega_0^2 x$ to give

$$\frac{d^2x}{dt^2} + \omega_0^2 x + f\left(\frac{dx}{dt}, x, t\right) - \omega_0^2 x = 0. \tag{2.25}$$

The term $\omega_0^2 x$ may be separated out of the term $f\left(\frac{dx}{dt}, x, t\right)$; if not, it is of a fictitious nature. The constant ω_0 may be determined by the form of Eq. (2.24) or may have to be chosen from other information. Introducing the new variables τ and v defined by

$$\tau = \omega_0 t, \qquad \text{and} \qquad v = \frac{dx}{d\tau}, \tag{2.26}$$

Eq. (2.25) may be written as

$$\frac{dv}{dx} = -\frac{x + \delta(v, x, \tau)}{v}, \tag{2.27}$$

where

$$\delta(v, x, \tau) = \frac{1}{\omega_0^2} f\left(\omega_0 v, x, \frac{\tau}{\omega_0}\right) - x. \tag{2.28}$$

The function $\delta(v, x, \tau)$, in general, depends upon all the variables v , x , and τ , but for small change in these variables it may be regarded to remain constant. This is the basic assumption of the method. If δ is constant, the variables of (2.27) can be separated and integrated to give

$$v^2 + (x+\delta)^2 = r^2 = \text{constant.} \tag{2.29}$$

This is the equation for a circle of radius r centered at the point ($x = -\delta$, $v = 0$); therefore δ corresponds the displacement of the center of the circle in the negative direction of the x axis. This displacement δ gives the method its name. Thus, for a small increment of τ, the solution curve may be approximated by a small arc of this circle.

The delta method is most immediately applicable to equations with oscillatory solutions. The constant ω_0 in (2.26) may preferably be chosen equal to the frequency of the oscillation, or more generally, ω_0 should be chosen such that the change in $\delta(v,x,\tau)$ should be as small as possible during the process of graphical computation. Figure 2.10 shows the graphical construction of this method. The procedure is as follows:

1. Locate the initial point $P_0(x_0, v_0)$ at $\tau = \tau_0$ in the x, v plane.
2. By making use Eq. (2.28), calculate the initial values of δ. Fix the point $Q_0(-\delta, 0)$ on the x axis.
3. Starting from P_0 draw a short circular arc with its center at Q_0. The arc P_0P_1 represents a portion of the solution curve. The arc must be short enough so that the change in δ is relatively small.
4. Repeat the above procedure to find the successive points on the solution curve.

The local errors in this procedure are estimated to be

$$\left.\begin{aligned} \varepsilon_x = \frac{1}{6}\left(\frac{d\delta}{d\tau}\right)_0 (\Delta\theta)^3 + O_4(\Delta\theta), \end{aligned}\right\} \tag{2.30}$$

$$\bar{\varepsilon}_v = \frac{1}{2}\left(\frac{d\delta}{d\tau}\right)_0 (\Delta\theta)^2 + \frac{1}{6}\left(\frac{d^2\delta}{d\tau^2}\right)_0 (\Delta\theta)^3 + O_4(\Delta\theta),$$

where $\left(\frac{d\delta}{d\tau}\right)_0$ and $\left(\frac{d^2\delta}{d\tau^2}\right)_0$ stand for $\left(\frac{d\delta}{d\tau}\right)$ and $\left(\frac{d^2\delta}{d\tau^2}\right)$ at $\tau = \tau_0$ respectively, and $\Delta\theta$ is the incremental angle of the radius line r for the individual circular arc.

The increment in time τ is readily found in this method. Since τ increases in a clockwise direction in the x, v plane, the positive increment $\Delta\theta$ is likewise taken in the same direction. Then we obtain the following relation

$$d\tau = \frac{dx}{v} = d\theta. \tag{2.31}$$

By using this relation, $\Delta\theta$ in (2.30) may be replaced by $\Delta\tau$ which is the time increment corresponding to the individual circular arc.

2.3.2 Modification of Method

In the process of the construction above mentioned, the value of δ calculated at the beginning of each step is used throughout that interval. Actually, it is more desirable to use the average values of v, x, and τ existing during the increment for calculating the value of δ.

Figure 2.11 shows the graphical construction of higher approximation which takes care of this consideration. The point P_0 indicates the initial condition (x_0, v_0) at $\tau = \tau_0$. The procedure is as follows:

1. By using (2.28) calculate the initial value of δ, and locate the point Q_0 ($-\delta_0$, 0) on the x axis.
2. Draw the circular arc P_0P_H with its center at Q_0, the incremental angle being chosen equal to $\Delta\tau/2$.

3. Again calculate $\delta_H = \delta\,(v_H, x_H, \tau_0 + \Delta\tau/2)$, where x_H, v_H are the coordinates of the point P_H. Locate $Q_H(-\delta_H, 0)$.

4. Draw the circular arc P_0P_1 with its center at Q_H, the incremental angle being equal to $\Delta\tau$. The arc P_0P_1 represents the solution curve during time interval $\Delta\tau$.

5. Repeat the above procedure to find the successive points on the solution curve.

The local errors in this procedure are estimated to be

$$\left.\begin{aligned} \varepsilon_x &= -\frac{1}{12}\left(\frac{d\delta}{d\tau}\right)_0(\Delta\tau)^3 + O_4(\Delta\tau), \\ \varepsilon_v &= \frac{1}{24}\left(\frac{d^2\delta}{d\tau^2}\right)_0(\Delta\tau)^3 + O_4(\Delta\tau). \end{aligned}\right\} \tag{2.32}$$

In comparison of (2.32) with (2.30), it is clear that the errors, particularly error of v, are reduced fairly well. The modified procedure may still be advantageous as compared with the basic procedure using the halved interval $\Delta\tau/2$.

Numerical Example

We consider an example of Duffing's equation

$$\frac{d^2x}{dt^2} + x + 0.25x^3 = 0.2\cos 1.2t. \tag{2.33}$$

In the equivalent δ-form this becomes

$$\left.\begin{aligned} &\frac{dv}{dx} = -\frac{x+\delta}{v}, \\ \text{where}\quad &\delta = -0.306x + 0.174x^3 - 0.139\cos\tau, \\ &\tau = 1.2t, \quad v = \frac{dx}{d\tau}. \end{aligned}\right\} \tag{2.34}$$

Figure 2.12 shows the phase-plane solution curve with the initial condition $x = 0$, $v = 0$ at $\tau = 0$. Using the relation (2.31), the phase-plane trajectory may readily be converted to the time-response curve shown in Fig. 2.13. The curves obtained by analog-computer analysis are shown dotted in the figures. They well agree with the curves obtained by the graphical method.

2.3.3 Double-Delta Method

Let us consider second-order differential equations of the type

$$g\left(\frac{dx}{dt}, x, t\right)\frac{d^2x}{dt^2} + f\left(\frac{dx}{dt}, x, t\right) = 0, \tag{2.35}$$

where $g(\frac{dx}{dt}, x, t)$ is a continuous and single-valued function as well as $f(\frac{dx}{dt}, x, t)$. Dividing throughout this equation by g, we obtain the equation of the type (2.24); hence we can apply the delta method to its solution. However, the graphical construction becomes impractical owing to the presence of the complicated term f/g.

We describe a somewhat different way of graphical construction for solving equation (2.35). Through addition and subtraction of the terms $\frac{d^2x}{dt^2}$ and $\omega_0^2 x$, the equation is rewritten as

$$[1 + g - 1]\frac{d^2x}{dt^2} + \omega_0^2 x + f - \omega_0^2 x = 0.$$

Introducing the variables τ and v as defined by (2.26), we have

$$\left.\begin{aligned} &\frac{dv}{dx} = -\frac{x + \delta_1}{v + \delta_2}, \\ \text{where} \quad &\delta_1 = \frac{1}{\omega_0^2} f(\omega_0 v, x, \frac{\tau}{\omega_0}) - x, \\ &\delta_2 = [g(\omega_0 v, x, \frac{\tau}{\omega_0}) - 1]v. \end{aligned}\right\} \tag{2.36}$$

If these δ-functions, δ_1 and δ_2, are assumed to be constant, (2.35) may be integrated to give

$$(v+\delta_2)^2+(x+\delta_1)^2 = r^2 = \text{constant.} \tag{2.37}$$

This is the equation for a circle of radius r centered at the point ($x = -\delta_1$, $v = -\delta_2$); hence there is no longer the restriction that the center of the circular arc has to be located on the x axis. See Fig. 2.14. The use of two δ-functions will save the labour of calculation as a whole. In this method of construction, however, it should be noted that the simple relation between $\Delta\tau$ and $\Delta\theta$ as given by (2.31) does not hold.

Numerical Example

We consider the response of the L-C-R series circuit as shown in Fig. 2.15. Following the notations in the figure, the circuit equation may be written as

$$n\frac{d\phi}{dt} + Ri + \frac{q}{C} = E, \tag{2.38}$$

where ϕ is the magnetic flux in the core L and n is the number of turns of the coil wound around the core. The nonlinear characteristic of the core is assumed to be

$$\phi = c_1(\tanh ni + c_2 ni), \tag{2.39}$$

where C_1 and C_2 are constants dependent on the nature of the core. Letting the numerical values of the parameters

$$\left.\begin{array}{lll} n = 1, & R = 0.20, & C = 2.50, \\ c_1 = 0.40, & c_2 = 0.20, & \end{array}\right\} \tag{2.40}$$

we obtain the differential equation

$$\left.\begin{aligned} &(1.2 - \tanh^2 \tfrac{dx}{dt})\frac{d^2x}{dt^2} + 0.5\frac{dx}{dt} + x = 2.5E, \\ \text{where} \quad &x = q. \end{aligned}\right\} \qquad (2.41)$$

Equation (2.41) is rewritten in the double-delta form as

$$\left.\begin{aligned} &\frac{dv}{dx} = -\frac{x+\delta_1}{v+\delta_2}, \\ \text{where} \quad &\delta_1 = 0.5v - 2.5E, \quad \delta_2 = 0.2v - v\cdot\tanh^2 v, \\ &\tau = t, \quad v = \frac{dx}{d\tau}. \end{aligned}\right\} \qquad (2.42)$$

The phase-plane trajectories starting from the origin ($x = 0$, $v = 0$) are shown in Fig. 2.16 for various values of E. Also plotted in the figure the trajectories obtained by using an analog computer. They show excellent agreement.

2.4 Conclusion

The results obtained in this investigation are summarized as follows:

1. The methods have extensive applications to autonomous and nonautonomous differential equations. Nonlinearity in the equations can be dealt with as readily as linearity.
2. First-order equations are solved by the slopeline method as well as certain second-order equations; by the delta method only second-order equations are dealt with.
3. In theory, any differential equations of the second order can be solved by the delta method or the double-delta method. However, numerical computations are needed in finding the value of δ. On the other hand the slopeline meth-

od, in which the procedure of integration contains only graphical works, is restricted to equations of the types as described in Section 2.2.

4. The methods are relatively simple to apply, even to complicated equations. The drafting instruments needed are a scale and a protractor in the slopeline method; in addition to them, a compass in the delta method.

5. The solution in graphical form is obtained fairly quickly, while the degree of accuracy is maintained satisfactorily high for practicable size of steps. However, small unavoidable errors at each step tend to accumulate, and the latter portion of a solution involving long duration is likely to become inaccurate.

6. The phase-plane trajectory is readily converted to the time-response curve, as the time increment for one step of trajectory construction is predetermined or measured at once.

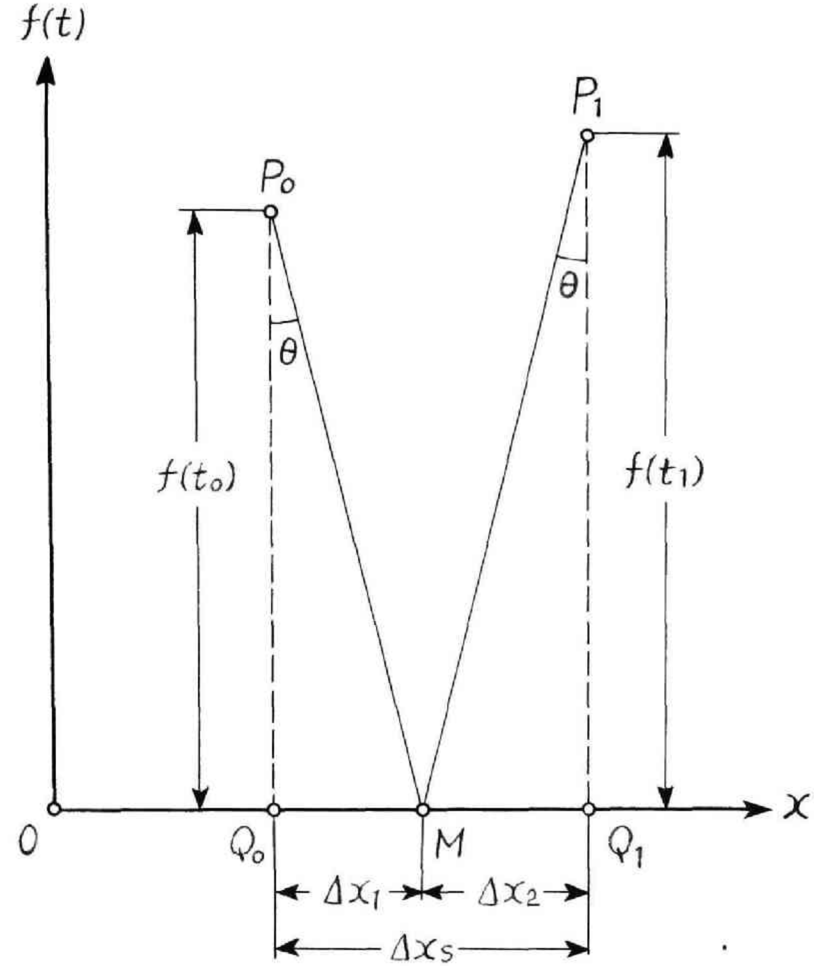

Fig. 2.1 Graphical construction for making Δx_s of Eq. (2.4).

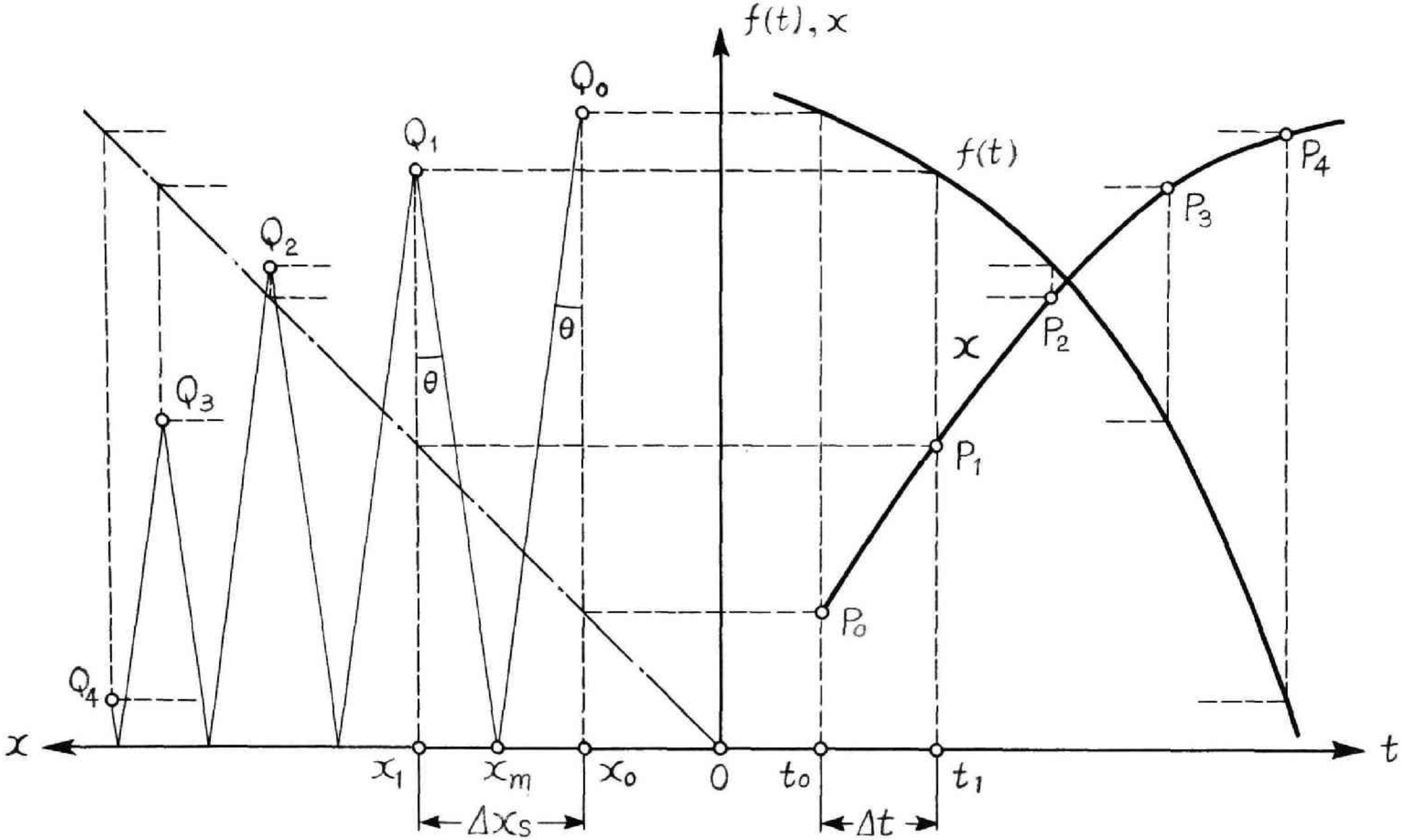

Fig. 2.2 Graphical process for solving Eq. (2.1).

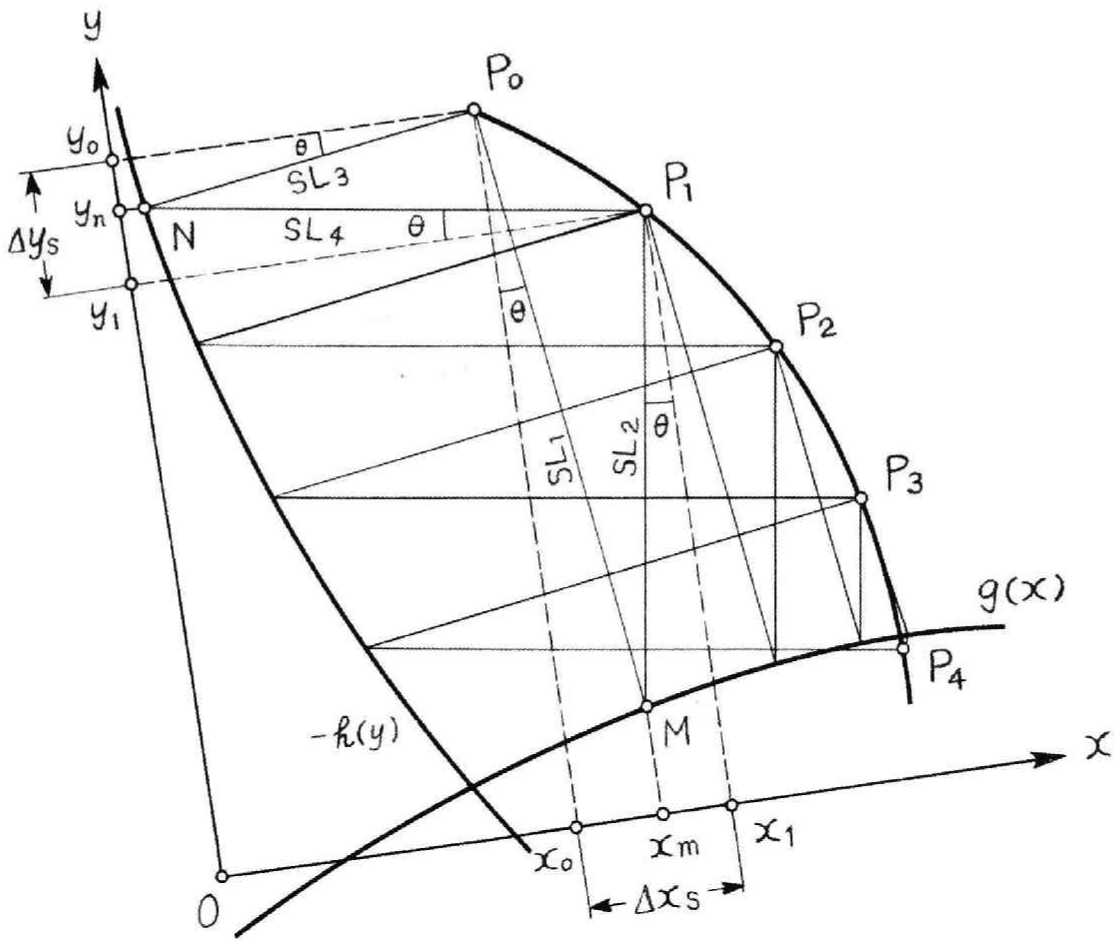

Fig. 2.3 Graphical process for solving Eqs. (2.7).

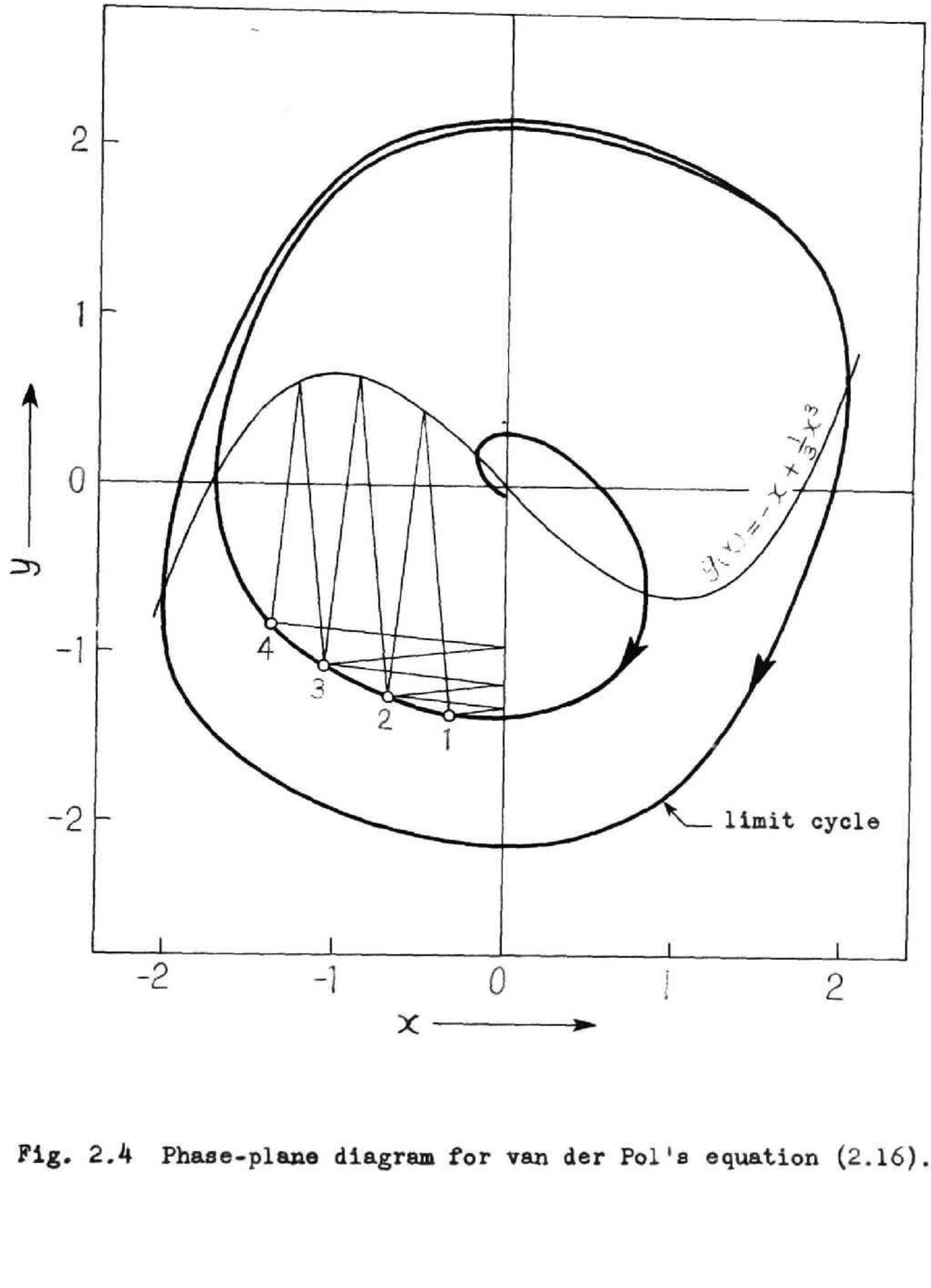

Fig. 2.4 Phase-plane diagram for van der Pol's equation (2.16).

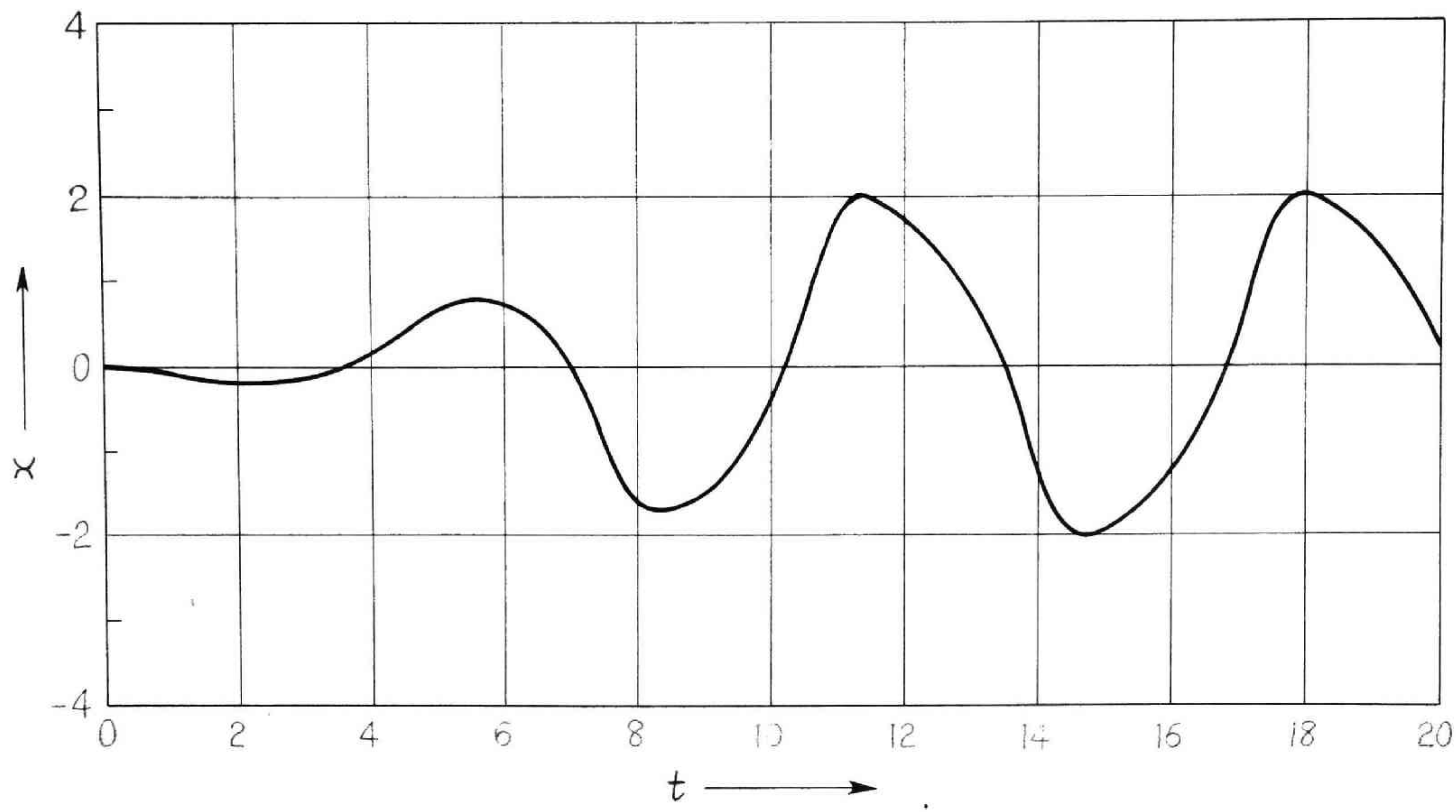

Fig. 2.5 Time-response curve converted from the phase-plane trajectory of Fig. 2.4.

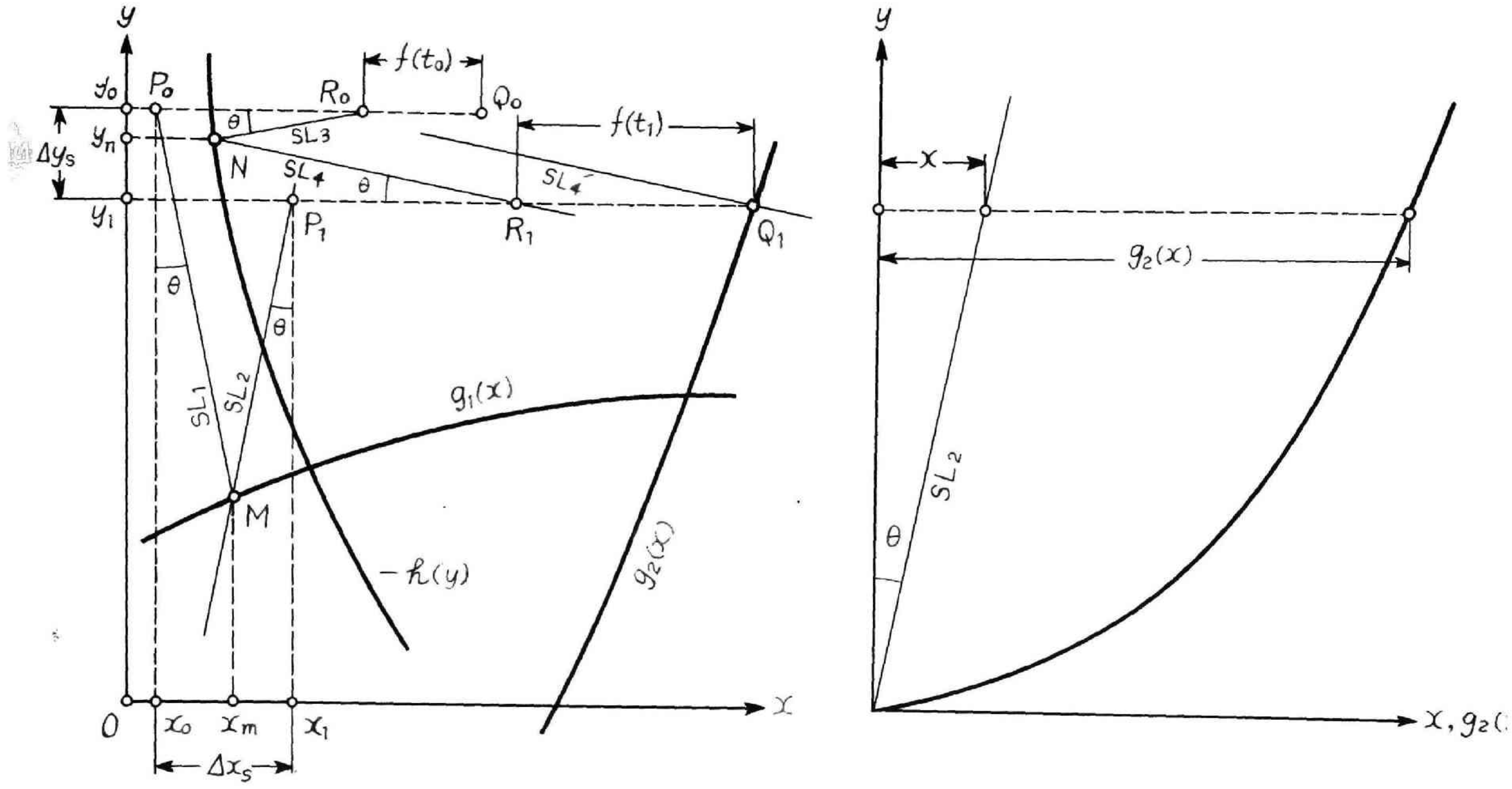

(a)

(b)

Fig. 2.6 Graphical process for solving Eqs. (2.17).

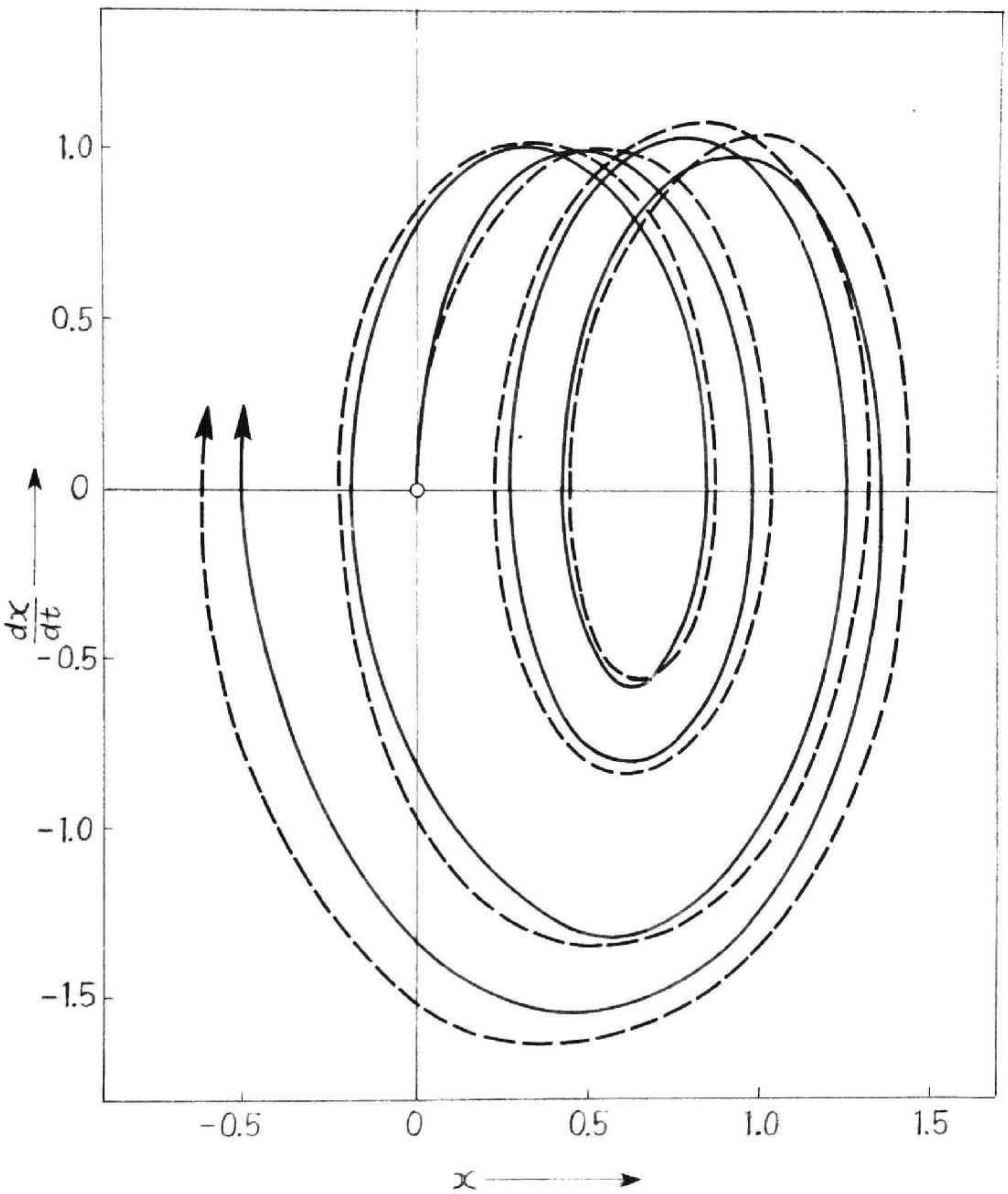

——— : Curve obtained by the slopeline method

– – – – : Curve obtained by the analog-computer analysis

Fig. 2.7 Phase-plane trajectories of the 1/2-harmonic oscillation in the transient state.

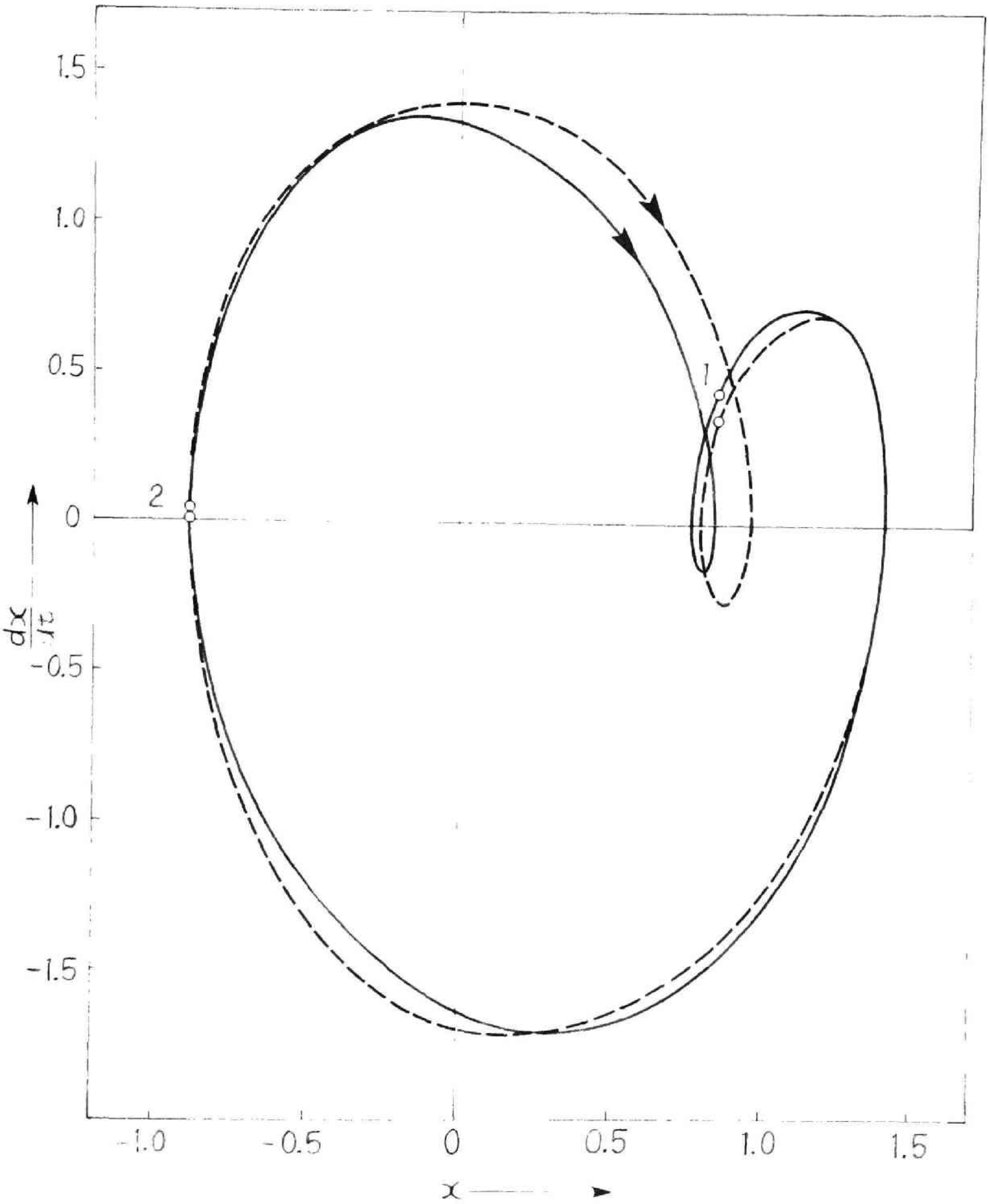

——— : Curve obtained by the slopeline method

– – – – : Curve obtained by the analog-computer analysis

Fig. 2.8 Phase-plane trajectories of the 1/2-harmonic oscillation in the steady state.

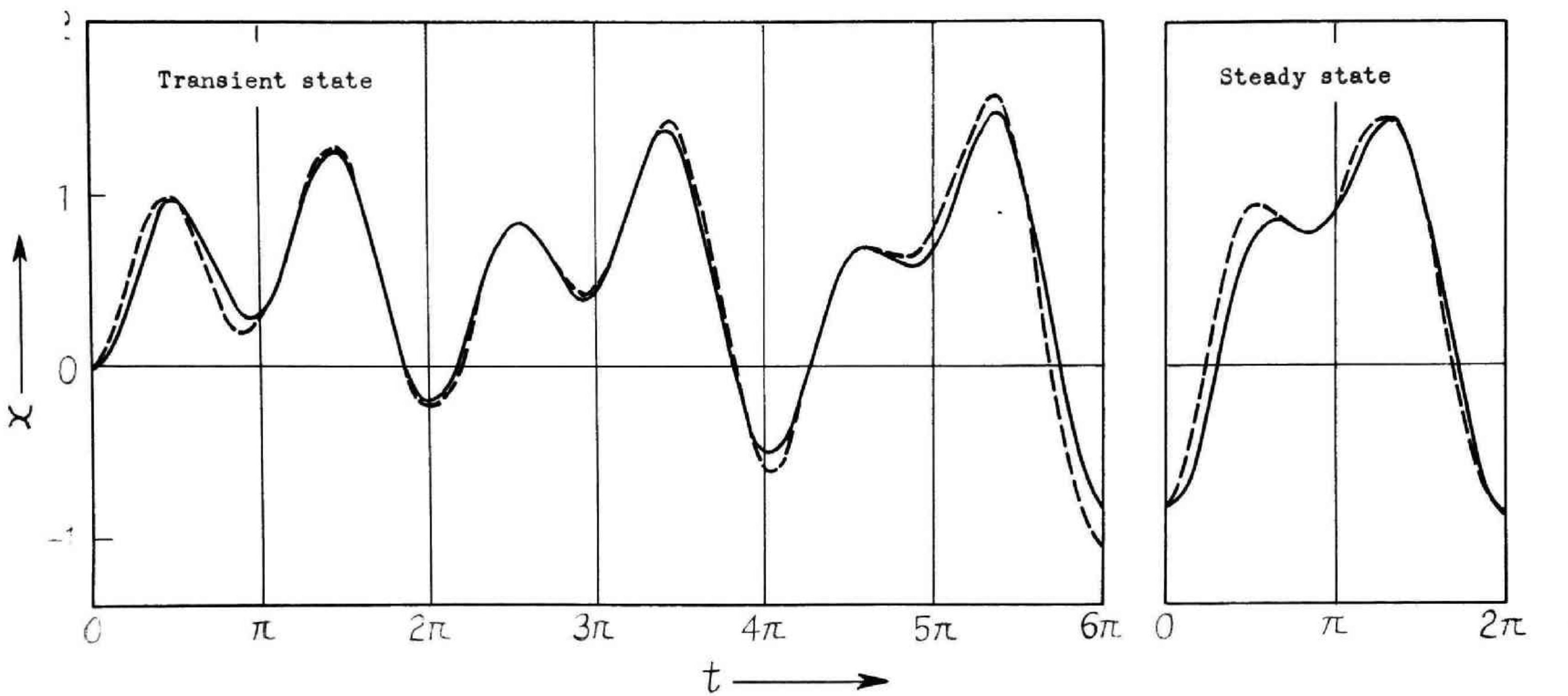

——————— : Curves obtained by the slopeline method

— — — — : Curves obtained by the analog-computer analysis

Fig. 2.9 Waveforms of the 1/2-harmonic oscillation converted from the phase-plane trajectories of Figs. 2.7 and 2.8.

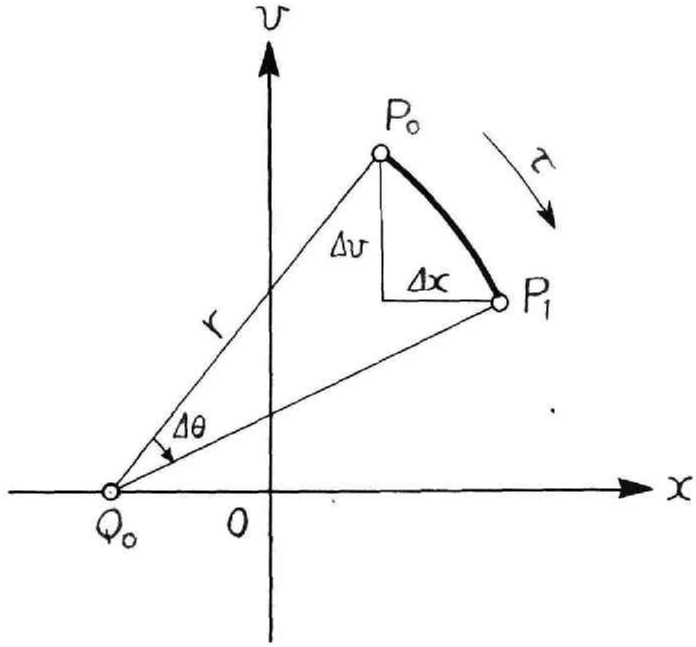

Fig. 2.10 Short arc of the solution curve constructed by the delta method.

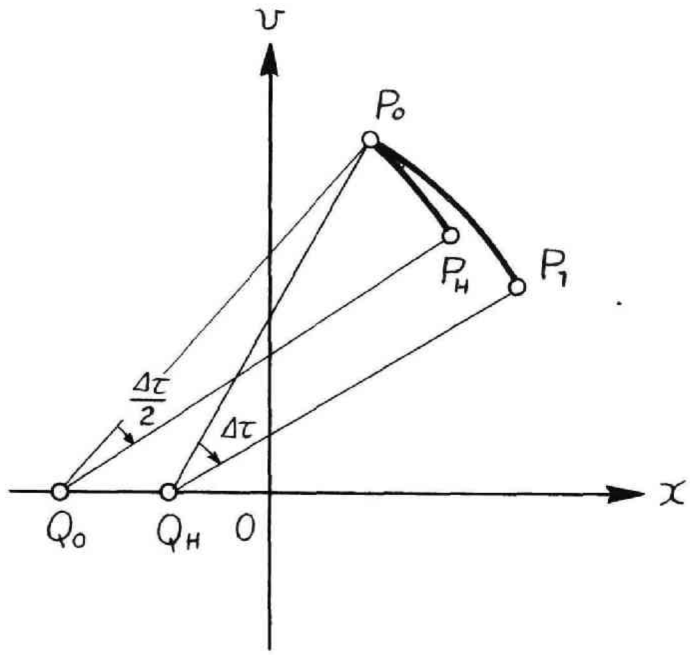

Fig. 2.11 Modified procedure of the delta method.

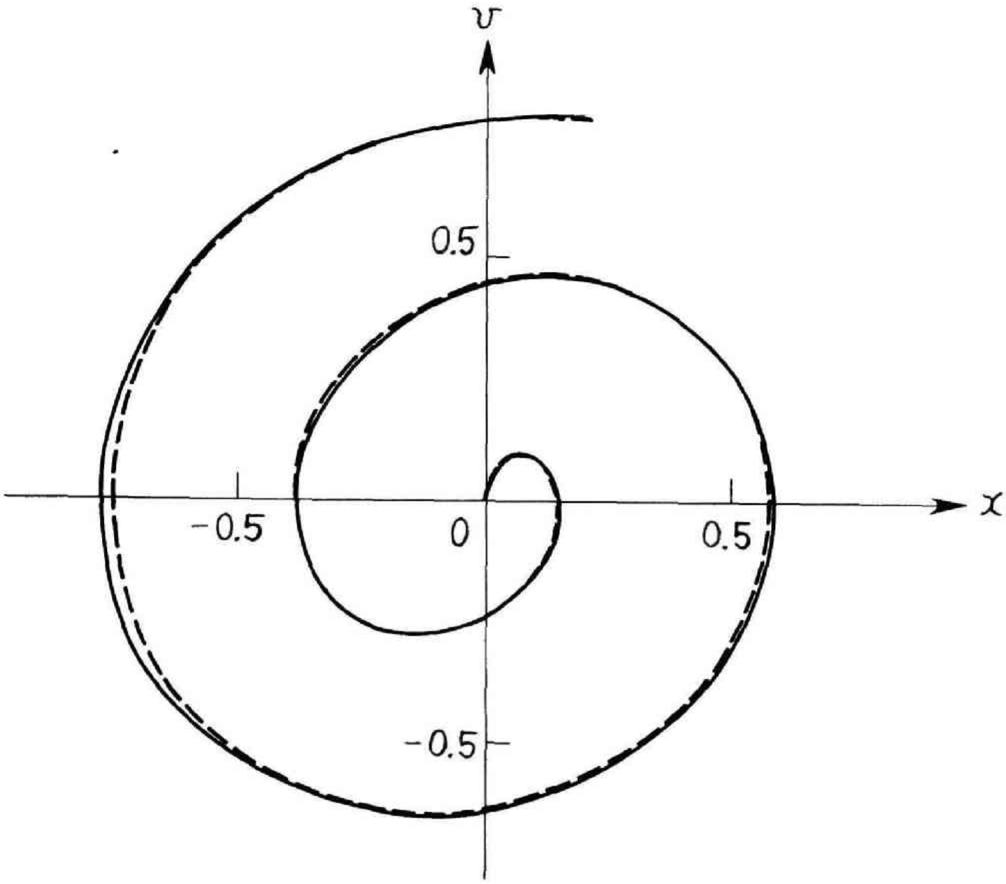

——————— : Curve obtained by the delta method

— — — — — : Curve obtained by the analog-computer analysis

Fig. 2.12 Phase-plane diagram for Eq. (2.34).

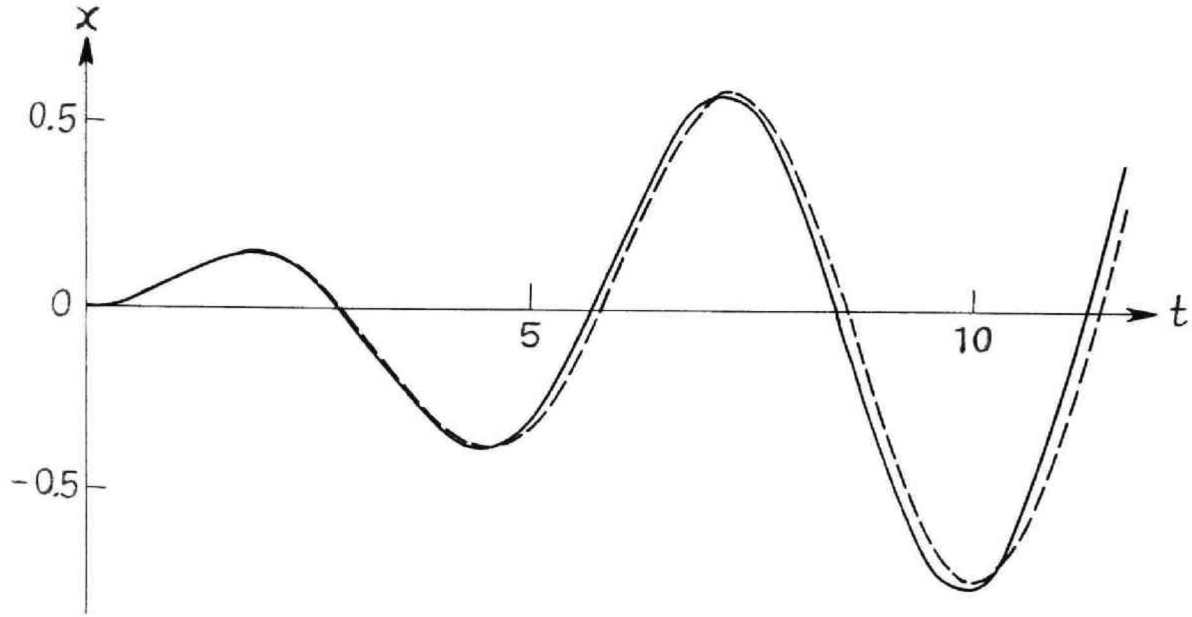

——— : Curve obtained by the delta method

– – – – – : Curve obtained by the analog-computer analysis

Fig. 2.13 Time-response curve converted from the phase-plane trajectory of Fig. 2.12.

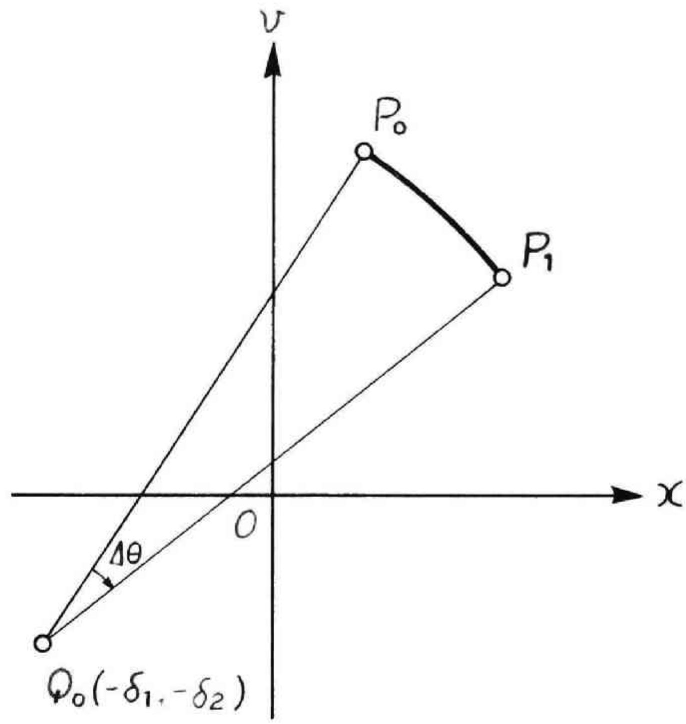

Fig. 2.14 Graphical construction for double-delta method.

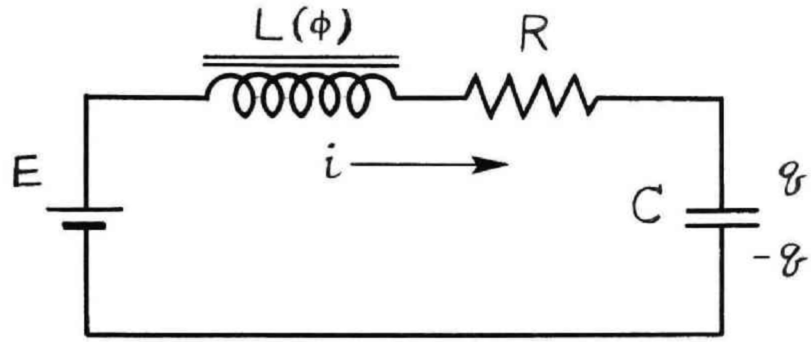

Fig. 2.15 L - C - R series circuit with d-c voltage applied.

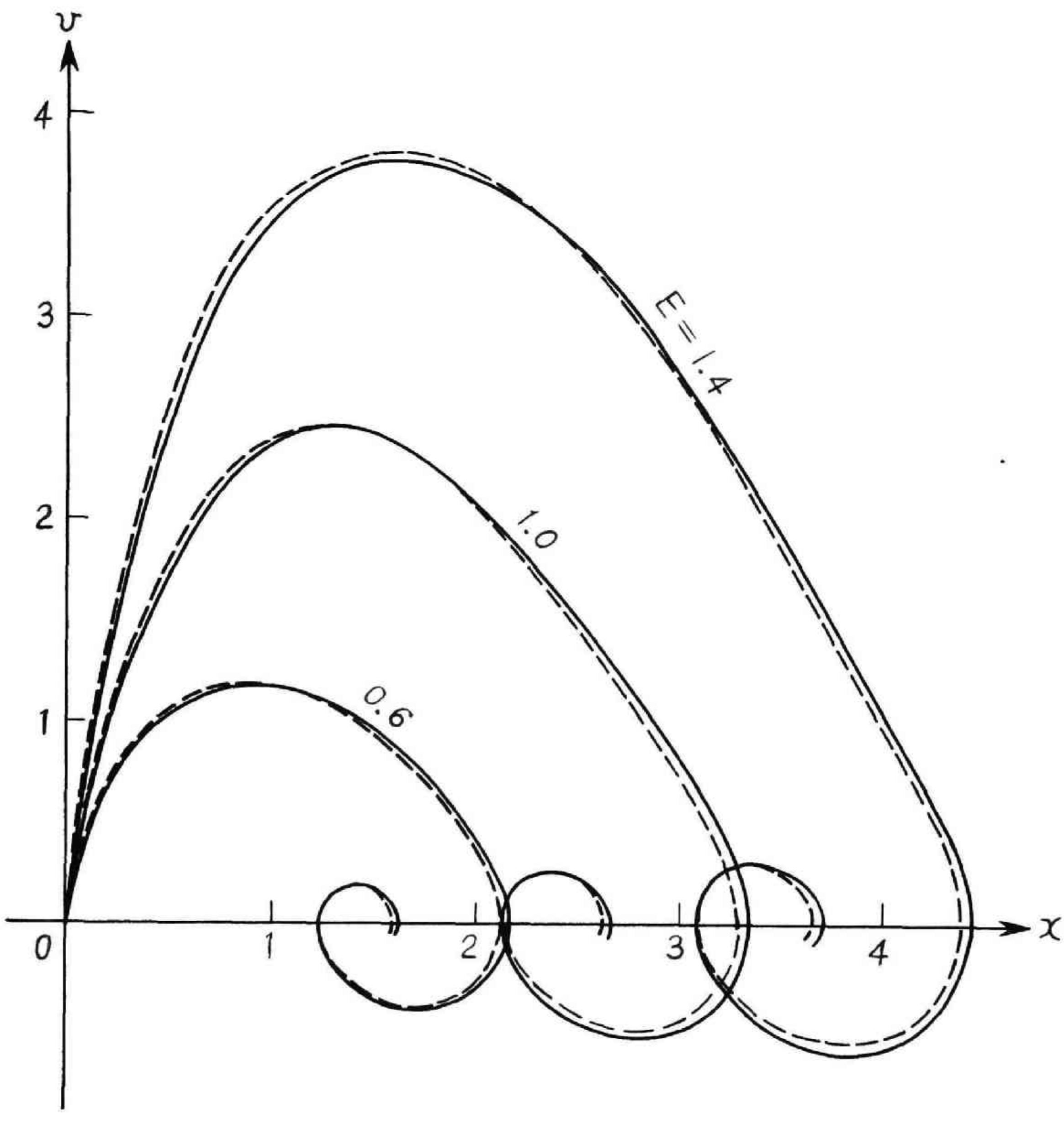

——— : Curves obtained by the delta method

– – – : Curves obtained by the analog-computer analysis

Fig. 2.16 Phase-plane diagram for Eq. (2.42).

CHAPTER III

SUBHARMONIC OSCILLATIONS OF ORDER ONE HALF

3.1 Introduction

Under the action of a periodic force a subharmonic oscillation, whose frequency is a fraction of that of the applied force, may occur in a nonlinear system. In this chapter we shall deal with the system described by

$$\frac{d^2v}{d\tau^2} + k\frac{dv}{d\tau} + f(v) = B\cos 2\tau + B_0, \tag{3.1}$$

where $f(v)$ characterizes the nonlinearity of the system, and subharmonic oscillations of order one half with period 2π will be investigated [8]. The steady-state oscillations have been discussed previously by making use of Hill's equation as a stability criterion [30, pp. 68-80]. An example of the transient state has also been reported [11]. In the present investigation, particular attention is directed toward obtaining the relationship between the initial conditions and the resulting subharmonic responses.

Subharmonic oscillations of order 1/2 may occur also in linear systems if their parameters vary periodically with time [22]. In a system governed by Mathieu's equation

$$\frac{d^2v}{d\tau^2} + [\theta_0 + 2\theta_1 \cos 2\tau]v = 0, \tag{3.2}$$

where the coefficient of v varies periodically with the period π, an oscillation having the period 2π will be excited provided that the parameters θ_0 and θ_1 are appropriately chosen. The term "parametric excitation" is applied to this kind of oscillation [31, pp. 308-313, 355-377]. A practical system designed to approximate (3.2) must contain a nonlinear term which will limit the final amplitude of the oscillation, but this need not alter the mechanism of build-up at low amplitude.

The mechanism of build-up of the 1/2-harmonic oscillation in the nonlinear system described by (3.1) is, to some extent, similar to that in a linear system with parametric excitation. However, subharmonic oscillations in nonlinear systems are usually much more complicated than those in linear systems. Depending on different values of the initial conditions, there may be various types of the steady-state responses even in the same system; under certain special cases of importance, quasi-periodic oscillations may occur where the amplitude of the oscillations vary periodically with time. An investigation on quasi-periodic oscillations will described in Chapter V.

3.2 The Fundamental Equations

From a number of experimental observations and a simplified analysis of subharmonic oscillations [30, pp. 49-51], it is concluded that a certain relationship may exist between the nonlinear characteristic and the order of subharmonics. In order to produce the subharmonic oscillation of order $1/\nu$ with ν odd, for instance, it is to be desired that the power-series expansion of $f(v)$ contains the term v^ν, so that the differential equation takes the form

$$\frac{d^2v}{d\tau^2} + k\frac{dv}{d\tau} + c_1 v + c_3 v^3 + \cdots + c_\nu v^\nu + \cdots = B\cos\nu\tau. \tag{3.3}$$

When ν is even, the term $\operatorname{sign} v\,|v^\nu|$ is considered instead of v^ν. The differential equation is then written as

$$\frac{d^2v}{d\tau^2} + k\frac{dv}{d\tau} + \operatorname{sign} v\,|v^\nu| + \cdots = B\cos\nu\tau + B_0. \tag{3.4}$$

where the unidirectional component B_0 is superposed on the periodic force $B\cos\nu\tau$.* These statements do not necessarily imply that the form of the nonlinearity has to be so chosen in order to produce the desired subharmonic oscillation. Subharmonics with ν even, for instance, may be found when the system is governed by (3.3) [30, p. 80]. However, the oscillation thus produced is stable for only limited ranges of the system parameters.

Since we are concerned with subharmonic oscillations of order 1/2, putting $\nu = 2$ and omitting the dispensable terms in (3.4), we obtain

$$\frac{d^2v}{d\tau^2} + k\frac{dv}{d\tau} + |v|v = B\cos 2\tau + B_0. \tag{3.5}$$

The expression $|v|v$ is, however, difficult to handle analytically, so expanding this into the power series in v and taking only the first two terms for simplicity's sake, we have

$$\frac{d^2v}{d\tau^2} + k\frac{dv}{d\tau} + c_1 v + c_3 v^3 = B\cos 2\tau + B_0. \tag{3.6}$$

The solution of this equation is assumed to take the form

$$v(\tau) = z(\tau) + x(\tau)\sin\tau + y(\tau)\cos\tau + w\cos 2\tau, \tag{3.7}$$

---

* The term B_0 can be eliminated by rendering the nonlinear term a non-odd function.

where only the non-oscillatory term $z(\tau)$, the subharmonic oscillation $x(\tau)\sin\tau + y(\tau)\cos\tau$, and the oscillation having the applied frequency $w\cos 2\tau$, are considered to be of prime importance.* The amplitude w is further approximated by

$$w = \frac{1}{1-\nu^2} B = -\frac{1}{3} B. \tag{3.8}$$

This approximation is legitimate in the case when the nonlinearity is small. However, this is still a permissive approximation even when the departure from linearity is large [30, p. 75].

Substituting (3.7) in (3.6) and equating the coefficients of the terms containing $\cos\tau$ and $\sin\tau$ and of the non-oscillatory term separately to zero, we obtain**

$$\left.\begin{aligned}
\dot{x} &= \tfrac{1}{2}\left[Ay - kx - 3c_3 wyz\right] \equiv X(x,y,z), \\
\dot{y} &= \tfrac{1}{2}\left[-Ax - ky - 3c_3 wxz\right] \equiv Y(x,y,z), \\
B_0 &= c_1 z + c_3\left[\left(\tfrac{3}{2}w^2 + \tfrac{3}{2}r^2 + z^2\right)z - \tfrac{3}{4}w(x^2-y^2)\right] \equiv Z(x,y,z), \\
\text{with}\quad A &= (1-c_1) - c_3\left(\tfrac{3}{2}w^2 + \tfrac{3}{4}r^2 + 3z^2\right), \\
r^2 &= x^2 + y^2,
\end{aligned}\right\} \tag{3.9}$$

---

* It is tacitly assumed that the damping coefficient k is so small that the term containing $\sin 2\tau$ is discarded in (3.7). The non-oscillatory term $z(\tau)$ appears when we deal with the subharmonic oscillation of even order (ν : even).

** Here and throughout this chapter dots over a quantity refer to differentiations with respect to the time τ.

under the assumptions that $x(\tau)$, $y(\tau)$, and $z(\tau)$ are slowly variable functions of τ so that $\ddot{x}$, $\ddot{y}$, and $\ddot{z}$ may be neglected, and that k is a sufficiently small quantity and, therefore, $k\dot{x}$, $k\dot{y}$, and $k\dot{z}$ may also be discarded.

Equations (3.9) play a significant role in the following investigation, since they serve as the fundamental equations in studying the transient state as well as the steady state of the oscillations.

3.3 Subharmonic Oscillations of Order 1/2 in the Steady State

In order to obtain the relationship between the initial conditions and the resulting responses, we have first to investigate the types of the steady-state oscillations under various combinations of the system parameters; and so the 1/2-harmonic oscillations in the steady state will be studied in this section.

3.3.1 Periodic Solutions

We consider the steady state in which $x(\tau)$, $y(\tau)$, and $z(\tau)$ in (3.7) are constant, so that

$$\dot{x} = 0, \quad \dot{y} = 0, \quad \text{and} \quad \dot{z} = 0. \tag{3.10}$$

Substituting these conditions in (3.9), the steady-state components r_0 $(=\sqrt{x_0^2+y_0^2})$ and z_0 of the periodic solution $v(\tau)$ are determined by

$$\left.\begin{aligned} A^2 + k^2 = (3c_3 w z_0)^2, \end{aligned}\right\} \tag{3.11}$$

$$c_1 Z_0 + c_3\left[\left(\frac{3}{2}r_0^2 + \frac{3}{2}\mu^2 + Z_0^2\right)Z_0 + \frac{Ar_0^2}{4c_3 Z_0}\right] = B_0,$$

and the components x_0, y_0, of the amplitude r_0 are found to be

$$\left.\begin{aligned} x_0 &= r_0\cos\theta, \qquad r_0\cos(\theta+\pi), \\ y_0 &= r_0\sin\theta. \qquad r_0\sin(\theta+\pi), \end{aligned}\right\} \tag{3.12}$$

where

$$\cos 2\theta = -\frac{A}{3c_3 w Z_0}, \qquad \sin 2\theta = -\frac{k}{3c_3 w Z_0}.$$

We see from (3.11) and (3.12) that, if the sign of B_0 is reversed, the sign of Z_0 and consequently those of $\cos 2\theta$ and $\sin 2\theta$ are also reversed, resulting in the shift in θ by $\pi/2$ radians. Hence, by reversing the sign of B_0, the components x_0, y_0 are given by

$$\left.\begin{aligned} x_0 &= r_0\cos(\theta+\pi/2), \qquad r_0\cos(\theta+3\pi/2), \\ y_0 &= r_0\sin(\theta+\pi/2), \qquad r_0\sin(\theta+3\pi/2), \end{aligned}\right\} \tag{3.13}$$

When $B_0 = 0$ in particular, four types of the 1/2-harmonic oscillations exist, each differing in phase by $\pi/2$ radians from the other.

3.3.2 Stability Investigation

In order to investigate the stability of the periodic solutions as given by (3.11), (3.12), and (3.13), we consider sufficiently small variations ξ, η, and ζ from the equilibrium state defined by

$$\xi = x - x_0, \quad \eta = y - y_0, \quad \zeta = z - Z_0. \tag{3.14}$$

Then, if these variations ξ, η, and ζ tend to zero with increasing τ, the solutions are stable. Substituting (3.14) in (3.9), we obtain

$$\left.\begin{aligned}
\dot{\xi} &= a_{11}\xi + a_{12}\eta + a_{13}\zeta, \\
\dot{\eta} &= a_{21}\xi + a_{22}\eta + a_{23}\zeta, \\
0 &= a_{31}\xi + a_{32}\eta + a_{33}\zeta,
\end{aligned}\right\}$$

with

$$\left.\begin{aligned}
a_{11} &= \left(\frac{\partial X}{\partial x}\right)_0 = -\frac{1}{2}\left[\frac{3}{2}c_3 x_0 y_0 + k\right], \\
a_{12} &= \left(\frac{\partial X}{\partial y}\right)_0 = \frac{1}{2}\left[A - \frac{3}{2}c_3 y_0^2 - 3c_3 w z_0\right], \\
a_{13} &= \left(\frac{\partial X}{\partial z}\right)_0 = -\frac{3}{2}c_3 y_0\left[w + 2z_0\right], \\
a_{21} &= \left(\frac{\partial Y}{\partial x}\right)_0 = -\frac{1}{2}\left[A - \frac{3}{2}c_3 x_0^2 + 3c_3 w z_0\right], \\
a_{22} &= \left(\frac{\partial Y}{\partial y}\right)_0 = \frac{1}{2}\left[\frac{3}{2}c_3 x_0 y_0 - k\right], \\
a_{23} &= \left(\frac{\partial Y}{\partial z}\right)_0 = \frac{3}{2}c_3 x_0\left[-w + 2z_0\right], \\
a_{31} &= \left(\frac{\partial Z}{\partial x}\right)_0 = \frac{3}{2}c_3 x_0\left[-w + 2z_0\right], \\
a_{32} &= \left(\frac{\partial Z}{\partial y}\right)_0 = \frac{3}{2}c_3 y_0\left[w + 2z_0\right], \\
a_{33} &= \left(\frac{\partial Z}{\partial z}\right)_0 = c_1 + c_3\left[\frac{3}{2}r_0^2 + \frac{3}{2}w^2 + 3z_0\right],
\end{aligned}\right\} \tag{3.15}$$

where $\left(\frac{\partial X}{\partial x}\right)_0, \ldots, \left(\frac{\partial Z}{\partial z}\right)_0$ stand for $\frac{\partial X}{\partial x}, \ldots, \frac{\partial Z}{\partial z}$ at $x = x_0$, $y = y_0$ and $z = z_0$. The characteristic equation of the system (3.15) is

$$\begin{vmatrix} a_{11}-\lambda & a_{12} & a_{13} \\ a_{21} & a_{22}-\lambda & a_{23} \\ a_{31} & a_{32} & a_{33} \end{vmatrix} = 0, \tag{3.16}$$

or

$$a_{33}\lambda^2 - \left\{ \begin{vmatrix} a_{11} & a_{13} \\ a_{31} & a_{33} \end{vmatrix} + \begin{vmatrix} a_{22} & a_{23} \\ a_{32} & a_{33} \end{vmatrix} \right\} \lambda + \begin{vmatrix} a_{11} & a_{12} & a_{13} \\ a_{21} & a_{22} & a_{23} \\ a_{31} & a_{32} & a_{33} \end{vmatrix} = 0. \tag{3.17}$$

By making use of the Routh-Hurwitz's criterion, the system (3.15) and consequently the periodic solutions are stable provided that

$$\left.\begin{aligned} & a_{33} > 0, \\ & \begin{vmatrix} a_{11} & a_{13} \\ a_{31} & a_{33} \end{vmatrix} + \begin{vmatrix} a_{22} & a_{23} \\ a_{32} & a_{33} \end{vmatrix} < 0, \\ & \begin{vmatrix} a_{11} & a_{12} & a_{13} \\ a_{21} & a_{22} & a_{23} \\ a_{31} & a_{32} & a_{33} \end{vmatrix} \equiv \Delta > 0, \end{aligned}\right\} \tag{3.18}$$

The first and the second conditions of (3.18) are fulfilled from the outset, because, by (3.15),

$$\left.\begin{aligned} & a_{33} = c_1 + c_3\left[\tfrac{3}{2} r_0^2 + \tfrac{3}{2} w^2 + 3z_0^2\right] > 0, \\ & \begin{vmatrix} a_{11} & a_{13} \\ a_{31} & a_{33} \end{vmatrix} + \begin{vmatrix} a_{22} & a_{23} \\ a_{32} & a_{33} \end{vmatrix} = -k\left\{c_1 + c_3\left[\tfrac{3}{2} r_0^2 + \tfrac{3}{2} w^2 + 3z_0^2\right]\right\} < 0. \end{aligned}\right\} \tag{3.19}$$

Hence the third inequality $\Delta > 0$ is an essential condition for the stability of the periodic solutions. Substitution of (3.15) in the determinant Δ leads to a lengthy expression; however, by virtue of (3.11) and (3.12), the stability condition ultimately leads to

$$\Delta = 6c_3 r_0^2 z_0 \left(1 - c_1 - \frac{3}{4} c_3 r_0^2 - 3c_3 z_0^2\right) \frac{dB_0}{dr_0^2} > 0, \tag{3.20}$$

It is, therefore, clear that the characteristic curve (r_0 versus B_0) has vertical tangents at the stability limits $dB_0/dr_0^2=0$.

3.3.3 Numerical Examples

In order to present a more concrete description of the 1/2-harmonic oscillations, some representative examples will be given in what follows. The nonlinearity in (3.6) is fixed by

$$c_1 v + c_3 v^3 = 0.3 v + 0.7 v^3. \tag{3.21}$$

The constants c_1, c_3 are so chosen that the difference between $|v|v$ and $c_1 v + c_3 v^3$ is small enough for the interval of v in which the 1/2-harmonics occur. These characteristics are compared in Fig. 3.1.

By making use of (3.11), the amplitude characteristics (r_0 versus B_0) are computed for several values of k and B, and illustrated in Fig. 3.2. The stability of the periodic solutions is investigated by (3.20), and the result is shown in the figure by distinguishing the characteristic curves with full lines and dotted lines corresponding to the stable and the unstable states respectively. It will be noticed that, since $x = 0$ and $y = 0$ satisfy (3.9), $v(\tau) = z_0 + w\cos 2\tau$ is another periodic solution. We see in Fig. 3.2 that various types of the 1/2-harmonic oscillations exist according to the different values of the system parameters. They are as follows:

Case 1 - $k = 0.20$, $B = 1.50$, and $B_0 = 0.50$ [Fig. 3.2(b)]

There are two 1/2-harmonic oscillations, differing only in phase by π radians. The periodic solution without 1/2-harmonic (i.e., $r_0 = 0$) is readily found to be unstable. Therefore all initial conditions lead to the 1/2-harmonic response.

Case 2 - $k = 0.20$, $B = 0.60$, and $B_0 = 0.40$ [Fig. 3.2(a)].

As regards the 1/2-harmonic oscillations, the situation is the same as in Case 1. However, the periodic solution with $r_0 = 0$ is stable; therefore the 1/2-harmonic oscillation occurs only when the initial condition is properly chosen.

Case 3 - $k = 0.20$, $B = 1.50$, and $B_0 = 0.25$ [Fig. 3.2(b)].

There are two different values for r_0 ; and, for each of these, two 1/2-harmonic oscillations exist, differing in phase by π radians. The periodic solution with $r_0 = 0$ is unstable; therefore all initial conditions lead to the 1/2-harmonic response.

Case 4 - $k = 0.10$, $B = 2.00$, and $B_0 = 0$ [Fig. 3.2(c)].

There are, as mentioned in Section 3.3.1, four 1/2-harmonic oscillations, each differing in phase by $\pi/2$ radians from the other. The periodic solution with $r_0 = 0$ is stable; therefore the 1/2-harmonic oscillation occurs only when the initial condition is properly chosen.

Case 5 - $k = 0.01$, $B = 1.80$, and $B_0 = 0.15$ [Fig. 3.2(d)].

There are three different values for r_0 ; and, for each of these, two 1/2-harmonic oscillations exist, differing in phase by π radians. The periodic solution with $r_0 = 0$ is unstable; therefore all initial conditions lead to the 1/2-harmonic response.

3.4 Subharmonic Oscillations of Order 1/2 in the Transient State

3.4.1 Phase-Plane Analysis

As mentioned before, our object is to study the solution of (3.6) in the transient state, which, with the lapse of time, ultimately yields the periodic solution. For this purpose it is useful to investigate the integral curves of the following equations derived from (3.9), i.e.,

$$\left.\begin{aligned} &\frac{dy}{dx} = \frac{Y(x,y,z)}{X(x,y,z)}\,, \\ \text{with} \qquad & \\ &Z(x,y,z) = B_0. \end{aligned}\right\} \qquad (3.22)$$

One will readily see from the third equation of (3.9) that Z is uniquely determined once the values of X and y are given. Since the time τ does not appear explicitly in (3.22), we can draw the integral curves in the x, y plane. The periodic solutions satisfy the conditions (3.10) and are, therefore, expressed by the singular points of (3.22), i.e., by the points at which $X(x,y,z)$ and $Y(x,y,z)$ both vanish.

Now suppose that an initial condition for the solution of (3.6) is prescribed by $v(0)$ and $\dot{v}(0)$; then $x(0)$, $y(0)$, and $z(0)$ corresponding to this initial condition are determined by (3.7) and (3.9), i.e.,

$$\left.\begin{aligned} v(0) &= z(0) + y(0) + w, \\ \dot{v}(0) &= \dot{z}(0) + x(0) + \dot{y}(0) \cong x(0), \\ c_1 Z(0) &= c_3\left\{\left[\tfrac{3}{2}w^2 + \tfrac{3}{2}r^2(0) + z^2(0)\right]z(0) - \tfrac{3}{4}w\left[x^2(0) - y^2(0)\right]\right\} = B_0. \end{aligned}\right\} \quad (3.23)$$

An initial condition is thus prescribed by a point whose coordinates are given by $x(0)$ and $y(0)$ in the x,y plane. Then the representative point $x(\tau)$, $y(\tau)$ moves, with increasing τ, along the integral curve which starts from the initial point $x(0)$, $y(0)$, and tends ultimately to a stable singular point.* Hence the transient-state solutions are correlated with the integral curves of (3.22), and the time response of $v(\tau)$ in the transient state is obtained by the line integral

$$\tau = \int \frac{ds}{\sqrt{X^2(x,y,z) + Y^2(x,y,z)}}, \quad ds = \sqrt{(dx)^2 + (dy)^2}, \tag{3.24}$$

where ds is the line element along the integral curve.

The character of the singular point reveals the behavior of the oscillation in the vicinity of the equilibrium state and consequently determines the stability of the periodic solution. The stable solution is correlated with the stable singular point such that a point $x(\tau)$, $y(\tau)$ on the neighboring integral curves tends to it with increasing τ.

The types of singular points are classified according to the roots λ's of the characteristic equation (3.17). By use of (3.19), the discriminant D of (3.17) becomes

$$D \equiv \left\{ \begin{vmatrix} a_{11} & a_{13} \\ a_{31} & a_{33} \end{vmatrix} + \begin{vmatrix} a_{22} & a_{23} \\ a_{32} & a_{33} \end{vmatrix} \right\}^2 - 4 a_{33} \Delta = a_{33}(a_{33} k^2 - 4\Delta). \tag{3.25}$$

It is also noted, from (3.19), that

---

* If the integral curve leads to a limit cycle with increasing τ, the representative point $x(\tau)$, $y(\tau)$ moves along the limit cycle repeatedly, so that the amplitude and the phase of the oscillation keep on varying periodically, resulting in a quasi-periodic oscillation. However, it will be verified without difficulty that the integral curves of (3.22) have no limit cycle provided that $X(x,y,z)$ and $Y(x,y,z)$ are given by (3.9).

$$\begin{vmatrix} a_{11} & a_{13} \\ a_{31} & a_{33} \end{vmatrix} + \begin{vmatrix} a_{22} & a_{23} \\ a_{32} & a_{33} \end{vmatrix} < 0, \quad \text{and} \quad a_{33} > 0. \tag{3.26}$$

Hence the singular points of the system (3.22) will be classified as follows:

(1) If $D \geqq 0$, and $\Delta > 0$, the characteristic roots λ are both real and of the negative sign, so that the singularity is a stable node.

(2) If $D > 0$, and $\Delta < 0$, the characteristic roots λ are real but of opposite signs, so that the singularity is a saddle point which is intrinsically unstable.

(3) If $D < 0$, the characteristic roots λ are conjugate complex, so that the singularity is a stable spiral.

3.4.2 Numerical Examples

Since the transient state of the oscillation is correlated with the integral curve of (3.22), it will be useful and illustrating to show the geometrical configuration of integral curves for representative cases.

Case 1 - We first consider the example corresponding to Case 1 in Section 3.3.3, where the system parameters are given by

$$k = 0.20, \qquad B = 1.50, \qquad \text{and} \qquad B_0 = 0.50.$$

As explained in Section 3.3.3, there are two 1/2-harmonic oscillations having the same amplitude but of opposite phases. The integral curves for this particular case are plotted in Fig. 3.3. As expected, there are three singularities 1, 2, and 3, the details of which are listed in Table 3.1.

Table 3.1. Singular Points of Fig. 3.3

Singular Point	x_o	y_o	z_o	λ_1, λ_2	μ_1, μ_2 *	Classification
1	0.204	0.900	0.441	$-0.100 \pm 0.370i$		Stable spiral
2	-0.204	-0.900	0.441	$-0.100 \pm 0.370i$		Stable spiral
3	0	0	0.603	0.171, -0.371	1.806, -1.806	Saddle (unstable)

* μ_1, μ_2 are the tangential directions of the integral curves at the singular points.

By (3.9) a representative point $x(\tau), y(\tau)$ moves, with increasing τ, along the integral curve in the direction of the arrows and tends ultimately to one of the stable singularities 1 and 2. Since the distance between the singular point and the origin shows the amplitude r_0, the singularities 1 and 2 represent the 1/2-harmonic oscillations having the same amplitude but of opposite phases. The singularity 3, i.e., the origin is a saddle point which is intrinsically unstable; the corresponding periodic state cannot be sustained, because any slight deviation from the saddle point will lead the oscillation to one of the stable spirals. The separatrices, i.e., the integral curves which enter the saddle point, divide the whole plane into two regions as indicated with different hatches. All integral curves in one of these regions tend to the stable singularity which is contained in that region. Hence the relationship existing between the initial condition $x(0), y(0)$ and the resulting 1/2-harmonic oscillation will be made clear. Since the origin is an unstable singularity, all initial conditions lead to the 1/2 harmonic response.

Case 2 - We consider the second example corresponding to Case 2 in Section 3.3.3, where the system parameters are given by

$$k = 0.20, \qquad B = 0.60, \quad \text{and} \quad B_0 = 0.40.$$

As explained in Section 3.3.3, there are, as in Case 1, two 1/2-harmonic oscillations. The integral curves for this particular case are plotted in Fig. 3.4. As expected, there are five singularities, 1 to 5, the details of which are listed in Table 3.2.

Table 3.2. Singular Points of Fig. 3.4

Singular Point	x_0	y_0	z_0	λ_1, λ_2	μ_1, μ_2 *	Classification
1	0.410	0.384	0.477	$-0.100 \pm 0.183i$		Stable spiral
2	-0.410	-0.384	0.477	$-0.100 \pm 0.183i$		Stable spiral
3	0.088	0.186	0.617	0.014,-0.214	1.579,-2.016	Saddle (unstable)
4	-0.088	-0.186	0.617	0.014,-0.214	1.579,-2.016	Saddle (unstable)
5	0	0	0.638	-0.009,-0.191	2.555,-2.555	Stable node

* μ_1, μ_2 are the tangential directions of the integral curves at the singular points.

In Fig. 3.4 we see that the singular points 1 and 2 represent the stable states of the 1/2-harmonic oscillations which have the same amplitude but differ in phase by π radians, while the singular points 3 and 4 represent the unstable states. Contrary to Case 1, the singular point 5, i.e., the origin is a stable spiral. Therefore the conclusion follows that any oscillation starting from a point (which prescribes an initial condition) in the shaded regions leads ultimately to one of the singularities 1 and 2, resulting in the 1/2-harmonic response; and that any oscillation which starts from the unshaded region leads ultimately to the origin, resulting in no 1/2-harmonic response.

Case 3 - The third example corresponds to Case 3 in Section 3.3.3, where the system parameters are given by

$$k = 0.20, \qquad B = 1.50, \qquad \text{and} \qquad B_0 = 0.25.$$

As explained in Section 3.3.3, there are two kinds of the 1/2-harmonic oscillations with different amplitudes. The integral curves for this particular case are plotted in Fig. 3.5. There are seven singularities, 1 to 7, the details of which are listed in Table 3.3.

Table 3.3. Singular Points of Fig. 3.5

Singular Point	x_0	y_0	z_0	λ_1, λ_2	μ_1, μ_2 *	Classification
1	0.376	0.883	0.265	$-0.100 \pm 0.090i$		Stable spiral
2	-0.376	-0.883	0.265	$-0.100 \pm 0.090i$		Stable spiral
3	0.586	0.586	0.190	0.098, -0.298	0.156, 5.322	Saddle (unstable)
4	-0.586	-0.586	0.190	0.098, -0.298	0.156, 5.322	Saddle (unstable)
5	0.407	0.176	0.263	$-0.100 \pm 0.055i$		Stable spiral
6	-0.407	-0.176	0.263	$-0.100 \pm 0.055i$		Stable spiral

7	0	0	0.375	0.086,-0.286	0.696,-0.696	Saddle (unstable)

* μ_1, μ_2 are the tangential directions of the integral curves at the singular points.

In Fig. 3.5 we see that the singular points 1 and 2 represent the stable states of the 1/2-harmonic oscillations having the same amplitude but of opposite phases; the same is true for the singularities 5 and 6. The singularities 3, 4, and 7 are saddle points. The separatrices divide the whole plane into four regions as indicated with different hatches. Since the origin is an unstable singularity like as in Case 1, all initial conditions lead to the 1/2-harmonic response.

Thus far, the behavior of the nonoscillatory component $Z(\tau)$ has not been illustrated. Since $Z(\tau)$ also varies as the values of $x(\tau)$ and $y(\tau)$, the integral curves are really on the surface which is determined by the third equation of (3.9). Fig. 3.6 shows the geometrical configuration of the integral curves in the x, y, z space. Their projections on the x, y plane are, as a matter of course, the same as the integral curves in Fig. 3.5.

By making use of (3.23), the regions of initial conditions and the stable singularities in Fig. 3.5 are reproduced on the $v(0)$, $\dot{v}(0)$ plane as illustrated in Fig. 3.7. Since, in the steady state,

$$\left.\begin{aligned} v(\tau) &= x_0 \sin\tau + y_0 \cos\tau + w\cos 2\tau + z_0, \\ \dot{v}(\tau) &= x_0 \cos\tau - y_0 \sin\tau - 2w\sin 2\tau, \end{aligned}\right\} \tag{3.27}$$

the periodic solutions correlated with the stable singularities 1, 2 and 5, 6 in Fig. 3.5 are shown by the closed curves I and II, respectively, where the coordinates are to be considered $v(\tau)$ and $\dot{v}(\tau)$ instead of $v(0)$ and $\dot{v}(0)$. The time required for a point $v(\tau)$, $\dot{v}(\tau)$ to complete one revolution along the curve I or II is 2π, or twice the period of the external force. A trajectory which starts from an initial point $v(0)$, $\dot{v}(0)$ in one of these regions, e.g., the region containing the point 1 (or 2), will tend to the closed curve I; the representative point $v(\tau)$, $\dot{v}(\tau)$ in the steady state will then pass through the point 1 (or 2) when $\tau = 2n\pi$, n being a sufficiently large positive integer. Similarly, initial conditions in the region containing the point 5 (or 6) will lead the oscillation to the steady state represented by the closed curve II, and the representative point $v(\tau)$, $\dot{v}(\tau)$ in the steady state will pass through the point 5 (or 6) when $\tau = 2n\pi$.

Case 4 - The fourth example corresponds to Case 4 in Section 3.3.3, where the system parameters are given by

$$k = 0.10, \qquad B = 2.00, \qquad \text{and} \qquad B_0 = 0.$$

As explained in Section 3.3.3, there are four 1/2-harmonic oscillations, each having the same amplitude but differing in phase by $\pi/2$ radians from the other. The integral curves for this particular case are plotted in Fig. 3.8. There are nine singularities, 1 to 9, the details of which are listed in Table 3.4.

Table 3.4. Singular Points of Fig. 3.8

Singular Point	x_0	y_0	z_0	λ_1, λ_2	μ_1, μ_2*	Classification
1	0.229	0.789	0.134	$-0.050 \pm 0.140i$		Stable spiral

2	-0.229	-0.789	0.134	$-0.050 \pm 0.140i$		Stable spiral
3	-0.789	0.229	-0.134	$-0.050 \pm 0.140i$		Stable spiral
4	0.789	-0.229	-0.134	$-0.050 \pm 0.140i$		Stable spiral
5	0.320	0.683	0.093	0.095, -0.195	0.301, 2.434	Saddle (unstable)
6	-0.320	-0.683	0.093	0.095, -0.195	0.301, 2.434	Saddle (unstable)
7	-0.683	0.320	-0.093	0.095, -0.195	-3.322, -0.411	Saddle (unstable)
8	0.683	-0.320	-0.093	0.095, -0.195	-3.322, -0.411	Saddle (unstable)
9	0	0	0	$-0.050 \pm 0.117i$		Stable spiral

* μ_1, μ_2 are the tangential directions of the integral curves at the singular points.

In Fig. 3.8 we see that the singular points 1, 2, 3, and 4 represent the stable states of the 1/2-harmonic oscillations, and that they are equidistant and equiangular about the origin. The angular distance between the adjacent singular points corresponds to one-half cycle, of the external force. The singular points 5, 6, 7, and 8 are saddle points; therefore the corresponding periodic solutions are unstable. Like as in Case 2, the singular point 9, i.e., the origion is a stable spiral. Therefore any oscillation starting from a point in the shaded regions leads ultimately to one of the singularities 1, 2, 3, and 4, resulting in the 1/2-harmonic response; however any oscillation which starts from the unshaded region leads ultimately to the origin, resulting in no 1/2-harmonic response. By making use of the third equation of (3.9), the integral curves in the x, y, z space are calculated and illustrated in Fig. 3.9.

The regions of initial conditions and the stable singularities in Fig.

3.8 are reproduced on the $v(0)$, $\dot{v}(0)$ plane as illustrated in Fig. 3.10. The periodic solutions correlated with the singularities 1, 2 and 3, 4 are also shown by the closed curves I and II respectively, where the coordinates are $v(\tau)$, $\dot{v}(\tau)$ instead of $v(0)$, $\dot{v}(0)$. Since these oscillations are the 1/2-harmonics, the time required for a point $v(\tau)$, $\dot{v}(\tau)$ to complete one revolution along the curve I or II is 2π. The singularity 9, i.e., the origin of Fig. 3.8 is correlated with the oscillation without 1/2-harmonic response; the periodic solution corresponding to it is represented by the closed curve III. The time required for a point $v(\tau)$, $\dot{v}(\tau)$ to complete one revolution along the curve III is π, or equal to the period of the external force.

Case 5 - The fifth example corresponds to Case 5 in Section 3.3.3, where the system parameters are given by

$$k = 0.01, \qquad B = 1.80, \qquad \text{and} \qquad B_0 = 0.15.$$

As explained in Section 3.3.3, there are three kinds of the 1/2-harmonic oscillations with different amplitudes. The integral curves for this particular case are plotted in Fig. 3.11. There are eleven singularities, 1 to 11, the details of which are listed in Table 3.5.

Table 3.5. Singular Points of Fig. 3.11

Singular Point	x_0	y_0	z_0	λ_1, λ_2	μ_1, μ_2 *	Classification
1	0.000	0.984	0.261	$-0.005 \pm 0.407i$		Stable spiral
2	-0.000	-0.984	0.261	$-0.005 \pm 0.407i$		Stable spiral

3	-0.850	0.066	-0.053	-0.005 ± 0.238i		Stable spiral
4	0.850	-0.066	-0.053	-0.005 ± 0.238i		Stable spital
5	0.705	0.284	0.012	0.161, -0.171	-0.143, -93.44	Saddle (unstable)
6	-0.705	-0.284	0.012	0.161, -0.171	-0.143, -93.44	Saddle (unstable)
7	-0.769	0.225	-0.015	0.121, -0.131	1.134, 19.60	Saddle (unstable)
8	0.769	-0.225	-0.015	0.121, -0.131	1.134, 19.60	Saddle (unstable)
9	0.209	0.005	0.182	-0.005 ± 0.142i		Stable spiral
10	-0.209	-0.005	0.182	-0.005 ± 0.142i		Stable spiral
11	0	0	0.211	0.063, -0.073		Saddle (unstable)

* μ_1, μ_2 are the tangential directions of the integral curves at the singular points.

In Fig. 3.11 we see that the singular points 1 and 2 represent the stable states of the 1/2-harmonic oscillations having the same amplitude but of opposite phases; the same is true for the pairs of the singularities 3, 4 and 9, 10. The singularities 5, 6, 7, 8, and 11 are saddle points. The separatrices divide the whole plane into six regions as illustrated with different hatches. Since the origin is an unstable singularity, like as in Case 1 and 3, all initial conditions lead to the 1/2-harmonic response.

3.5 Analog-Computer Analysis

3.5.1 The Fundamental Equation and the Computer Block Diagram

As mentioned in Section 3.2, the fundamental equation for subharmonic oscillations of order 1/2 is considered in the form

$$\frac{d^2v}{d\tau^2}+k\frac{dv}{d\tau}+|v|v=B\cos\tau+B_0. \tag{3.28}$$

The phase trajectories on the $v(\tau)$, $\dot{v}(\tau)$ plane and the time-response curves (v vs τ) will be sought and compared with foregoing analysis.

Fig. 3.12 shows the schematic diagram of the computer connection. The symbols in the figure follow the conventional notation.* The nonlinear characteristic $|v|v$ is readily obtained by the servomultiplier as indicated in the figure.

3.5.2 Computer Solutions

Among the numerical examples in Section 3.4.2, two cases will be investigated by the analog computer.

Case 1 - $k = 0.20$, $B = 1.50$, and $B_0 = 0.25$.

Fig. 3.13 is obtained by the following procedure. A point $v(0)$, $\dot{v}(0)$, i.e., one of the initial conditions, is first prescribed on the $v(\tau)$, $\dot{v}(\tau)$ plane of the computer recorder. Then the solution curve, i.e., the trajectory of the point $v(\tau)$, $\dot{v}(\tau)$ which starts from the initial point $v(0)$, $\dot{v}(0)$ will ultimately tend to one of the closed curves I and II. By repeating this process for different values of the initial conditions, the whole plane is divided into four regions; the region containing the point m (= 1, 2, 5, or 6) is so determined that the representative point $v(\tau)$, $\dot{v}(\tau)$ which has started from this region passes through the point m when $\tau = 2n\pi$, n being

---

* The integrating amplifiers in the block diagram integrate the inputs with respect to the machine time t (in seconds), which is, in this particular case, two times the dimensionless time τ , i.e., $t = 2\tau$.

a sufficiently large positive integer.*

Fig. 3.13 shows a satisfactory agreement with the theoretical result as given in Fig. 3.7. Therefore the assumptions used in deriving (3.9) may be accepted. The time-response curves of the 1/2-harmonic oscillations are shown in Fig. 3.14. The calculated curves in Fig. 3.14(a) are obtained by substituting the steady-state values x_0, y_0, and z_0 of Table 3.3 into (3.27). The curves in Fig. 3.14(b) are obtained by making use of the analog computer. As indicated in the figure, there are four 1/2-harmonics having two different waveforms, and for each of these, two oscillations differing in phase by π radians.

Case 2 - $k = 0.10$, $B = 2.00$, and $B_0 = 0$.

Proceeding analogously to a consideration of the first case, we obtain Fig. 3.15, which again shows an agreement with the theoretical result as given in Fig. 3.10. Contrary to the preceding case, an initial condition prescribed in the unshaded region results in the oscillation without 1/2-harmonic. The time-response curves are illustrated in Fig. 3.16. Curves 1, 2, 3, and 4 show the 1/2-harmonic oscillations; curve 9, the oscillation without 1/2-harmonic response.

3.6 Conclusion

Subharmonic oscillations of order 1/2 have been investigated. The differential equation which governs the system takes the form

---

* A cycle indicator which counts every two cycles of the external force $B\cos 2\tau$ is used for this purpose.

$$\frac{d^2v}{d\tau^2} + k\frac{dv}{d\tau} + f(v) = B\cos 2\tau + B_0,$$

where the nonlinear term $f(v)$ is given by

$$f(v) = |v|v \qquad \text{for analog-computer analysis,}$$

$$\cong c_1 v + c_3 v^3 \quad \text{for phase-plane analysis.}$$

Particular attention has been directed to the relationship existing between the initial conditions and the resulting 1/2-harmonic responses, and the examples illustrating this relationship have been given. In addition, Fig. 3.17 shows a list of representative patterns of the initial conditions which lead to the 1/2-harmonic responses. These patterns are explained as follows:

(a) All initial conditions lead to one of the two 1/2-harmonic oscillations having the same amplitude but differing in phase by π radians.

(b) Initial conditions lead either to the 1/2-harmonic response or to the oscillation without 1/2-harmonic. The 1/2-harmonic oscillations have the same amplitude but differ in phase by π radians.

(c) All initial conditions lead to the 1/2-harmonic response. The 1/2-harmonics have two different amplitudes, and, for each of these, two oscillations exist, differing in phase by π radians.

(d) Initial conditions lead either to the 1/2-harmonic response or to the oscillation without 1/2-harmonic. The 1/2-harmonic oscillations have the same amplitude, but each differs in phase by $\pi/2$ radians from the other.

(e) All initial conditions lead to the 1/2-harmonic response. The 1/2-

harmonics have three different amplitudes, and, for each of these, two oscillations exist, differing in phase by π radians.

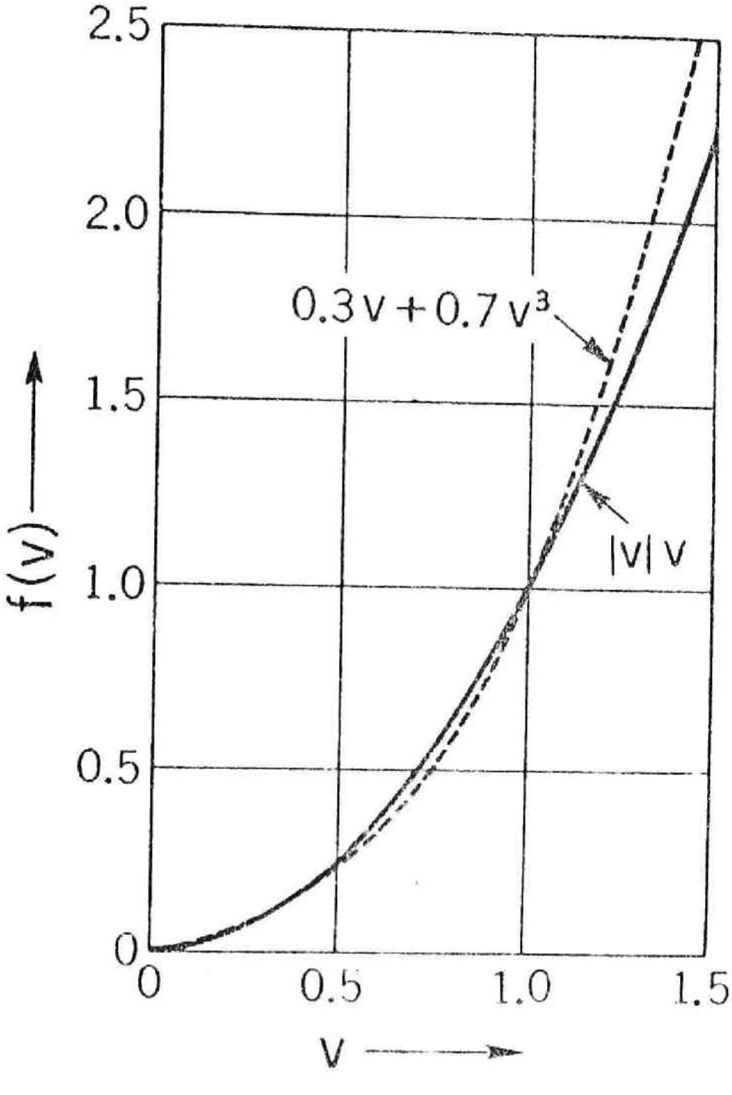

Fig. 3.1 Nonlinear characteristic $|v|v$ and its approximation by power-series expansion.

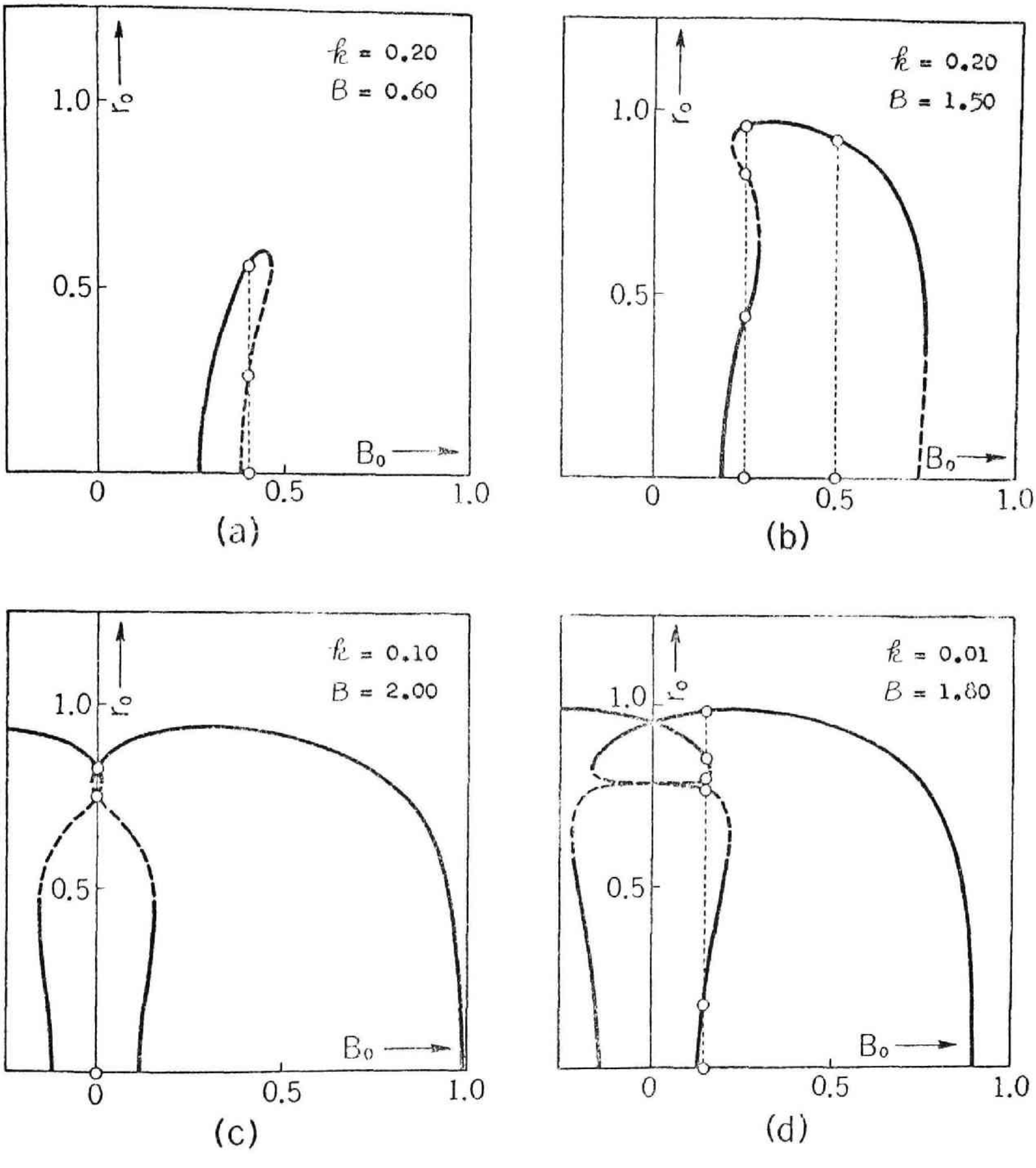

Fig. 3.2 Amplitude characteristics of 1/2-harmonic oscillations.

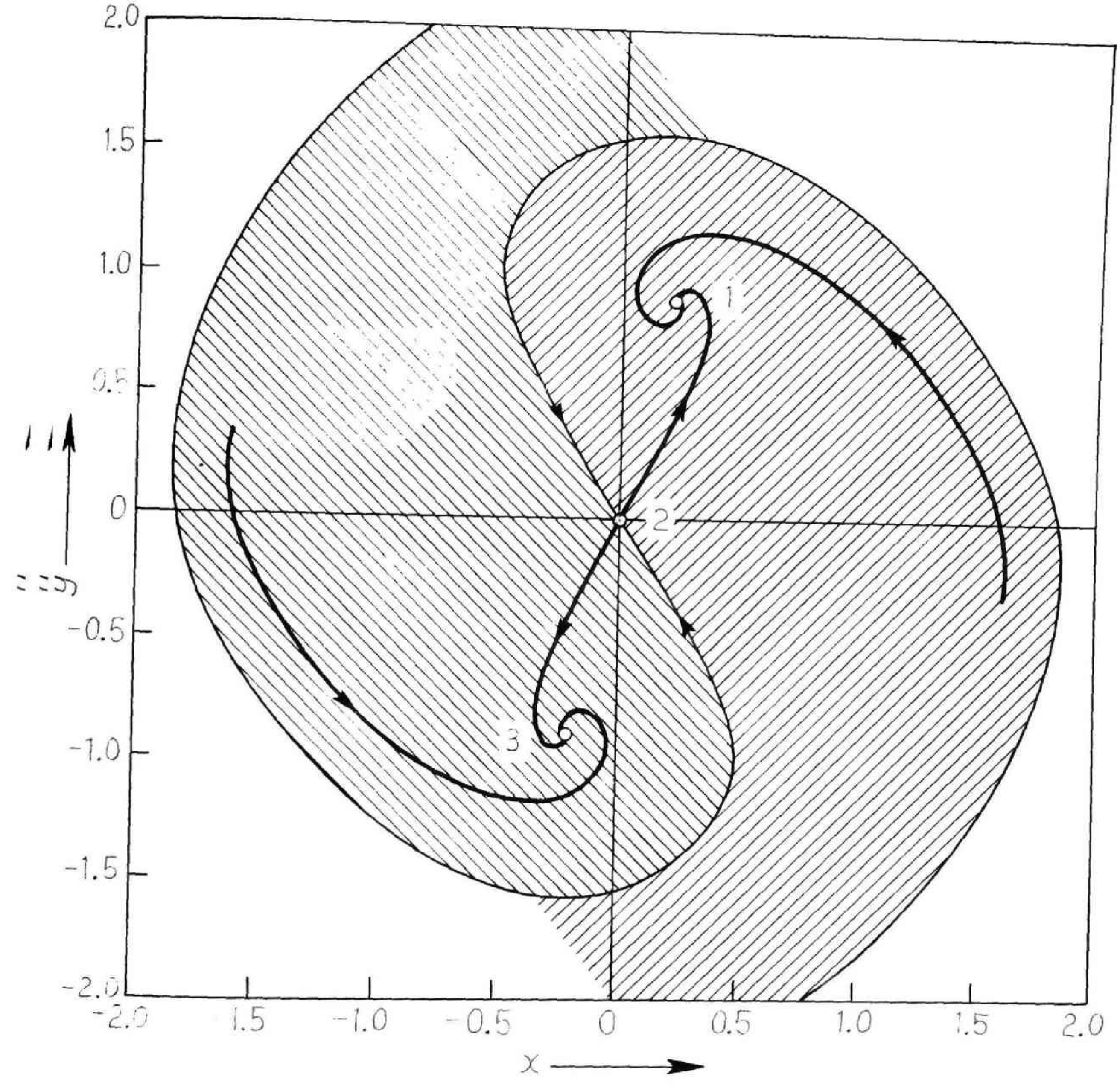

Fig. 3.3 Integral curves of (3.22) in the x, y plane, the system parameters being $k = 0.20$, $B = 1.50$, and $B_0 = 0.50$.

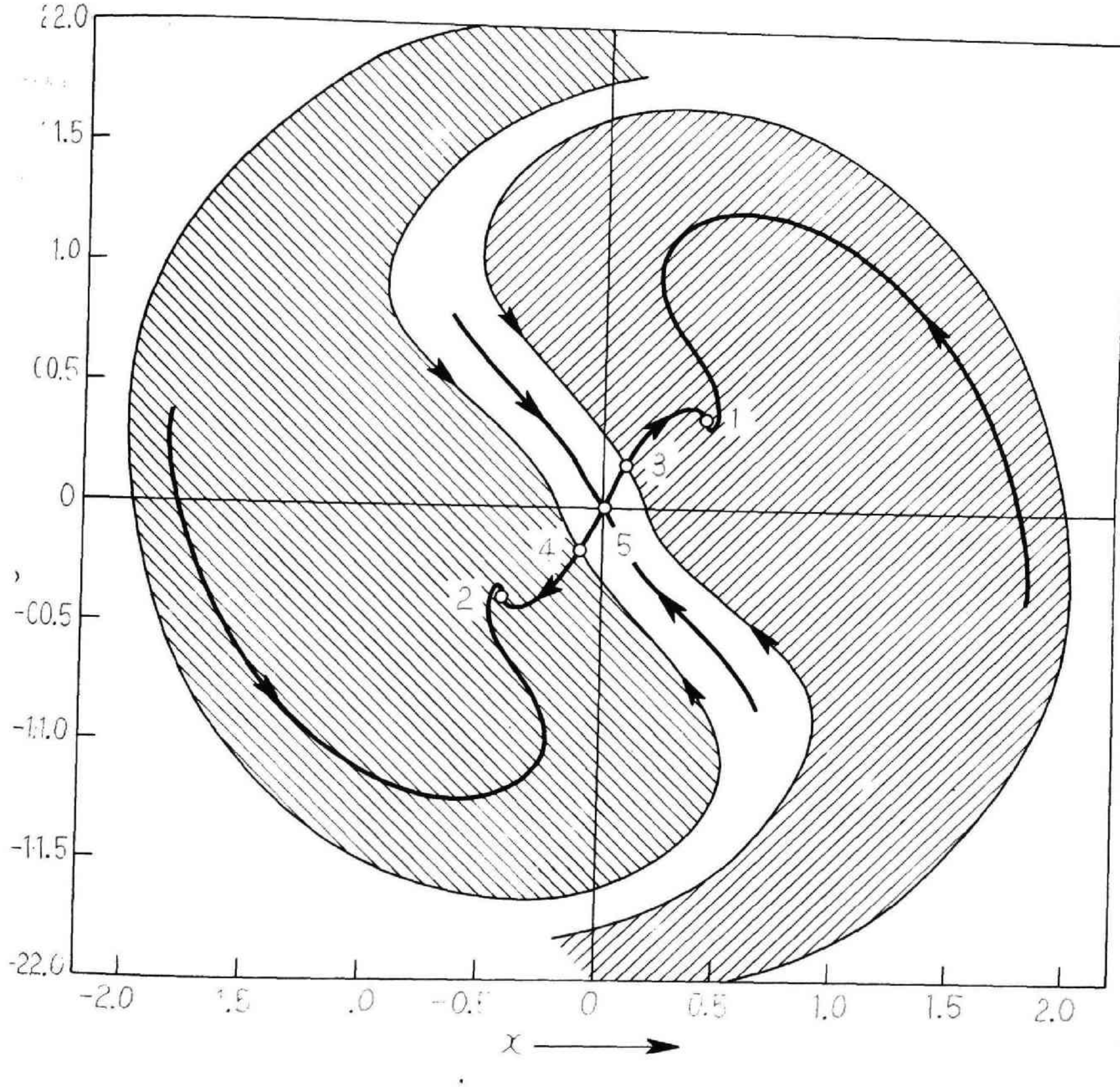

Fig. 3.4 Integral curves of (3.22) in the x, y plane, the system parameters being $k=0.20$, $B=0.60$, and $B_0=0.40$.

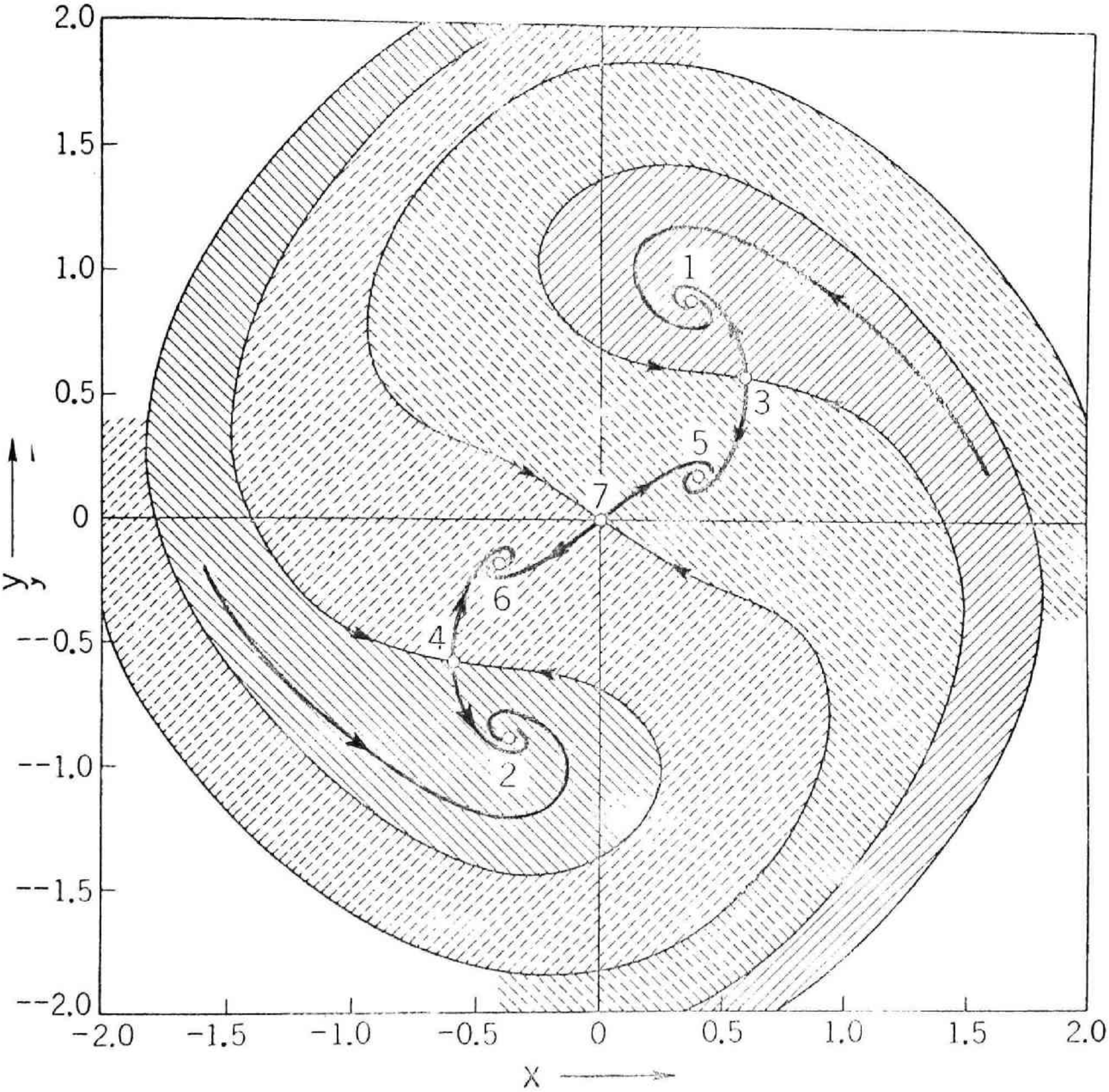

Fig. 3.5 Integral curves of (3.22) in the x, y plane, the system parameters being k =0.20, B =1.50, and B_0=0.25.

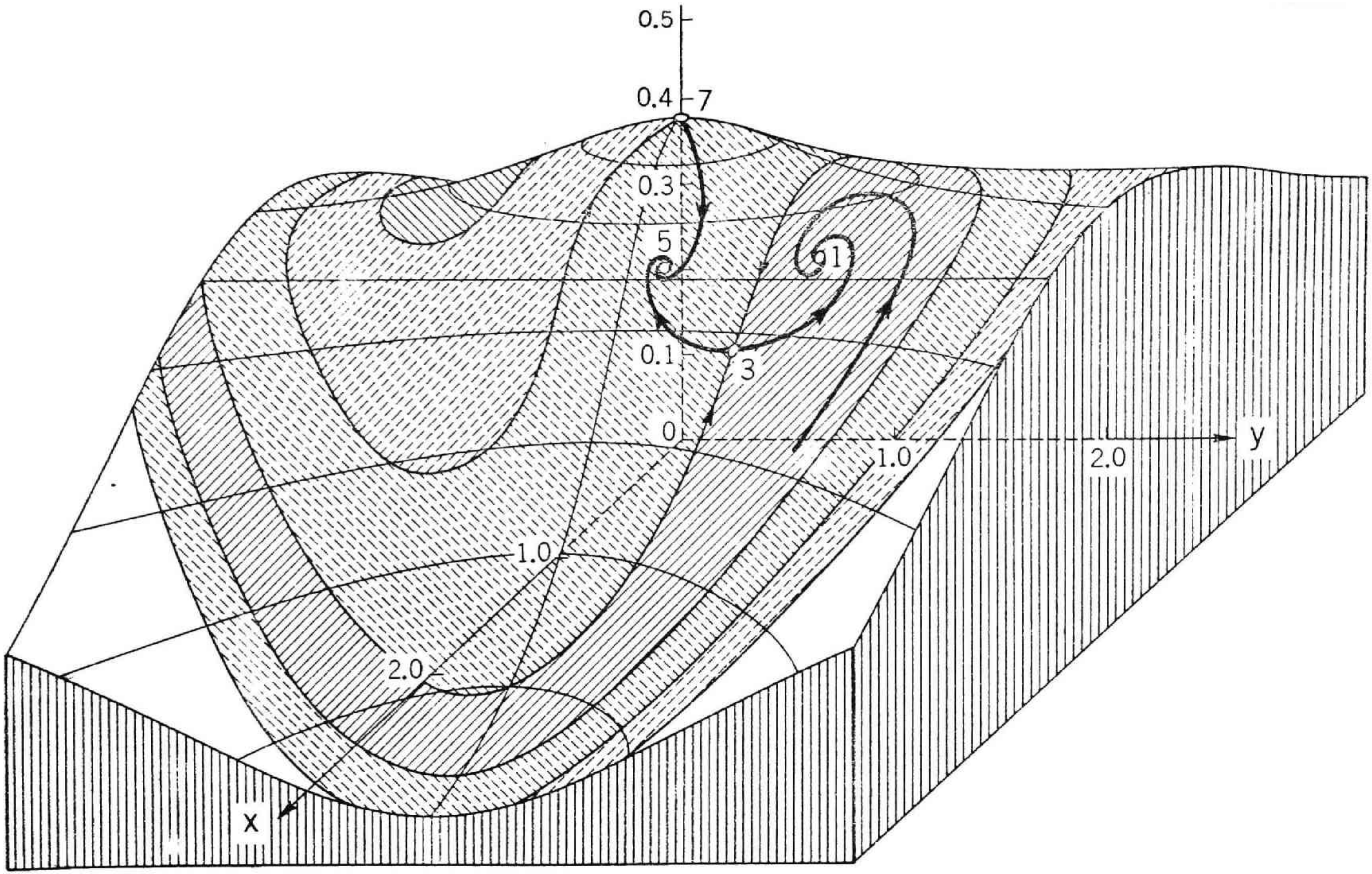

Fig. 3.6 Integral curves of (3.22) in the x, y, z space, the system parameters being k =0.20, B =1.50, and B_0 =0.25.

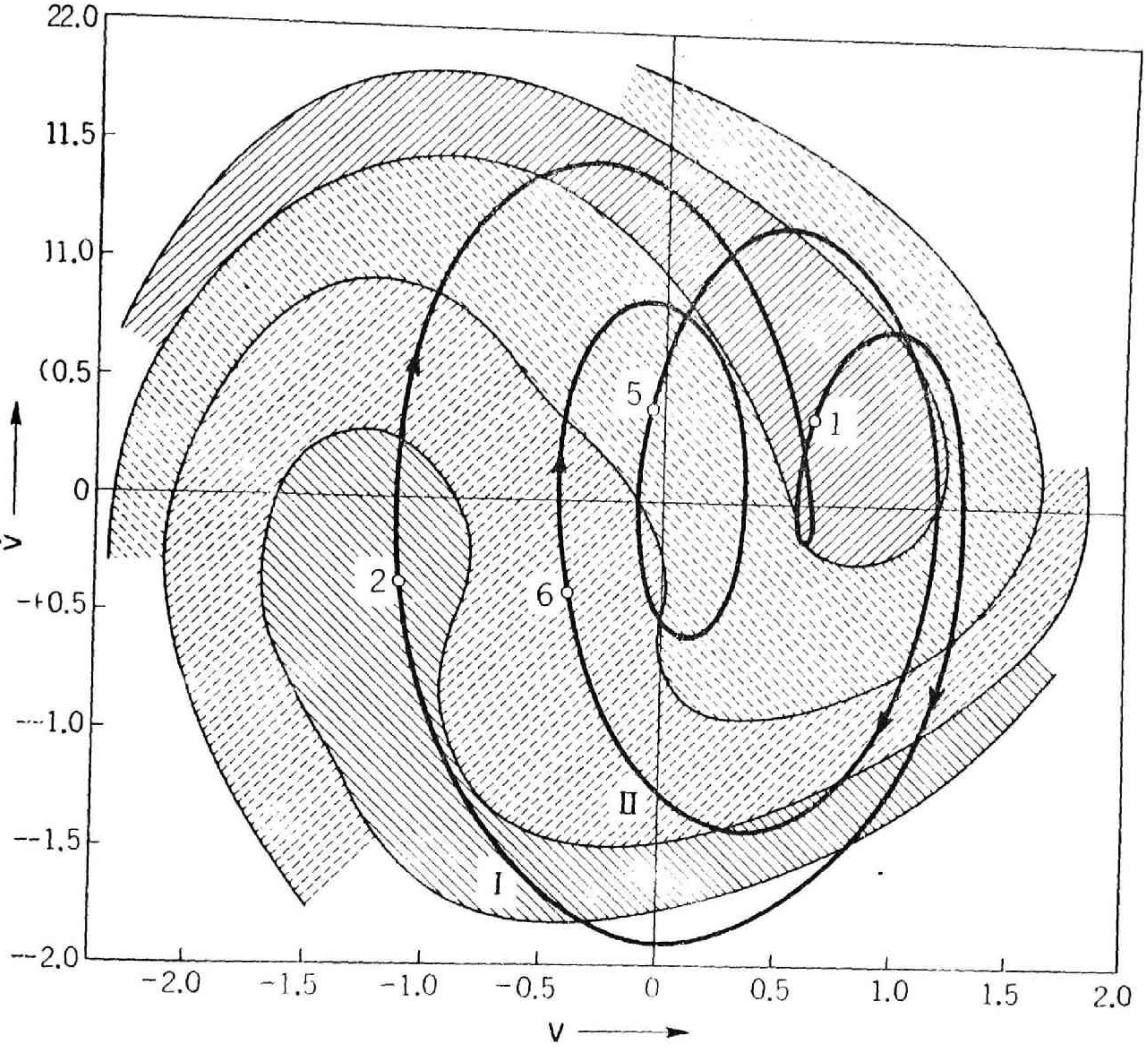

Fig. 3.7 Regions of initial conditions leading to the 1/2-harmonic responses, and the trajectories of the periodic solutions correlated with the stable singularities in Fig. 3.5.

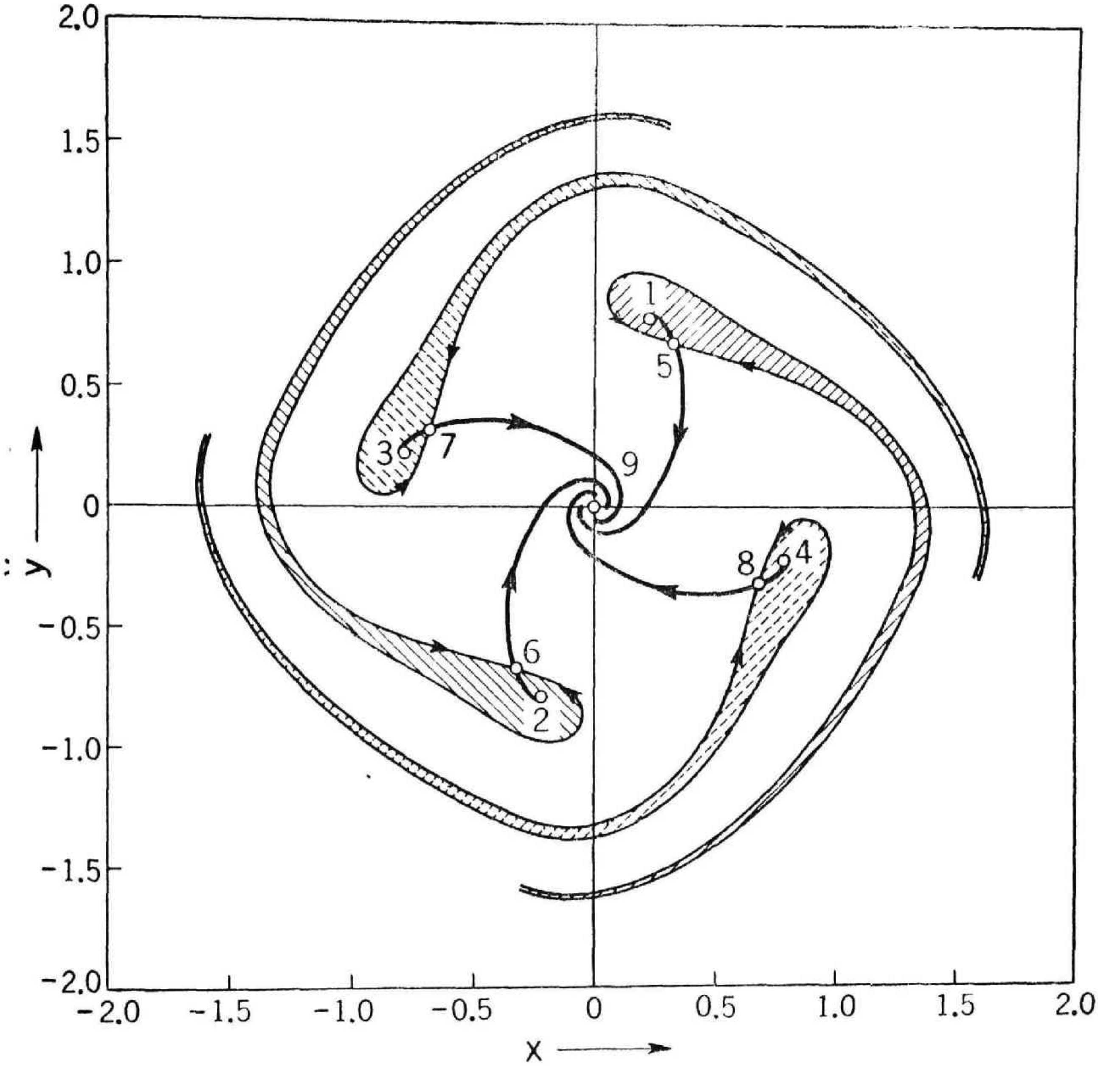

Fig. 3.8 Integral curves of (3.22) in the x, y plane, the system parameters being k =0.10, B =2.00, and B_0=0.

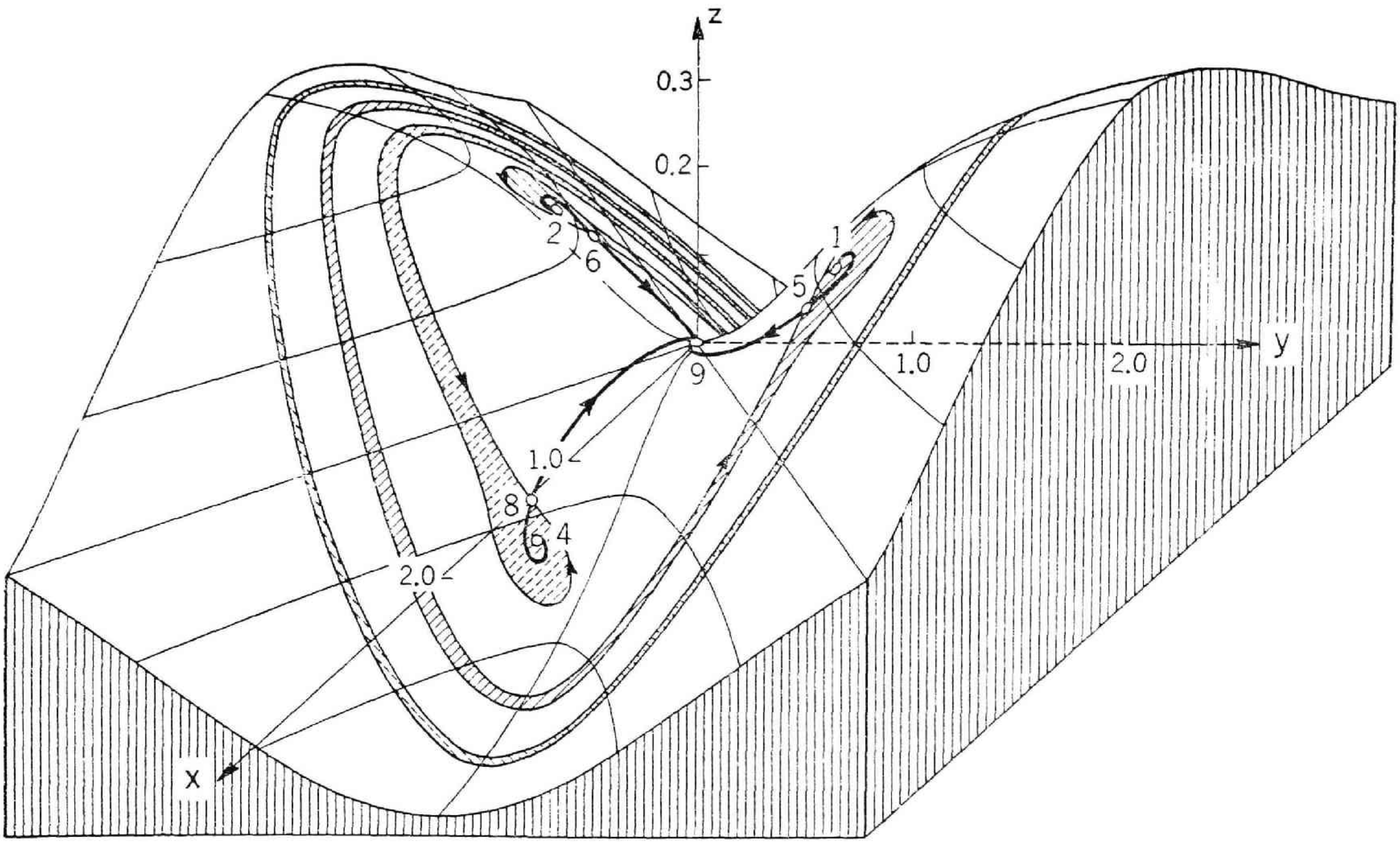

Fig. 3.9 Integral curves of (3.22) in the x, y, z space, the system parameters being k =0.10, B =2.00, and B_0 =0.

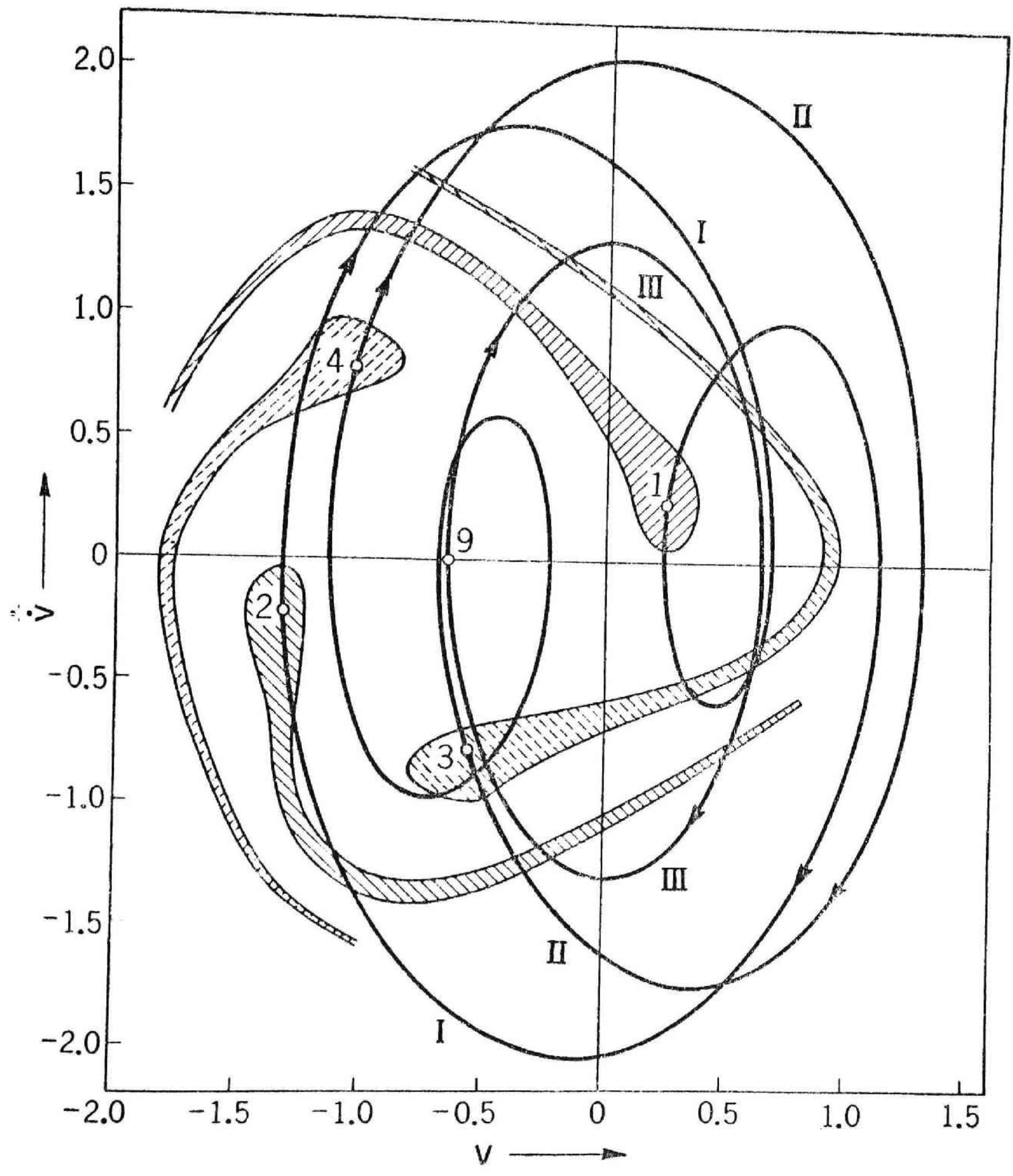

Fig. 3.10 Regions of initial conditions leading to the 1/2-harmonic responses, and the trajectories of the periodic solutions correlated with the stable singularities in Fig. 3.8.

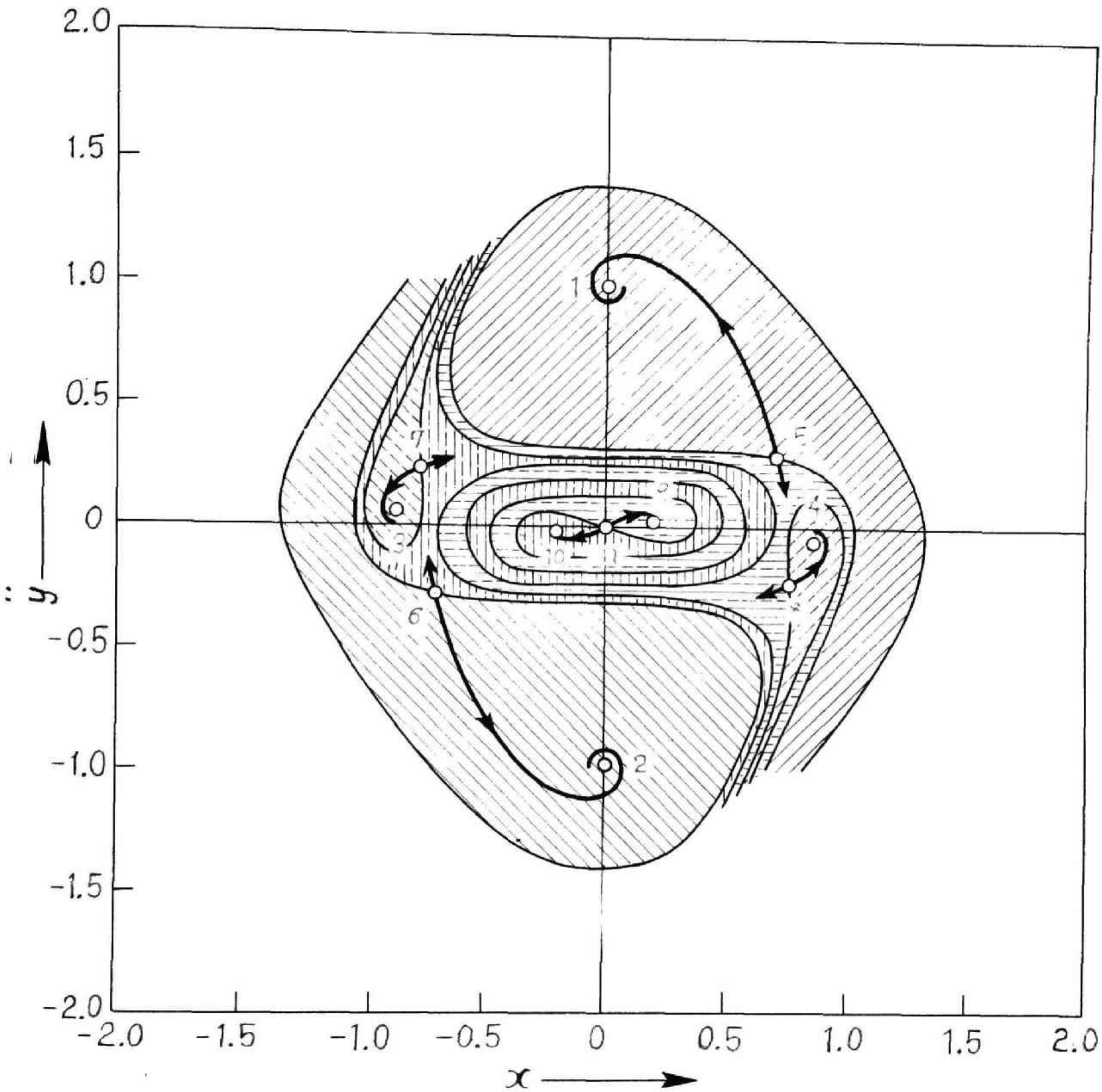

Fig. 3.11 Integral curves of (3.22) in the x, y plane, the system parameters being $k=0.01$, $B=1.80$, and $B_0=0.15$.

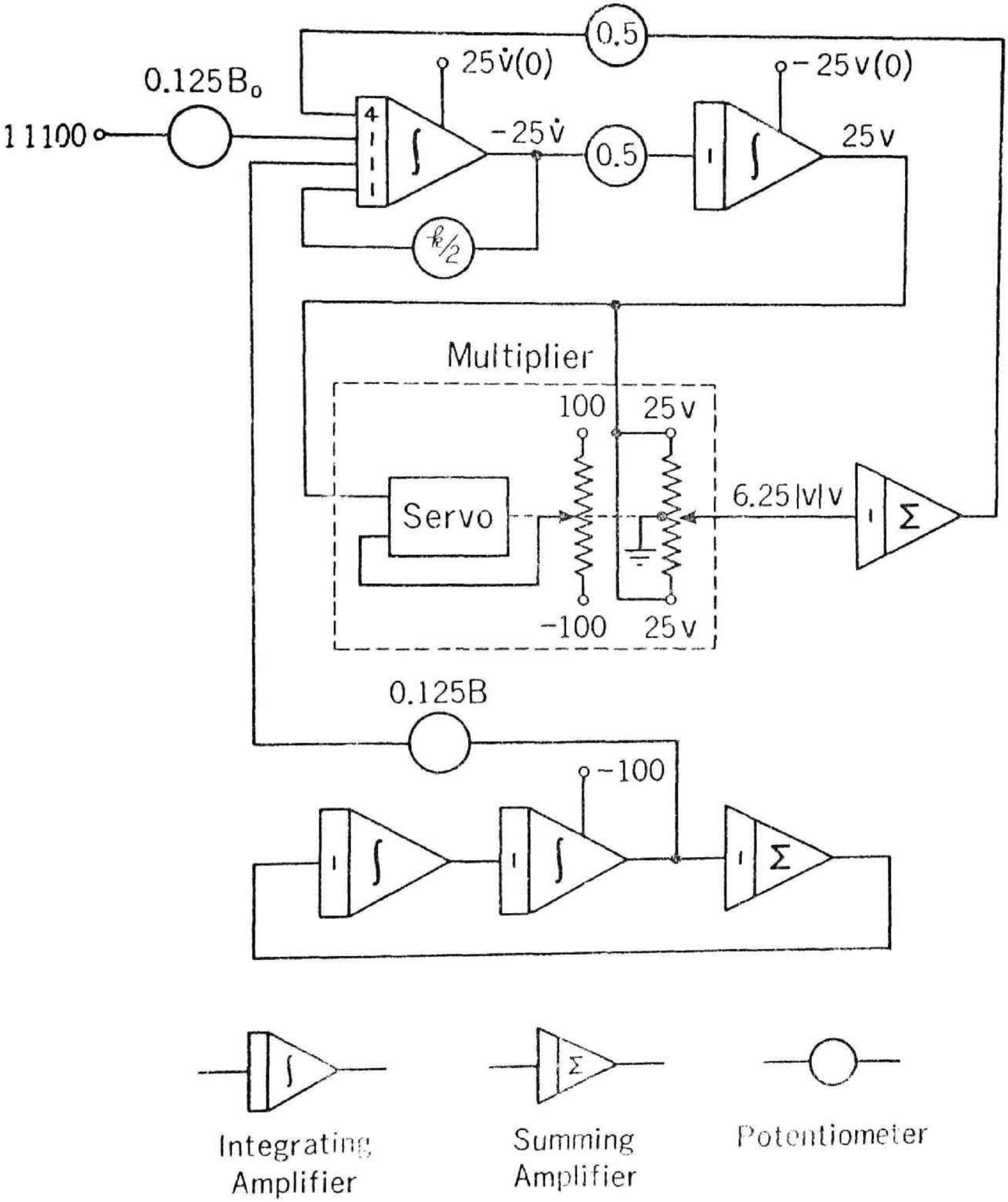

Fig. 3.12 Computer block diagram for (3.28).

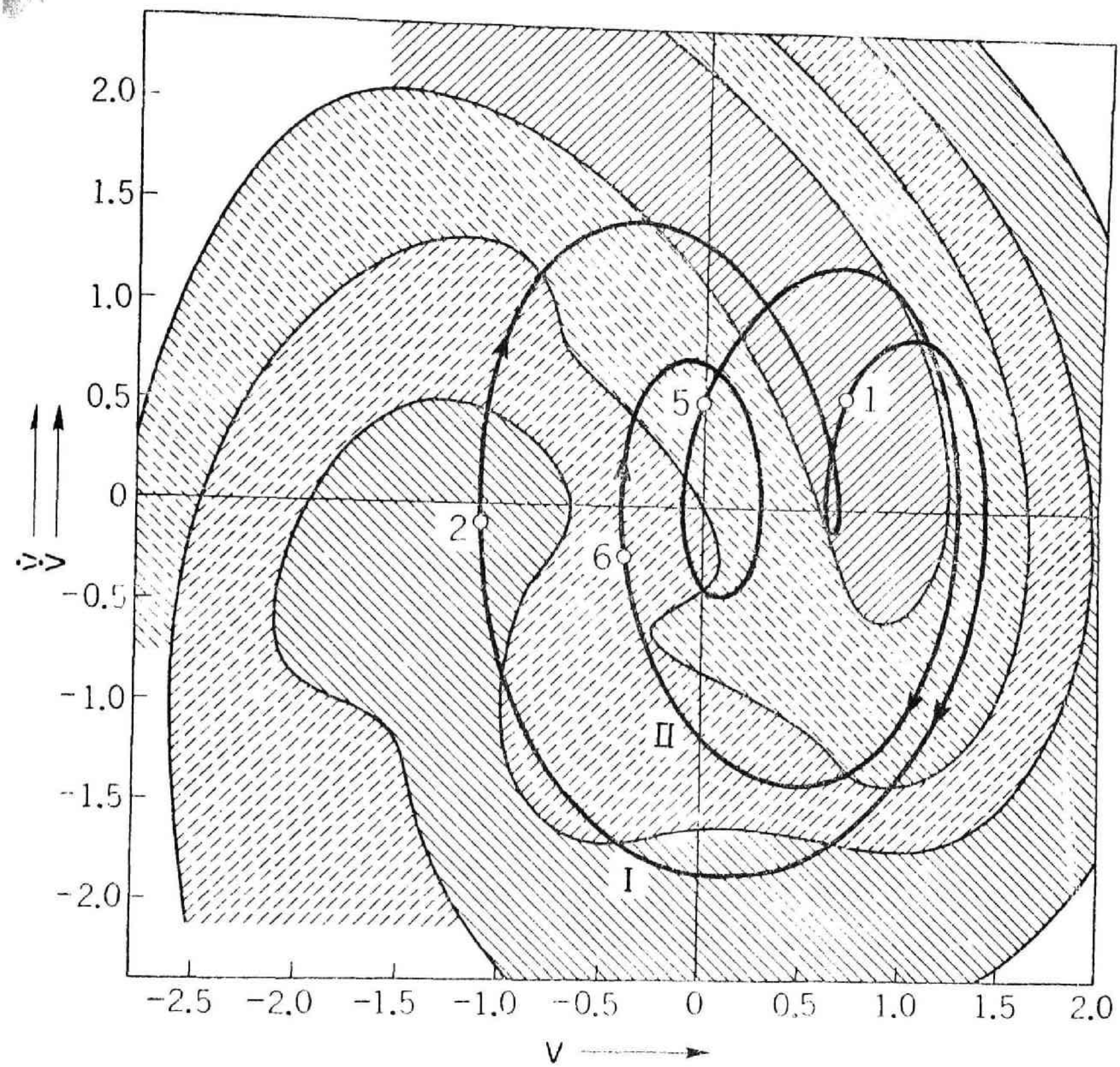

Fig. 3.13 Regions of initial conditions leading to the 1/2-harmonic responses and the trajectories of the periodic solutions, both obtained by analog-computer analysis (See Fig. 3.7).

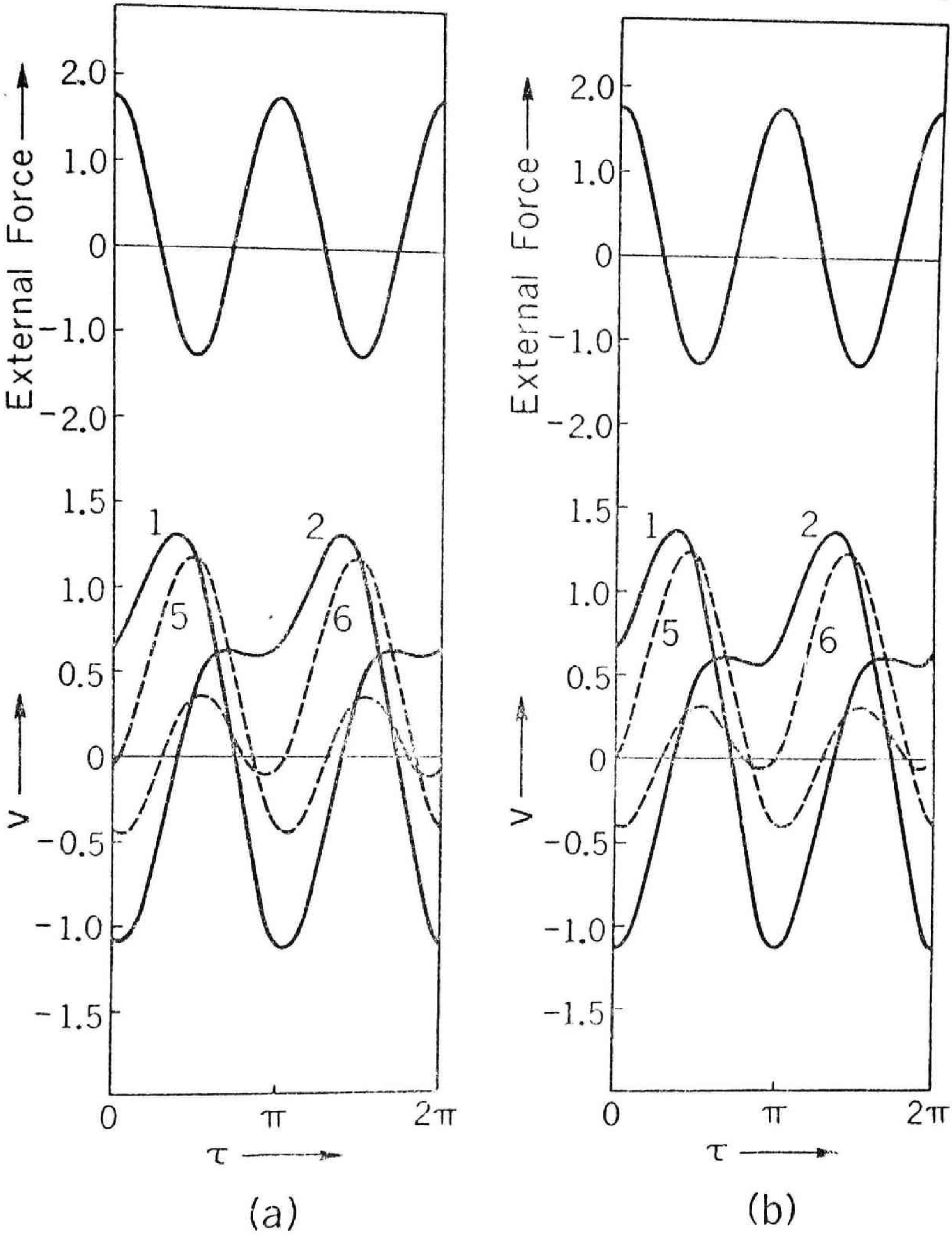

Fig. 3.14 Waveforms of the 1/2-harmonic oscillations in the case when k =0.20, B =1.50, and B_0=0.25. (a) Obtained by phase-plane analysis. (b) Obtained by analog-computer analysis.

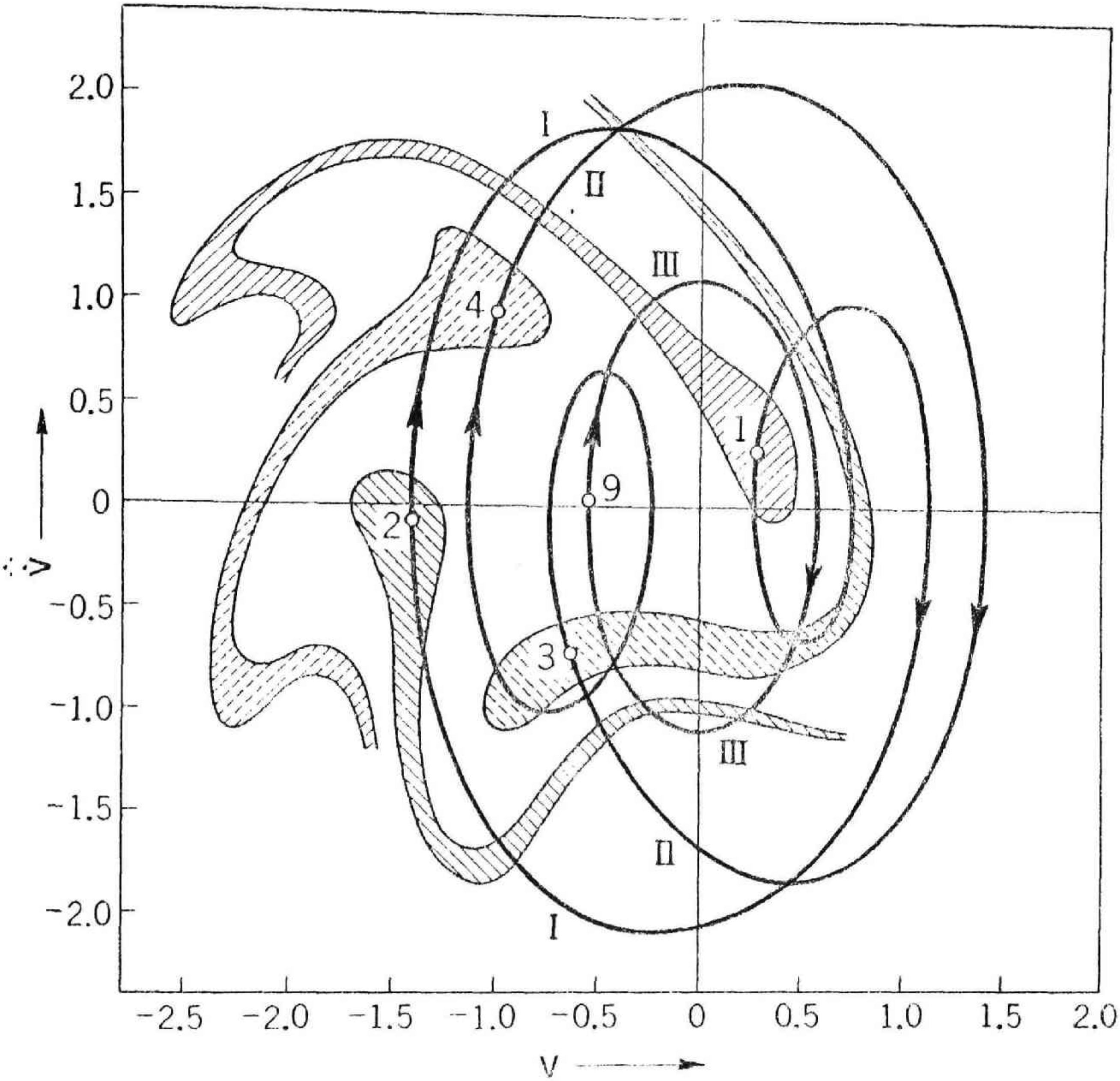

Fig. 3.15 Regions of initial conditions leading to the 1/2-harmonic responses and the trajectories of the periodic solutions, both obtained by analog-computer analysis (See Fig. 3.10).

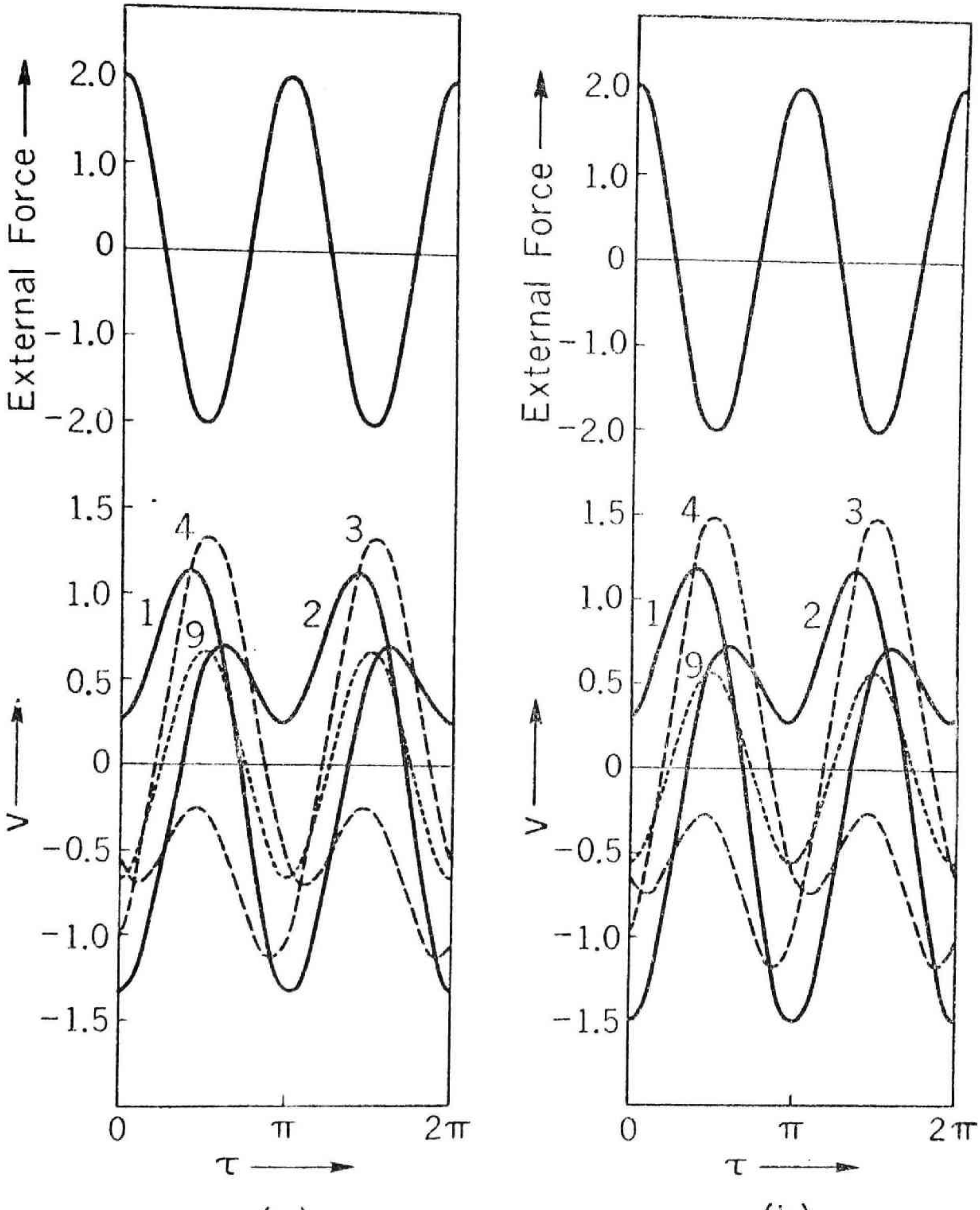

Fig. 3.16 Waveforms of the harmonic and the 1/2-harmonic oscillations in the case when k =0.10, B =2.00, and B_0 =0. (a) Obtained by phase-plane analysis. (b) Obtained by analog-computer analysis.

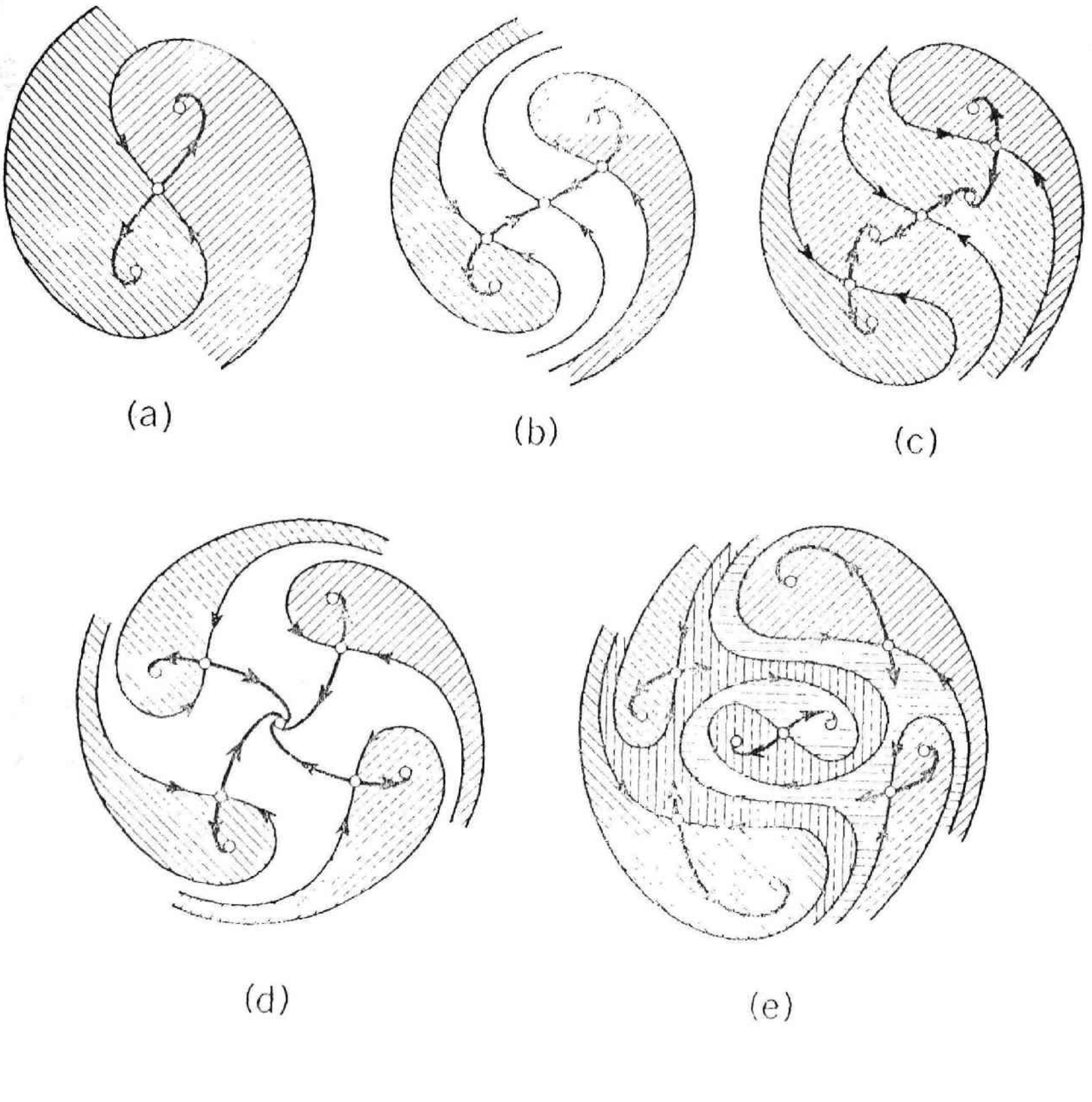

Fig. 3.17 Patterns of initial conditions leading to the 1/2-harmonic responses.

CHAPTER IV

INITIAL CONDITIONS LEADING TO DIFFERENT TYPES OF PERIODIC SOLUTIONS

4.1 Introduction

In the preceding chapter, we investigated the subharmonic oscillations of order 1/2 and particular attention was directed toward obtaining the relationship between the initial conditions and the resulting 1/2-harmonic oscillations. Now we are concerned with investigation of such relationship for various types of periodic oscillations in systems governed by Duffing's equation

$$\frac{d^2v}{d\tau^2} + k\frac{dv}{d\tau} + f(v) = g(\tau), \tag{4.1}$$

where k is a constant, $f(v)$ is a polynomial of v, and $g(\tau)$ is periodic in the time τ [8, 11, 12, 30].

The method of analysis is quite different from the method which was used in the preceding chapter. The latter has been extensively used for the study of harmonic and subharmonic oscillations in the transient state [30, pp. 81-124; 11]. Let us take a glance at this method before going into present investigation. For simplicity we confine the problem to the analysis of harmonic response under the impression of the external force $g(\tau) = B\cos\tau$. We write the solution of (4.1) as

$$v(\tau) = x(\tau)\sin\tau + y(\tau)\cos\tau,$$

where it is assumed that the amplitudes $x(\tau)$ and $y(\tau)$ are slowly varying functions of the time τ. Under this condition we may derive a set of simultaneous equations of the form

$$\frac{dx}{d\tau} = X(x, y) \qquad \frac{dy}{d\tau} = Y(x, y), \tag{4.2}$$

where $X(x,y)$ and $Y(x,y)$ are the polynomials of x and y that may readily be found. Upon elimination of τ in (4.2), the integral curves, i.e., the trajectories of the representative point (x, y), are plotted in the x, y plane. A singular point, for which $X(x,y) = 0$ and $Y(x,y) = 0$, is correlated with a periodic solution of (4.1). For certain values of k and B, there exist three singularities, i.e., two stable spirals and one saddle point which is directly unstable. The integral curve which tends to the saddle point with increasing τ is the separatrix which divides the coordinates plane into two domains, such that any initial conditions prescribed in each of them will lead to a particular type of harmonic oscillation. These domains will be called the domains of attraction.

This method of analysis is very effective for the study of harmonic and subharmonic oscillations in the transient state. However it has the following drawbacks. First, if the initial conditions are prescribed at values which are far different from those of the steady state, the assumption that the amplitude and phase of the oscillation vary slowly does not hold; therefore the result obtained by this method is not quite accurate. The second and more serious drawback is that, if a number of steady-state responses are to be expected, this method is practically inapplicable, since the analysis is compelled to resort to the graphical solution in a higher-dimensional phase space.

The present chapter describes the method of analysis which is applicable under such situation.* We consider the behavior of a point whose coordinates are given by $v(\tau)$ and $\dot{v}(\tau)$ in the $v, \dot{v}$ plane (dots over v refer to differentiation with respect to τ). An initial condition is then defined by a point prescribed at $\tau = 0$. Special attention is directed toward location of the points at the instants of $\tau = 2\pi, 4\pi, 6\pi, \ldots$. Mathematically, these points will be obtained as the successive images of the initial point under iterations of the mapping from $\tau = 2n\pi$ to $2(n+1)\pi$, where $n = 0, 1, 2, \ldots$. As expected from the foregoing analysis for harmonic response, there exist three fixed points, P_1, P_2, and P_3, of the mapping corresponding to the periodic solutions of (4.1) (see Fig. 4.1). P_1 and P_2 are stable, while P_3 is directly unstable. Through P_3 there are two curves, C_1 and C_2, which are invariant under the mapping. Points on C_2 approach P_3 under iterations of the mapping, while points on C_1 approach P_3 under iterations of the inverse mapping. Hence the successive images of an initial point will tend either to P_1 or to P_2, depending on which side of C_2 is the initial point. Thus the curve C_2 is the boundary between the domains of attraction, in each of them any initial conditions leading to a particular type of harmonic oscillations. The behavior of the loci of images is analogous to that of the integral curves in the neighborhood of the saddle point in the x, y plane.

The domains of attraction leading to different types of periodic solutions may be determined by the following procedure.

1. A periodic solution may be expanded into Fourier series, assuming the harmonic or subharmonic frequency as its least frequency. If the periodic solution, either stable or unstable, does exist, the coefficients of the principal terms of the Fourier series may be determined by the method of harmonic

---

* A similar method of analysis has also been studied by K. W. Blair and W. S. Loud [4]. The reader is suggested to refer to their paper for the mathematical consideration of the analysis.

balance.

2. A small variation ξ from the periodic solution is governed by the variational equation of (4.1), i.e.,

$$\frac{d^2\xi}{d\tau^2} + k\frac{d\xi}{d\tau} + \left[\frac{df}{dv}\right]_{v=v_0}\xi = 0, \tag{4.3}$$

where v_0 is the periodic solution. Equation (4.3) takes the form of Hill's equation and may be solved by an approximate method. Thus we can distinguish between the stable and unstable fixed points and also determine the slope of the invariant curve C_2 at the unstable fixed point P_3 (see Fig. 4.1).

3. The boundary between the domains of attraction is invariant curve C_2, which is the locus of the images that approach the unstable fixed point from both sides. These curves are obtained by starting just on either side of the unstable fixed point and integrating the original equation (4.1) for decreasing time, i.e., by using negative time in (4.1). A digital computer may be used for numerical integration. It is found that, if two initial points are prescribed not exactly on C_2 but on both sides of C_2 sufficiently close to each other, the loci of the images which have started these points nearly coincide with each other after several iterations of the mapping.

Two examples of the domains of attraction are illustrated in the present chapter. The first deals with the domains of attraction leading to the harmonic oscillation and the subharmonic oscillations of order 1/3. The second example is concerned with the domains of attraction for harmonic oscillation, the subharmonic oscillations of order 1/2 and of order 1/3.

The domains of attraction calculated by the above procedure agree well with those obtained by analog-computer analysis.

4.2 Symmetrical System

As an example of (4.1) we shall consider Duffing's equation of the form

$$\frac{d^2 v}{d\tau^2} + k\frac{dv}{d\tau} + v^3 = B\cos\tau. \tag{4.4}$$

This equation is unchanged if the sign of v is reversed and τ is shifted by π radians. Therefore the system governed by (4.4) will be called the symmetrical system. Since the nonlinearity is cubic in v, one may expect a periodic solution with harmonic frequency or subharmonic frequency of order 1/3 as its least frequency.* If the system parameters, k and B, are appropriately chosen, the periodic solution might be assumed to take the form

$$v_0(\tau) = x_1 \sin\tau + y_1 \cos\tau \tag{4.5}$$

for harmonic response, and

$$v_0(\tau) = x_{1/3} \sin\frac{1}{3}\tau + y_{1/3}\cos\frac{1}{3}\tau + x_1 \sin\tau + y_1\cos\tau \tag{4.6}$$

for subharmonic response. Terms of frequency other than those that appear in (4.5) and (4.6) are ignored to this order of approximation. It depends on the initial conditions that which response, (4.5) or (4.6), will actually occur. This problem will be studied in the following sections.

---

* A subharmonic oscillation of order 1/2 may exist over a smaller range of the system parameters. See Appendix III. However, since this type of oscillation is apt to occur when the system is unsymmetrical, this case will be deferred to Section 4.3.

4.2.1 Determination of the Coefficients of the Periodic Solutions

The coefficients of the periodic solutions, (4.5) and (4.6), may be determined by the method of harmonic balance. Substituting (4.6) into (4.4) and equating the coefficients of the terms containing $\sin\tau$, $\cos\tau$, $\sin\frac{1}{3}\tau$, and $\cos\frac{1}{3}\tau$ separately to zero, we obtain

$$\left.\begin{aligned}
&A_1 x_1 + k y_1 + \frac{1}{4}(x_{1/3}^2 - 3y_{1/3}^2)x_{1/3} = 0,\\
&k x_1 - A_1 y_1 - \frac{1}{4}(3x_{1/3}^2 - y_{1/3}^2)y_{1/3} - B = 0,\\
&\frac{9}{4}(x_{1/3}^2 - y_{1/3}^2)x_1 + \frac{9}{2}x_{1/3}y_{1/3}y_1 + A_{1/3}x_{1/3} + k y_{1/3} = 0,\\
&\frac{9}{2}x_{1/3}y_{1/3}x_1 - \frac{9}{4}(x_{1/3}^2 - y_{1/3}^2)y_1 + k x_{1/3} - A_{1/3}y_{1/3} = 0,
\end{aligned}\right\} \tag{4.7}$$

where

$$A_1 = 1 - \frac{3}{4}(R_1 + 2R_{1/3}), \quad A_{1/3} = \frac{1}{3} - \frac{9}{4}(2R_1 + R_{1/3}),$$

$$R_1 = r_1^2 = x_1^2 + y_1^2, \quad R_{1/3} = r_{1/3}^2 = x_{1/3}^2 + y_{1/3}^2,$$

from which one may derive the relations to determine R_1 and $R_{1/3}$, namely,

$$\left.\begin{aligned}
&(9A_1R_1 - A_{1/3}R_{1/3})^2 + k^2(9R_1 + R_{1/3})^2 = 81B^2R_1,\\
&\left[A_{1/3}^2 + k^2 - \frac{81}{16}R_1R_{1/3}\right]R_{1/3} = 0.
\end{aligned}\right\} \tag{4.8}$$

Through use of (4.7) and (4.8) the coefficients of the periodic solutions are found to be

$$\left.\begin{aligned}
x_1 &= \frac{k(9R_1 + R_{1/3})}{9B},\\
y_1 &= -\frac{(9A_1R_1 - A_{1/3}R_{1/3})}{9B},
\end{aligned}\right\} \tag{4.9}$$

and

$$x_{1/3} = r_{1/3}\cos\theta_{1/3}, \quad r_{1/3}\cos(\theta_{1/3} + \frac{2}{3}\pi), \quad r_{1/3}\cos(\theta_{1/3} + \frac{4}{3}\pi),$$

$$\left.\begin{array}{l} y_{1/3} = r_{1/3}\sin\theta_{1/3}, \quad r_{1/3}\sin(\theta_{1/3}+\frac{2}{3}\pi), \quad r_{1/3}\sin(\theta_{1/3}+\frac{4}{3}\pi), \\ \text{where} \\ \cos 3\theta_{1/3} = -\dfrac{-4(A_{1/3}x_1-ky_1)}{9R_1 r_{1/3}}, \quad \sin 3\theta_{1/3} = \dfrac{-4(kx_1+A_{1/3}y_1)}{9R_1 r_{1/3}}. \end{array}\right\} \tag{4.10}$$

From the second equation of (4.8) one sees that either

$$A_{1/3}^2 + k^2 - \frac{81}{16}R_1R_{1/3} = 0 \quad \text{or} \quad R_{1/3} = 0.$$

When $R_{1/3}=0$ there will be no subharmonic response, and (4.9) with $R_{1/3}=0$ gives the coefficients of the harmonic oscillation (4.5).*

4.2.2 Stability Investigation of the Periodic Solutions

The stability of the periodic solution will be investigated by considering the behavior of a small variation $\xi(\tau)$ from the periodic solution $v_0(\tau)$. If

---

* When the amplitude of the harmonic oscillation is not small, the accompanying third-harmonic component is to be considered as well. Several methods of improving the approximation were described in Chapter I. In this chapter, the following procedure is carried out for improvement if necessary.

The harmonic oscillation of the second approximation is written as

$$v_0(\tau) = (x_1+\delta x_1)\sin\tau + (y_1+\delta y_1)\cos\tau + x_3\sin 3\tau + y_3\cos 3\tau,$$

where the correction terms associated with δx_1, δy_1, x_3, and y_3 are considered to be relatively small. Proceeding in the same manner as before and discarding terms of order higher than the first in δx_1, δy_1, x_3, and y_3, we obtain a set of linear algebraic equations to determine these correction terms.

the variation $\xi(\tau)$ tends to zero with increasing τ, the periodic solution is stable; if $\xi(\tau)$ diverges, the periodic solution is unstable. The variation $\xi(\tau)$ is defined by

$$v(\tau) = v_0(\tau) + \xi(\tau). \tag{4.11}$$

Substituting this into (4.4) and introducing a new variable $\eta(\tau)$ defined by

$$\xi(\tau) = e^{-\frac{1}{2}k\tau} \cdot \eta(\tau), \tag{4.12}$$

we obtain

$$\frac{d^2\eta}{d\tau^2} + \left(-\frac{1}{4}k^2 + 3 v_0^2\right)\eta = 0. \tag{4.13}$$

Inserting $v_0(\tau)$ as given by (4.6) into (4.13) leads to a Hill's equation of the form

$$\left.\begin{aligned}
&\frac{d^2\eta}{d\tau^2} + \left[\theta_0 + 2\sum_{n=1}^{3}\theta_n \cos\left(2n\frac{\tau}{3} - \varepsilon_n\right)\right]\eta = 0,\\
&\text{where}\\
&\theta_0 = -\frac{1}{4}k^2 + \frac{3}{2}(R_1 + R_{1/3}),\\
&\theta_n^2 = \theta_{ns}^2 + \theta_{nc}^2, \qquad \varepsilon_n = \tan^{-1}\theta_{ns}/\theta_{nc},\\
&\theta_{1s} = \frac{3}{2}(x_1 y_{1/3} - y_1 x_{1/3} + x_{1/3} y_{1/3}), \qquad \theta_{1c} = \frac{3}{2}(x_1 x_{1/3} + y_1 y_{1/3} - \frac{1}{2}x_{1/3}^2 + \frac{1}{2}y_{1/3}^2),\\
&\theta_{2s} = \frac{3}{2}(x_1 y_{1/3} + y_1 x_{1/3}), \qquad \theta_{2c} = \frac{3}{2}(-x_1 x_{1/3} + y_1 y_{1/3}),\\
&\theta_{3s} = \frac{3}{2}x_1 y_1, \qquad \theta_{3c} = \frac{3}{2}(-\frac{1}{2}x_1^2 + \frac{1}{2}y_1^2).
\end{aligned}\right\} \tag{4.14}$$

By Floquet's theory the solution of (4.14) may be written in the form

$$\eta(\tau) = c_1 e^{\mu\tau}\phi(\tau) + c_2 e^{-\mu\tau}\psi(\tau), \tag{4.15}$$

where $\mu\,(>0)$ is the characteristic exponent dependent upon the parameters θ's, $\phi(\tau)$ and $\psi(\tau)$ are periodic in τ, c_1 and c_2 are arbitrary constants. From (4.12) and (4.15) one sees that the variation $\xi(\tau)$ tends to zero with increasing τ, provided that the damping $k/2$ is greater than μ. Hence the stability condition for the periodic solution $v_0(\tau)$ is given by $\frac{1}{2}k-\mu>0$. Upon computing μ to a first approximation, this condition leads to [17 ; 30 , pp. 3-22]

$$\left[\theta_0-\left(\frac{n}{3}\right)^2\right]^2+2\left[\theta_0+\left(\frac{n}{3}\right)^2\right]\left(\frac{k}{2}\right)^2+\left(\frac{k}{2}\right)^4>\theta_n^2, \quad n=1,\,2,\,3. \tag{4.16}$$

Substituting the parameters θ's as given by (4.14) into (4.16), we obtain

$$\left.\begin{aligned}
&\left(R_1+R_{1/3}-\tfrac{2}{27}\right)^2-\left(R_1+\tfrac{1}{4}R_{1/3}+\tfrac{2}{9}R_{1/3}\right)R_{1/3}+\tfrac{4}{81}k^2>0, && \text{for } n=1,\\
&\left(R_1+R_{1/3}-\tfrac{8}{27}\right)^2-R_1R_{1/3}+\tfrac{16}{81}k^2>0, && \text{for } n=2,\\
&\left(R_1+R_{1/3}-\tfrac{2}{3}\right)^2-\tfrac{1}{4}R_1^2+\tfrac{4}{9}k^2>0, && \text{for } n=3,
\end{aligned}\right\} \tag{4.17}$$

If the condition for $n=m$ is not satisfied, the periodic solution, (4.5) or (4.6), becomes unstable owing to the build-up of a self-excited oscillation having the frequency $m/3$.

(a) Harmonic Response

Since $R_{1/3}=0$ in this case, the first and second conditions of (4.17) are satisfied. The third condition is reduced to

$$\frac{27}{16}R_1^2-3R_1+k^2+1>0. \tag{4.18}$$

This is the stability condition for the periodic solution (4.5).

(b) Subharmonic Response (1/3-Harmonic)

For any combinations of R_1 and $R_{1/3}$ calculated from (4.8), one can verify that the second and third conditions of (4.17) are satisfied. By virtue of

(4.8) the first condition leads to

$$R_1 + \frac{2}{3} R_{V3} - \frac{8}{9} > 0. \tag{4.19}$$

This is the stability condition for the periodic solution (4.6).

See Appendix III as for the regions in which the harmonic and 1/3-harmonic oscillations are sustained.

4.2.3 Domains of Attraction leading to Harmonic and 1/3-Harmonic Responses

As mentioned earlier in Section 4.1, the boundary between the two domains of attraction for harmonic response is the locus of the images $[v_0(2n\pi),\ \dot{v}_0(2n\pi)]$ that approach the directly unstable fixed point with increasing time. This locus may be obtained by integrating the Duffing's equation (4.4) for decreasing time, i.e., by using negative time in the equation. The initial conditions, i.e., the initial points of integration should be on the invariant curve C_2 and may preferably be close to the unstable fixed point P_3 (see Fig. 4.1). The location of the fixed points may readily be determined from the periodic solutions, (4.5) and (4.6), in which the coefficients are to be found by using (4.8) through (4.10). The stability of the fixed points will be studied by conditions (4.18) and (4.19). We are particularly interested in the fixed points that are directly unstable. The slope of the invariant curve C_2 at the unstable fixed point may be determined by the following procedure. From (4.12) and (4.15) the variation $\xi(\tau)$ from the periodic solution $v_0(\tau)$ is given by

$$\xi(\tau) = c_1 e^{(-\frac{1}{2}k+\mu)\tau}\phi(\tau) + c_2 e^{(-\frac{1}{2}k-\mu)\tau}\psi(\tau). \tag{4.20}$$

In the neighborhood of the unstable fixed point, the images on the invariant curves C_1 and C_2 satisfy the condition that

$$\frac{\dot{\xi}(0)}{\xi(0)}=\frac{\dot{\xi}(T)}{\xi(T)}=\frac{\dot{\xi}(2T)}{\xi(2T)}=\cdots \text{ (= slope of the invariant curve)},$$

where $T=2\pi$ for harmonic response and $T=6\pi$ for subharmonic response. Hence it follows that either C_1 or C_2 must be zero. On the invariant curve C_2 the successive images approach the unstable fixed point with increasing time. Therefore these images are represented by the points $[\xi(nT), \dot{\xi}(nT)]$, where $\xi(\tau)$ is given by

$$\xi(\tau)=c_2 e^{(-\frac{1}{2}k-\mu)\tau}\,\psi(\tau).$$

Hence the slope of the invariant curve C_2, i.e., the direction of the boundary at the unstable fixed point is given by*

$$\alpha=\frac{\dot{\xi}(0)}{\xi(0)}=-\left(\frac{1}{2}k+\mu\right)+\frac{\dot{\psi}(0)}{\psi(0)}. \tag{4.21}$$

Thus the initial point of integration may be located on the line segment which passes through the unstable fixed point with slope α.

Numerical Example

We consider the Duffing's equation

---

* The reader is suggested to refer to Reference 30, pp. 127-137 for the calculation of the characteristic exponent μ and the periodic function $\psi(\tau)$ in the solution (4.15). The results of the numerical calculation for the particular examples will be shown in Appendix IV.

$$\frac{d^2 v}{d\tau^2} + 0.1\,\frac{dv}{d\tau} + v^3 = 0.15\cos\tau. \tag{4.22}$$

For these particular values of the parameters, i.e., $k = 0.1$ and $B = 0.15$ in (4.4),* the periodic solutions, (4.5) and (4.6), are determined from (4.8), (4.9), and (4.10). Their stability is studied by conditions (4.18) and (4.19). The result is shown in what follows. For harmonic response,

$$v_{01} = 0.011\sin\tau - 0.153\cos\tau,$$

$$v_{02} = 0.960\sin\tau + 0.686\cos\tau + 0.019\sin 3\tau - 0.040\cos 3\tau,$$

$$v_{03} = 0.806\sin\tau - 0.716\cos\tau + 0.023\sin 3\tau + 0.037\cos 3\tau,$$

v_{01}, v_{02} being stable, while v_{03} unstable. For subharmonic response,

$$v_{04} = 0.063\sin\tfrac{1}{3}\tau + 0.358\cos\tfrac{1}{3}\tau + 0.032\sin\tau - 0.180\cos\tau,$$

$$v_{05} = -0.342\sin\tfrac{1}{3}\tau - 0.124\cos\tfrac{1}{3}\tau + 0.032\sin\tau - 0.180\cos\tau,$$

$$v_{06} = 0.278\sin\tfrac{1}{3}\tau - 0.234\cos\tfrac{1}{3}\tau + 0.032\sin\tau - 0.180\cos\tau,$$

$$v_{07} = 0.149\sin\tfrac{1}{3}\tau + 0.226\cos\tfrac{1}{3}\tau + 0.025\sin\tau - 0.171\cos\tau,$$

$$v_{08} = -0.271\sin\tfrac{1}{3}\tau + 0.016\cos\tfrac{1}{3}\tau + 0.025\sin\tau - 0.171\cos\tau,$$

$$v_{09} = 0.122\sin\tfrac{1}{3}\tau - 0.242\cos\tfrac{1}{3}\tau + 0.025\sin\tau - 0.171\cos\tau,$$

---

* These parameters are chosen such that both types of periodic solutions, (4.5) and (4.6), exist for (4.22) depending on different values of the initial conditions.

v_{04}, v_{05}, v_{06} being stable, while v_{07}, v_{08}, v_{09} unstable.

By use of these values one may readily locate the fixed points in the v, $\dot{v}$ plane. For harmonic response, the fixed points are invariant under iterations of the mapping from $\tau = 2n\pi$ to $2(n+1)\pi$; while, for subharmonic response, the fixed points are invariant under every third iterate of the mapping. We are particularly interested in the fixed points that are directly unstable, since the boundaries between domains of attraction contain such points. The direction of the boundary curve at the unstable fixed point may be calculated through use of (4.21). The fixed points and the related properties thus calculated are listed in Table 4.1.

Table 4.1 Fixed Points and Related Properties correlated with the Periodic Solutions of (4.22)

Fixed Point	Response	v	$\dot{v}$	α^*	Stability
1	Harmonic	-0.153	0.011		Stable
2	Harmonic	0.646	1.016		Stable
3	Harmonic	-0.679	0.876	-0.020	Unstable
4	1/3-Harmonic	0.178	0.053		Stable
5	1/3-Harmonic	-0.304	-0.082		Stable
6	1/3-Harmonic	-0.413	0.124		Stable
7	1/3-Harmonic	0.056	0.075	-0.644	Unstable
8	1/3-Harmonic	-0.155	-0.065	-0.164	Unstable
9	1/3-Harmonic	-0.413	0.066	0.263	Unstable

* α is the direction of the boundary curve between domains of attraction

at the unstable fixed point.

The trajectories, i.e., the loci of the points $[v_0(\tau), \dot{v}_0(\tau)]$, of the stable solutions are shown in Fig. 4.2. The small circles in the figure indicate the location of the fixed points of the mapping. It is noted that the fixed points, 4, 5, and 6, correlated with the subharmonic oscillation lie on the same trajectory and that, under iterations of the mapping, these fixed points are transferred successively to the points that follow in the direction of the arrows. Following the procedure as described in Section 4.1, successive images of the mapping for harmonic response are shown in Fig. 4.3. The boundary between the two domains of attraction is shown in thick line, on which the image points approach the unstable fixed point 3 (in the direction of the arrows) with increasing time. Also plotted in Fig. 4.4 is the whole diagram of the domains of attraction leading to the harmonic and subharmonic responses. The boundaries between the domains of attraction were obtained by starting just on both sides (in the direction of α) of the unstable fixed points and integrating (4.22) for decreasing time. Both analog and digital computers were used for this purpose. The domains of attraction for subharmonic response have narrowing tails as they extend to infinity or as they come close to the domain of harmonic response containing the fixed point 2. These extremely narrow tails are omitted in the figure, since the computation becomes too laborious.

4.3 Unsymmetrical System

We shall consider an unsymmetrical system governed by

$$\frac{d^2 v}{d\tau^2} + k\,\frac{dv}{d\tau} + v^3 = B\cos\tau + B_0, \tag{4.23}$$

where the unsymmetry appears as the unidirectional component of the external force.* In addition to the responses as mentioned in Section 4.2, the subharmonic oscillation of order 1/2 may also be expected in this case. The periodic solution of (4.23) might be assumed to take the form

$$v_0(\tau) = x_1 \sin\tau + y_1 \cos\tau + z \tag{4.24}$$

for harmonic response, and

$$v_0(\tau) = x_{1/2}\sin\tfrac{1}{2}\tau + y_{1/2}\cos\tfrac{1}{2}\tau + x_1\sin\tau + y_1\cos\tau + z \tag{4.25}$$

or

$$v_0(\tau) = x_{1/3}\sin\tfrac{1}{3}\tau + y_{1/3}\cos\tfrac{1}{3}\tau + x_1\sin\tau + y_1\cos\tau + z \tag{4.26}$$

for subharmonic response. Since the system is unsymmetrical, the constant term z of zero frequency is added to the solution. If the system parameters, k, B, and B_0, are appropriately chosen, the resulting response will be one of the types as given by (4.24), (4.25), and (4.26), depending on different values of the initial conditions.

4.3.1 Periodic Solutions and Conditions for Stability

Proceeding analogously to Section 4.2.1, the coefficients of the periodic solutions are determined. The conditions for stability of the periodic solutions are also derived by solving the variational equations of the Hill's type.

---

* Equation (4.1) with unsymmetrical nonlinearity may readily be transformed to one with symmetrical nonlinearity but with unsymmetrical external force.

(a) Harmonic Response

The coefficients of the periodic solution (4.24) are found to be

$$\left.\begin{aligned} &x_1 = \frac{kR_1}{B}, \qquad y_1 = \frac{-A_1R_1}{B}, \\ &\text{where} \\ &A_1 = 1 - \frac{3}{4}(R_1 + 4Z), \\ &R_1 = r_1^2 = x_1^2 + y_1^2, \quad Z = z^2, \end{aligned}\right\} \tag{4.27}$$

in which the unknown quantities R_1 and Z may be determined by solving the simultaneous equations

$$\left.\begin{aligned} &(A_1^2 + k^2)R_1 = B^2, \\ &\left(\tfrac{3}{2}R_1 + Z\right)z = B_0. \end{aligned}\right\} \tag{4.28}$$

The stability condition of the same kind as (4.16) may be derived, from which we obtain

$$\left.\begin{aligned} &\left(R_1 + 2Z - \tfrac{1}{6}\right)^2 - 4R_1Z + \tfrac{1}{9}k^2 > 0, \qquad \text{for} \qquad n = 1, \\ &\left(R_1 + 2Z - \tfrac{2}{3}\right)^2 - \tfrac{1}{4}R_1^2 + \tfrac{4}{9}k^2 > 0, \qquad \text{for} \qquad n = 2. \end{aligned}\right\} \tag{4.29}$$

If the condition for $n = m$ is not satisfied, the periodic solution (4.24) becomes unstable owing to the build-up of a self-excited oscillation having the frequency $m/2$.

(b) Subharmonic Response (1/2-Harmonic)

The coefficients of the periodic solution (4.25) are found to be

$$x_1 = \frac{k(4R_1 + R_{1/2})}{4B},$$

$$
\left.
\begin{aligned}
& y_1 = \frac{-(4A_1R_1 - A_{1/2}R_{1/2})}{4E}, \\
& x_{1/2} = r_{1/2}\cos\theta_{1/2}, \quad r_{1/2}\cos(\theta_{1/2}+\pi), \\
& y_{1/2} = r_{1/2}\sin\theta_{1/2}, \quad r_{1/2}\sin(\theta_{1/2}+\pi),
\end{aligned}
\right.
$$

where

$$
\left.
\begin{aligned}
& A_1 = 1 - \tfrac{3}{4}(R_1 + 2R_{1/2} + 4Z), \quad A_{1/2} = \tfrac{1}{2} - \tfrac{3}{2}(2R_1 + R_{1/2} + 4Z), \\
& R_1 = r_1^2 = x_1^2 + y_1^2, \quad R_{1/2} = r_{1/2}^2 = x_{1/2}^2 + y_{1/2}^2, \quad Z = z^2, \\
& \cos 2\theta_{1/2} = \frac{-(kx_1 + A_{1/2}y_1)}{6R_1Z}, \quad \sin 2\theta_{1/2} = \frac{A_{1/2}x_1 - ky_1}{6R_1Z},
\end{aligned}
\right\} \quad (4.30)
$$

in which the unknown quantities R_1, $R_{1/2}$, and Z may be determined by solving the simultaneous equations

$$
\left.
\begin{aligned}
& (4A_1R_1 - A_{1/2}R_{1/2})^2 + k^2(4R_1 + R_{1/2})^2 - 16E^2R_1 = 0, \\
& A_{1/2}^2 + k^2 - 36R_1Z \doteq 0, \\
& \frac{3}{2}(R_1 + R_{1/2} + \tfrac{2}{3}Z)z + \frac{A_{1/2}R_{1/2}}{8z} - E_0 = 0.
\end{aligned}
\right\} \quad (4.31)
$$

The stability conditions may also be written as

$$
\left.
\begin{aligned}
& (R_1 + R_{1/2} + 2Z - \tfrac{1}{24})^2 + (R_1 + R_{1/2} - \tfrac{1}{3})R_{1/2} + \tfrac{1}{36}k^2 > 0, && \text{for } n = 1, \\
& (R_1 + R_{1/2} + 2Z - \tfrac{1}{6})^2 - (4R_1Z + \tfrac{1}{4}R_{1/2}^2 + \tfrac{1}{3}A_{1/2}R_{1/2}) + \tfrac{1}{9}k^2 > 0, && \text{for } n = 2, \\
& (R_1 + R_{1/2} + 2Z - \tfrac{3}{8})^2 - R_1R_{1/2} + \tfrac{1}{4}k^2 > 0, && \text{for } n = 3, \\
& (R_1 + R_{1/2} + 2Z - \tfrac{2}{3})^2 - \tfrac{1}{4}R_1^2 + \tfrac{4}{9}k^2 > 0, && \text{for } n = 4.
\end{aligned}
\right\} \quad (4.32)
$$

If the condition for $n = m$ is not satisfied, the periodic solution (4.25) becomes unstable owing to the build-up of a self-excited oscillation having the frequency $m/4$. The condition for $n = 4$ is superfluous in this particular case, since it is always satisfied by the coefficients of (4.25). Therefore the conditions for $n = 1$, 2, and 3 must be ascertained for stability of the periodic solution.

(c) Subharmonic Response (1/3-Harmonic)

The coefficients of the periodic solution (4.26) are found to be

$$
\left.
\begin{aligned}
& x_1 = \frac{k(9R_1 + R_{1/3})}{9B}, \\
& y_1 = \frac{-(9A_1R_1 - A_{1/3}R_{1/3})}{9B}, \\
& x_{1/3} = r_{1/3}\cos\theta_{1/3},\ r_{1/3}\cos(\theta_{1/3} + \tfrac{2}{3}\pi),\ r_{1/3}\cos(\theta_{1/3} + \tfrac{4}{3}\pi), \\
& y_{1/3} = r_{1/3}\sin\theta_{1/3},\ r_{1/3}\sin(\theta_{1/3} + \tfrac{2}{3}\pi),\ r_{1/3}\sin(\theta_{1/3} + \tfrac{4}{3}\pi), \\
\text{where}\quad & A_1 = 1 - \tfrac{3}{4}(R_1 + 2R_{1/3} + 4Z), \quad A_{1/3} = \tfrac{1}{3} - \tfrac{9}{4}(2R_1 + R_{1/3} + 4Z), \\
& R_1 = r_1^2 = x_1^2 + y_1^2, \quad R_{1/3} = r_{1/3}^2 = x_{1/3}^2 + y_{1/3}^2, \quad Z = z^2, \\
& \cos 3\theta_{1/3} = \frac{-4(A_{1/3}x_1 - ky_1)}{9R_1 r_{1/3}}, \quad \sin 3\theta_{1/3} = \frac{-4(kx_1 + A_{1/3}y_1)}{9R_1 r_{1/3}},
\end{aligned}
\right\} \quad (4.33)
$$

in which the unknown quantities R_1, $R_{1/3}$, and Z may be determined by solving the simultaneous equations

$$
\left.
\begin{aligned}
& (9A_1R_1 - A_{1/3}R_{1/3})^2 + k^2(9R_1 + R_{1/3})^2 - 81B^2R_1 = 0, \\
& A_{1/3}^2 + k^2 - \frac{81}{16}R_1R_{1/3} = 0,
\end{aligned}
\right\} \quad (4.34)
$$

$$-\frac{3}{2}\left(R_1+R_{1/3}+\frac{2}{3}Z\right)z-B_3=0.$$

The stability conditions are

$$\left.\begin{array}{ll}
\left(R_1+R_{1/3}+2Z-\frac{1}{54}\right)^2-4R_{1/3}Z+\frac{1}{81}k^2>0, & \text{for } n=1,\\[2mm]
\left(R_1+R_{1/3}+2Z-\frac{2}{27}\right)^2-\left(R_1+\frac{1}{4}R_{1/3}+\frac{2}{9}R_{1/3}\right)R_{1/3}+\frac{4}{81}k^2>0, & \text{for } n=2,\\[2mm]
\left(R_1+R_{1/3}+2Z-\frac{1}{5}\right)^2-4R_1Z+\frac{1}{9}k^2>0. & \text{for } n=3,\\[2mm]
\left(R_1+R_{1/3}+2Z-\frac{8}{27}\right)^2-R_1R_{1/3}+\frac{16}{81}k^2>0, & \text{for } n=4,\\[2mm]
\left(R_1+R_{1/3}+2Z-\frac{25}{54}\right)^2+\frac{25}{81}k^2>0, & \text{for } n=5,\\[2mm]
\left(R_1+R_{1/3}+2Z-\frac{2}{3}\right)^2-\frac{1}{4}R_1^2+\frac{4}{9}k^2>0, & \text{for } n=6.
\end{array}\right\}\quad(4.35)$$

If the condition for $n=m$ is not satisfied, the periodic solution (4.26) becomes unstable owing to the build-up of a self-excited oscillation having the frequency $m/6$. The conditions for $n=4$, 5, and 6 are superfluous in this particular case, since they are always satisfied by the coefficients of (4.26). Therefore the conditions for $n=1$, 2, and 3 must be ascertained for stability of the periodic solution.

See Appendix III as for the regions in which the harmonic, 1/2-harmonic, and 1/3-harmonic oscillations are sustained.

4.3.2 Domains of Attraction leading to Harmonic, 1/2-Harmonic, and 1/3-Harmonic Responses

Proceeding analogously to Section 4.2.3 we may determine, in the $v, \dot{v}$ plane, the domains of attraction leading to the respective types of oscillations.

Numerical Example

We consider the Duffing's equation

$$\frac{d^2 v}{d\tau^2} + 0.05\frac{dv}{d\tau} + v^3 = 0.14\cos\tau + 0.005. \tag{4.36}$$

For these particular values of the parameters, i.e., $k = 0.05$, $B = 0.14$, and $B_0 = 0.005$ in (4.23),* the periodic solutions are first sought by using the relations in Section 4.3.1. Then their stability is investigated also. The fixed points of the mapping in the v, $\dot{v}$ plane and the related properties are listed in Table 4.2.

Table 4.2 Fixed Points and Related Properties correlated with the Periodic Solutions of (4.36)

Fixed Point	Response	v	$\dot{v}$	α**	Stability
1	Harmonic	-0.036	0.008		Stable
2	Harmonic	1.111	0.665		Stable
3	Harmonic	-0.996	0.513	1.054	Unstable
4	1/2-Harmonic	0.415	0.080		Stable
5	1/2-Harmonic	-0.638	-0.001		Stable
6	1/2-Harmonic	0.235	0.166	-0.601	Unstable

* These parameters are chosen such that three types of periodic solutions, (4.24), (4.25), and (4.26), exist for (4.36) depending on different values of the initial conditions.

7	1/2-Harmonic	-0.597	-0.088	2.994	Unstable
8	1/3-Harmonic	0.241	0.027		Stable
9	1/3-Harmonic	-0.313	-0.102		Stable
10	1/3-Harmonic	-0.571	0.123		Stable
11	1/3-Harmonic	0.045	0.071	-0.674	Unstable
12	1/3-Harmonic	-0.187	-0.066	-0.194	Unstable
13	1/3-Harmonic	-0.357	0.030	0.199	Unstable

** α is the direction of the boundary curve between domains of attraction at the unstable fixed point.

The trajectories of the stable solutions are shown in Fig. 4.5. The small circles in the figure indicate the location of the fixed points of the mapping. The domains of attraction leading to harmonic, 1/2-harmonic, and 1/3-harmonic responses are also shown in Fig. 4.6. The boundaries between the domains of attraction were obtained by starting just on both sides (in the direction of α) of the unstable fixed points and integrating (4.36) for decreasing time. Similarly to the case of Fig. 4.4, the domain of attraction leading to the fixed point 2 exist outside of those domains, but is omitted in the figure.

4.4 Conclusion

The domains of attraction leading to the different types of the periodic solutions have been determined by making use of the mapping theorem in the phase plane. This method of analysis does not resort to the method of variation of parameters which assume the slowly varying amplitude and phase of the oscillation during the transient state. Therefore the results obtained in this chapter are superior to those described in the earlier reports [11, 30].

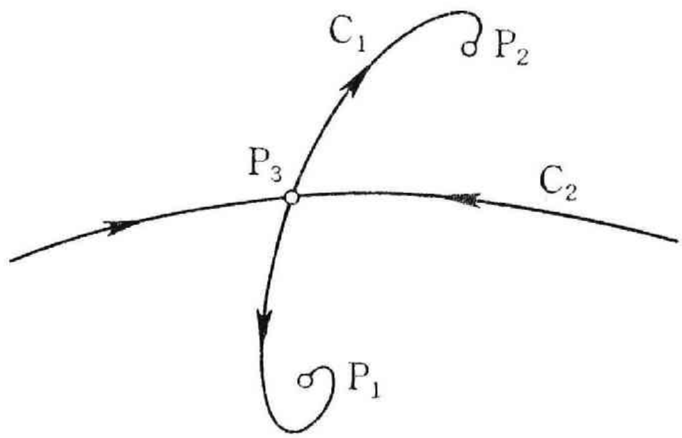

Fig. 4.1 Fixed points and invariant curves under the mapping.

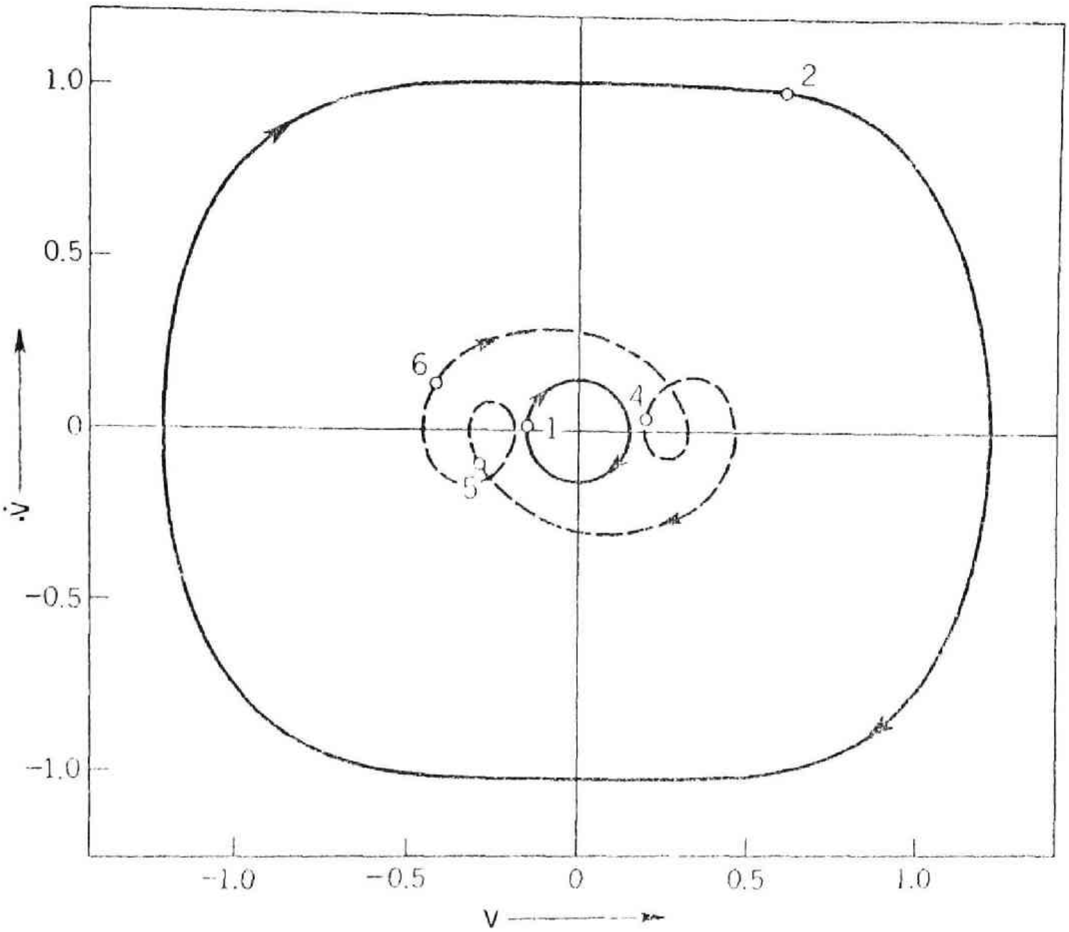

Fig. 4.2 Trajectories of the stable solutions for Eq. (4.22).

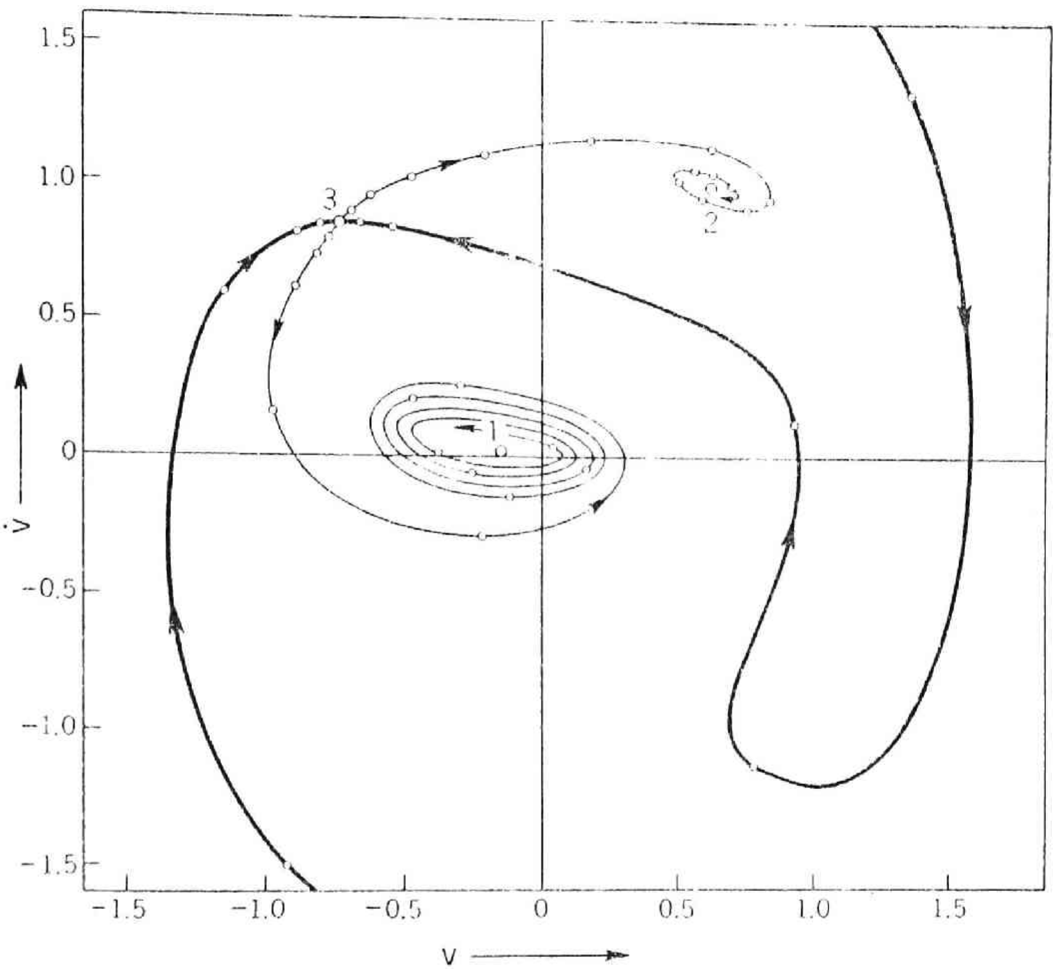

Fig. 4.3 The loci of image points under iterations of the mapping (harmonic response).

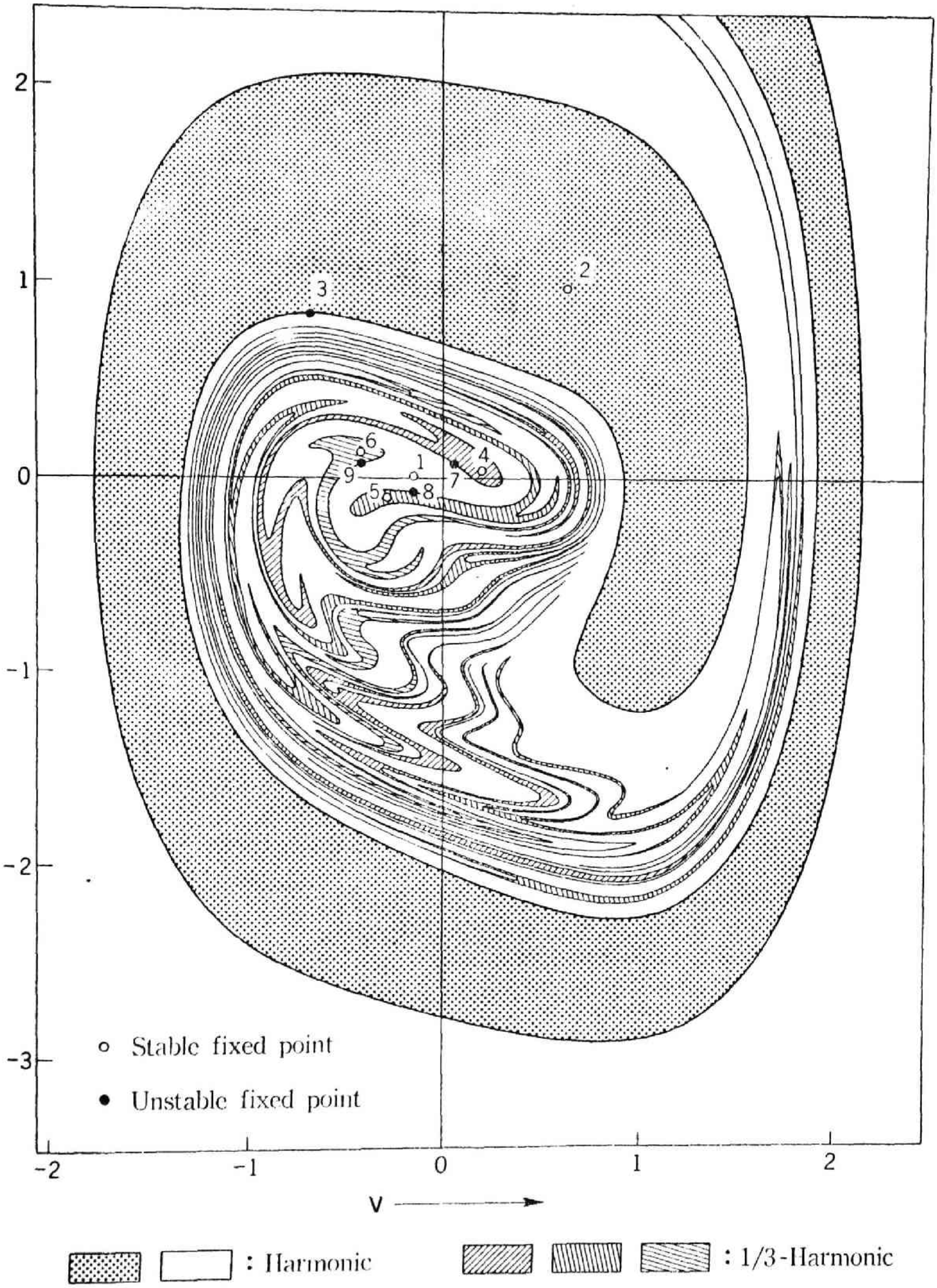

Fig. 4.4 Domains of attraction leading to harmonic and 1/3-harmonic responses.

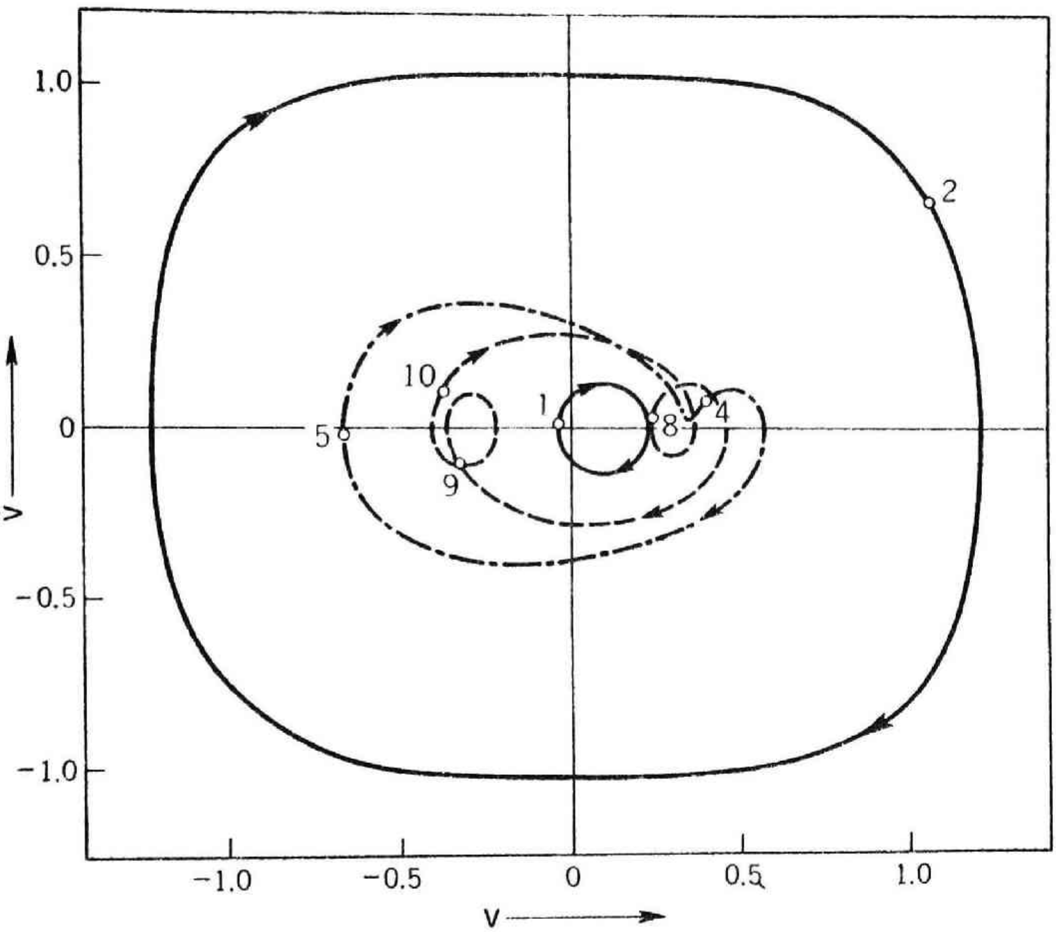

Fig. 4.5 Trajectories of the stable solutions for Eq. (4.36).

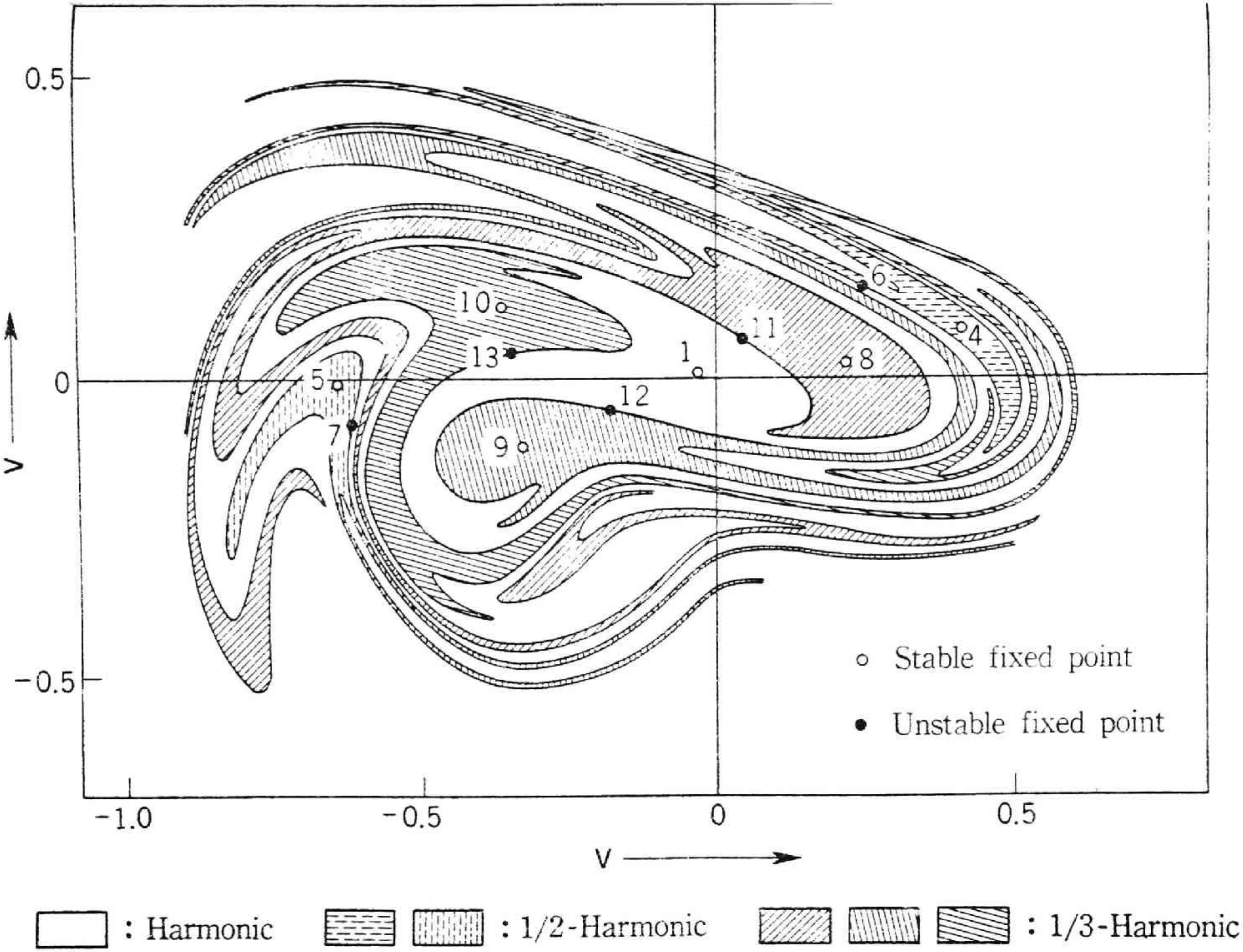

Fig. 4.6 Domains of attraction leading to harmonic, 1/2-harmonic, and 1/3-harmonic responses.

CHAPTER V

QUASI-PERIODIC OSCILLATIONS

5.1 Introduction

When a periodic force is applied to a nonlinear system, the steady-state response of the system may usually, but not necessarily, be periodic. When it is periodic, as described in the two chapters preceding, the fundamental period of the response is the same as the period of the applied force or equal to an integral multiple of that period. There are also certain special cases in which the response of a nonlinear system is not periodic even when subjected to a periodic applied force. This chapter deals with the so-called "quasi-periodic oscillation" where the amplitude and phase of the oscillation vary slowly but periodically in the steady-state [27, 30, 18]. The ratio between the period for amplitude variation and the period of the applied force is in general irrational, and thus there is no periodicity in the quasi-periodic oscillation.

An experimental investigation has been reported by W. T. Thomson [27] concerning the quasi-periodic oscillation in a magnetic amplifier circuit. This kind of oscillation also occurs in a logical circuit with parametric excitation and in various systems with nonlinear elements [24; 30, pp. 105-116; 6; 3 , pp. 283-294]. Two representative cases of the quasi-periodic oscillation are studied in the present chapter. The first is the case in which a harmonic oscillation in a resonant nonlinear circuit becomes unstable and chages into a quasi-periodic oscillation. The second case deals with the quasi-periodic oscillation which develops from a subharmonic oscillation of order 1/2 in a parametric excitation circuit.

5.2 Quasi-Periodic Oscillations in a Resonant Circuit with D-C Superposed

The circuit schematic is shown in Fig. 5.1. Under the impression of a sinusoidal voltage $E_1 \sin\omega t$, the resulting harmonic oscillation may have one of two different amplitudes, depending on the initial conditions. This phenomenon is known by the name ferroresonance which occurs owing to the nonlinearity of the saturable iron cores L_1 and L_2. Furthermore, when a D-C bias is superposed as in the figure, a quasi-periodic oscillation may also occur.

5.2.1 The Circuit Equations

Following the notations in Fig. 5.1, the circuit equations may be written as follows:

$$\left.\begin{aligned} & n\frac{d}{dt}(\phi_1+\phi_2)+R_1 i_R = E_1 \sin\omega t, \\ & n\frac{d}{dt}(\phi_1-\phi_2)+R_2 i_2 = E_0, \\ & R_1 i_R = \frac{1}{C}\int i_C\,dt, \quad i_1 = i_R + i_C, \end{aligned}\right\} \tag{5.1}$$

where ϕ_1 and ϕ_2 are the magnetic fluxes in the cores L_1 and L_2 respectively, and n is the number of turns of the coils wound around the cores (the same number of turns is assumed for each coil). The nonlinear characteristics of the cores are assumed to be

$$c_3\phi_1^3 = ni_1 + ni_2, \quad c_3\phi_2^3 = ni_1 - ni_2, \tag{5.2}$$

where c_3 is a constant dependent on the nature of the cores. Introducing the dimensionless variables u_1, u_2, v_1, v_2, k_1, k_2, and τ defined by

$$\left.\begin{aligned} & i_1 = I_n u_1, \quad i_2 = I_n u_2, \quad \phi_1 = \Phi_n v_1, \quad \phi_2 = \Phi_n v_2, \end{aligned}\right\} \tag{5.3}$$

$$k_1 = \frac{1}{\omega C R_1}, \quad k_2 = \omega C R_2, \quad \tau = \omega t - \tan^{-1} k,$$

and fixing the base quantities I_n and Φ_n in (5.3) by

$$n\omega^2 C \Phi_n = I_n, \quad c_3 \Phi_n^3 = n I_n, \tag{5.4}$$

Equations (5.1) and (5.2) may be written in normalized form as follows:*

$$\left.\begin{aligned} &\ddot{a} + k_1 \dot{a} + u_1 = B\cos\tau, \\ &\dot{b} + k_2 u_2 = B_0, \end{aligned}\right\} \tag{5.5}$$

and

$$v_1^3 = u_1 + u_2, \quad v_2^3 = u_1 - u_2, \tag{5.6}$$

where

$$\left.\begin{aligned} &v_1 + v_2 = a, \quad v_1 - v_2 = b, \\ &B = \frac{E_1}{n\omega\Phi_n}\sqrt{1 + k_1^2}, \quad B_0 = \frac{E_0}{n\omega\Phi_n}. \end{aligned}\right\} \tag{5.7}$$

Substituting (5.6) into (5.5), we obtain the simultaneous equations with respect to the variables a and b, i.e.,

$$\left.\begin{aligned} &\ddot{a} + k_1 \dot{a} + \frac{1}{8}(a^2 + 3b^2)a = B\cos\tau, \\ &\dot{b} + \frac{1}{8} k_2 (3a^2 + b^2) b = B_0. \end{aligned}\right\} \tag{5.8}$$

Since we are concerned with the harmonic oscillation which has the same frequency as the impressed voltage, the variables a and b may be assumed to

---

* Here and throughout this chapter dots over a quantity refer to differentiations with respect to τ.

take the form

$$\left.\begin{aligned} a &= x(\tau)\sin\tau + y(\tau)\cos\tau, \\ b &= z(\tau), \end{aligned}\right\} \tag{5.9}$$

where $x(\tau)$, $y(\tau)$, and $z(\tau)$ are slowly-varying functions of the time τ.

Substituting (5.9) into (5.8) and equating the coefficients of the terms containing $\cos\tau$ and $\sin\tau$ and the nonoscillatory terms separately to zero, we obtain

$$\left.\begin{aligned} \dot{x} &= \frac{1}{2}[-k_1 x + Ay + B] \equiv X(x, y, z), \\ \dot{y} &= \frac{1}{2}[-Ax - k_1 y] \equiv Y(x, y, z), \\ \dot{z} &= B_0 - \frac{1}{16}k_2(3r^2 + 2z^2)z \equiv Z(x, y, z), \end{aligned}\right\} \tag{5.10}$$

with

$$A = 1 - \frac{3}{32}(r^2 + 4z^2), \quad r^2 = x^2 + y^2,$$

under the assumptions that $x(\tau)$, $y(\tau)$, and $z(\tau)$ are slowly-varying functions of the time τ so that $\ddot{x}(\tau)$, $\ddot{y}(\tau)$, and $\ddot{z}(\tau)$ may be neglected, and that k_1 is a sufficiently small quantity and hence $k_1\dot{x}(\tau)$, $k_1\dot{y}(\tau)$, and $k_1\dot{z}(\tau)$ are also discarded. The results which will be obtained from (5.10) may not account for the occurrence of a pronounced higher harmonic or subharmonic oscillation. But, as far as we deal with the harmonic oscillation, (5.10) may be considered to be legitimate.

5.2.2 Periodic Solutions and Conditions for Stability

We consider the periodic state in which $x(\tau)$, $y(\tau)$, and $z(\tau)$ in (5.9) are constant, so that

$$\dot{x} = 0, \quad \dot{y} = 0, \quad \dot{z} = 0.$$

Substituting these conditions in (5.10), the components x_0, y_0, and z_0 of the periodic solution are determined by

$$\left.\begin{aligned} &k_1 x_0 - A y_0 = B, \\ &A x_0 + k_1 y_0 = 0, \\ &\frac{1}{16} k_2 (3 r_0^2 + 2 z_0^2) z_0 = B_0, \\ \text{with} \quad &A = 1 - \frac{3}{32}(r_0^2 + 4 z_0^2), \quad r_0^2 = x_0^2 + y_0^2. \end{aligned}\right\} \tag{5.11}$$

Eliminating x_0 and y_0 from the first and second equations of (5.11) leads to

$$(A^2 + k_1^2) r_0^2 = B^2. \tag{5.12}$$

Equation (5.12), together with the third equation of (5.11), determines the values of r_0 and z_0, and the components x_0, y_0, of the amplitude r_0 are found to be

$$x_0 = \frac{k_1 r_0^2}{B}, \qquad y_0 = -\frac{A r_0^2}{B}, \tag{5.13}$$

The periodic solution, i.e., the equilibrium state of the system (5.10) is correlated with the singular point (x_0, y_0, z_0) in the x, y, z phase space. If the singular point is stable, the corresponding periodic solution is also stable; if not, it is unstable. The stability of the singular point is studied by the behavior of integral curves in the neighborhood of that singular point. To this end we consider sufficiently small variations ξ, η, and ζ from the equilibrium state defined by

$$\xi = x - x_0, \quad \eta = y - y_0, \quad \zeta = z - z_0. \tag{5.14}$$

Then, if these variations ξ , η , and ζ tend to zero with increasing τ, the solutions are stable. Substituting (5.14) into (5.10), we obtain

$$\left.\begin{aligned}
\dot{\xi} &= a_{11}\xi + a_{12}\eta + a_{13}\zeta, \\
\dot{\eta} &= a_{21}\xi + a_{22}\eta + a_{23}\zeta, \\
\dot{\zeta} &= a_{31}\xi + a_{32}\eta + a_{33}\zeta, \\
\text{with} & \\
a_{11} &= \left(\frac{\partial X}{\partial x}\right)_0 = \frac{1}{2}\left(-\frac{3}{16}x_0 y_0 - k_1\right), \\
a_{12} &= \left(\frac{\partial X}{\partial y}\right)_0 = \frac{1}{2}\left(A - \frac{3}{16}y_0^2\right), \\
a_{13} &= \left(\frac{\partial X}{\partial z}\right)_0 = -\frac{3}{8}y_0 z_0, \\
a_{21} &= \left(\frac{\partial Y}{\partial x}\right)_0 = \frac{1}{2}\left(-A + \frac{3}{16}x_0^2\right), \\
a_{22} &= \left(\frac{\partial Y}{\partial y}\right)_0 = \frac{1}{2}\left(\frac{3}{16}x_0 y_0 - k_1\right), \\
a_{23} &= \left(\frac{\partial Y}{\partial z}\right)_0 = \frac{3}{8}x_0 z_0, \\
a_{31} &= \left(\frac{\partial Z}{\partial x}\right)_0 = -\frac{3}{8}k_2 x_0 z_0, \\
a_{32} &= \left(\frac{\partial Z}{\partial y}\right)_0 = -\frac{3}{8}k_2 y_0 z_0, \\
a_{33} &= \left(\frac{\partial Z}{\partial z}\right)_0 = -\frac{3}{16}k_2\left(r_0^2 + 2z_0^2\right),
\end{aligned}\right\} \qquad (5.15)$$

where $\left(\frac{\partial X}{\partial x}\right)_0, \ldots, \left(\frac{\partial Z}{\partial z}\right)_0$ stand for $\frac{\partial X}{\partial x}, \ldots, \frac{\partial Z}{\partial z}$ at $x = x_0$, $y = y_0$, and $z = z_0$. The characteristic equation of the system (5.15) is

$$\left.\begin{aligned}
&\begin{vmatrix} a_{11}-\lambda & a_{12} & a_{13} \\ a_{21} & a_{22}-\lambda & a_{23} \\ a_{31} & a_{32} & a_{33}-\lambda \end{vmatrix} = 0, \\
&\text{or} \\
&\lambda^3 + b_1\lambda^2 + b_2\lambda + b_3 = 0, \\
&\text{where} \\
&b_1 = -(a_{11}+a_{22}+a_{33}), \\
&b_2 = \begin{vmatrix} a_{11} & a_{12} \\ a_{21} & a_{22} \end{vmatrix} + \begin{vmatrix} a_{11} & a_{13} \\ a_{31} & a_{33} \end{vmatrix} + \begin{vmatrix} a_{22} & a_{23} \\ a_{32} & a_{33} \end{vmatrix}, \\
&b_3 = -\begin{vmatrix} a_{11} & a_{12} & a_{13} \\ a_{21} & a_{22} & a_{23} \\ a_{31} & a_{32} & a_{33} \end{vmatrix} \equiv \Delta.
\end{aligned}\right\} \tag{5.16}$$

By making use of the Routh-Hurwitz's criterion, the system (5.15), and consequently the periodic solutions, are stable provided that

$$\left.\begin{aligned}
&b_1 > 0, \\
&b_1 b_2 - b_3 > 0, \\
&b_3 > 0.
\end{aligned}\right\} \tag{5.17}$$

The first condition of (5.17) is fulfiled from the outset, because, by (5.15)

$$b_1 = -(a_{11}+a_{22}+a_{33}) = k_1 + \frac{3}{16} k_2 (r_0^2 + 2z_0^2) > 0. \tag{5.18}$$

By virtue of (5.15) and (5.16), b_2 and b_3 are written as

$$\left.\begin{aligned} b_2 &= \frac{1}{4}\left[\frac{B^2}{r_0^2} - \frac{3}{16}Ar_0^2 + \frac{3}{4}k_1k_2(r_0^2+2z_0^2)\right], \\ b_3 &= -\Delta = \frac{3}{64}k_2\left[\frac{B^2}{r_0^2}(r_0^2+2z_0^2) - \frac{3}{16}Ar_0^2(r_0^2+6z_0^2)\right]. \end{aligned}\right\} \tag{5.19}$$

Substituting (5.18) and (5.19) into the second condition of (5.17), we obtain

$$k_1\left(\frac{B^2}{r_0^2} - \frac{3}{16}Ar_0^2\right) + \frac{3}{4}k_2\Big\{k_1\left[k_1 + \frac{3}{64}k_2(r_0^2+2z_0^2)\right] (r_0^2+2z_0^2) - \frac{3}{8}Ar_0^2z_0^2\Big\} > 0. \tag{5.20}$$

The third condition of (5.17) is rewritten as

$$\frac{3}{4}\left(1 - \frac{3}{32}r_0^2 - \frac{3}{8}z_0^2\right)r_0^2z_0\frac{dB_0}{dr_0^2} = \left(\frac{B^2}{r_0^2} - \frac{3}{16}Ar_0^2\right)z_0\frac{dB_0}{dz_0^2} > 0. \tag{5.21}$$

After all, the conditions for stability are given by the inequalities (5.21) and (5.22).

Numerical analysis of the periodic solutions shows that various types of the oscillations exist according to the different values of the system parameters. They are as follows:

Case 1 - There exists only one unstable periodic solution.

Case 2 - There exists only one stable periodic solution.

Case 3 - There exist three periodic solutions; one of them is stable and the others are unstable.

Case 4 - There exist three periodic solutions; two of them are stable and the other one is unstable.

Case 5 - There exist five periodic solutions; two of them are stable and the others are unstable.

5.2.3 Quasi-Periodic Oscillations

As mentioned in the preceding section, when an oscillation is represented by a stable singular point in x , y , z space, the oscillation has invariable amplitude and phase angle. In contrast with this, when a representative point, whose coordinates are $x(\tau)$, $y(\tau)$, and $z(\tau)$, keeps on moving along a limit cycle with increasing time τ, the amplitude and phase of the oscillation vary slowly but periodically; i.e., a quasi-periodic oscillation occurs. The ratio between the period for amplitude variation and the period of the applied force is in general irrational, and thus there is no periodicity in the quasi-periodic oscillation.

It is very difficult to discuss rigorously the existence and the stability of limit cycles in general. But, if there is no stable singular point in a system, as in Case 1 in the preceding section, we may presume that there exists at least one stable limit cycle. In order to explain the occurrence of the quasi-periodic oscillation in such a system, now we consider a special case in which k_2 and B_0 are much less than k_1. Under this condition, one obtains $\dot{z} \ll \dot{x}$ and $\dot{z} \ll \dot{y}$, so that the behavior of the representative point (x, y, z) is first governed by

$$\dot{x} = \frac{1}{2}\left[-k_1 x + Ay + B\right], \quad \dot{y} = \frac{1}{2}\left[-Ax - k_1 y\right],$$

and the point approaches the characteristic curve defined by $\dot{x} = 0$ and $\dot{y} = 0$, or

$$(A^2 + k_1^2) r^2 = B^2. \tag{5.22}$$

During this transient $Z(\tau)$ is held nearly constant. After this period $\dot{x}$, $\dot{y}$, and $\dot{z}$ will all be of the same order in magnitude. In Fig. 5.2 is shown the characteristic curve (5.22) for which k_1=0.20 and B =0.50. Also plotted in the figure is the curve represented by

$$\dot{z} = B_0 - \frac{1}{16} k_2 (3r^2 + 2z^2) z = 0, \tag{5.23}$$

for a particular case of $B_0 = k_2$. The intersection P of these curves represents an equilibrium state, since the point P is satisfied by (5.11). However, it will readily be verified by (5.20) that this equilibrium state is unstable. Since $\dot{z}$ is negative in the region above the curve (5.23) and positive below the curve, the representative point will gradually move in the direction of the arrows with increasing τ. Hence, discontinuous jumps occur at the limiting points Q and R , and the representative point keeps on moving near the limit cycle represented by the thick line in the figure.

The description so far explains the occurrence of the limit cycle for the case in which the system parameters k_2 and B_0 are very small. The shape of the limit cycle in an actual system will be different more or less from that illustrated in Fig. 5.2. Further, the time required for the representative point to complete one revolution along the limit cycle decreases with the increase in k_2 and B_0 . A more concrete example of the limit cycle will be given in the following section.

We confined the consideration to the system where only one unstable equilibrium state exists. However we can expect the existence of limit cycles also in the system where the stable equilibrium states exist in addition to the unstable ones. We obtained several examples of such cases by making use of an analog computer.

5.2.4 Numerical Examples

A numerical analysis of the system (5.10) was carried out for the parameters as given by

$$k_1=0.20, \quad k_2=0.03, \quad B=0.50, \quad \text{and} \quad B_0=0.03. \qquad (5.24)$$

In this case there are no stable equilibrium state. After a sufficiently long period of time τ, a representative point moves along the limit cycle as illustrated in Fig. 5.3 or 5.4. Figure 5.3 shows the projections of the limit cycle on the x, y and x, z phase planes, while Fig. 5.4 shows the limit cycle in the x, y, z space. The time intervals between two successive points on the curves are 2π or equal to one cycle of the applied force. The time required for the representative point to complete one revolution along the limit cycle is $2\pi \times 15.5...$; thus a nonperiodic oscillation occurs. Since the projection of the limit cycle on the x, y plane does not contain the origin in its interior, the quasi-periodic oscillation is synchronized with the applied force, even though the waveform is affected by amplitude and phase modulation. The projection of the limit cycle on the r^2, z^2 plane is shown dotted in Fig. 5.2, and compared with the limit cycle theoretically obtained under the condition that $k_2 \to 0$.

5.2.5 Analog-Computer Analysis

Corresponding to the numerical analysis in the preceding section, the case when

$$k_1=0.20, \quad k_2=0.03, \quad B=0.50, \quad \text{and} \quad B_0=0.03,$$

was investigated. The waveforms of a and b in (5.7) are shown in Fig. 5.5. The successive points on the curves show the instants when $\tau = 2n\pi$, n being 1, 2, 3,.... We see in the figure that the amplitude and phase of a, as well as the quantity b, vary slowly with the period $2\pi \times 17.1$.... This fact assures the assumption in Section 5.2.1 that the responses may take the form as

$$\left.\begin{aligned} a &= x(\tau)\sin\tau + y(\tau)\cos\tau, \\ b &= z(\tau), \end{aligned}\right\}$$

where $x(\tau)$, $y(\tau)$, and $z(\tau)$ are slowly varying functions of time τ. These quantities $x(\tau)$, $y(\tau)$, and $z(\tau)$ are evaluated from the waveforms of a and b, thus we obtain the limit cycle as shown in Fig. 5.6. The numerical solution described in the preceding section is found to be in satisfactory agreement with the solution obtained in the present section.

5.3 Quasi-Periodic Oscillations in a Parametric Excitation Circuit

The circuit schematic is shown in Fig. 5.7. Under the impression of a sinusoidal voltage $E_1 \sin 2\omega t$, this circuit produces an oscillation which has the fundamental frequency ω, i.e., a subharmonic oscillation of order 1/2. The mechanism which produces this kind of oscillation is known as parametric excitation, and this principle is applied to logical circuits in digital computers.

5.3.1 The Circuit Equations

Following the notations in Fig. 5.7, the circuit equations are written as

$$n\frac{d}{dt}(\phi_1 + \phi_2) + R_1 i_1 = E_1 \sin 2\omega t,$$

$$\left.\begin{aligned} n\frac{d}{dt}(\phi_1-\phi_2) &= -\frac{1}{C}\int i_c dt = -R_2 i_R, \\ i_2 &= i_R + i_c. \end{aligned}\right\} \tag{5.25}$$

It is assumed that the current i_0 is kept constant owing to the high inductance L_0. Proceeding analogously to Section 5.2.1, Eqs. (5.25) are transformed into

$$\dot{a} + k_1 u_1 = B\sin 2\tau,$$
$$\ddot{b} + k_2\dot{b} + u_2 = 0,$$

where

$$i_1 = I_n u_1, \quad i_2 = I_n u_2, \quad \phi_1 = \Phi_n v_1, \quad \phi_2 = \Phi_n v_2,$$
$$v_1 + v_2 = a, \quad v_1 - v_2 = b, \quad \tau = \omega t,$$
$$k_1 = \omega C R_1, \quad k_2 = \frac{1}{\omega C R_2}, \quad B = \frac{E_1}{n\omega\Phi_n}, \tag{5.26}$$

and the base quantities I_n and Φ_n are fixed by the same equations as (5.4). The nonlinearlities of the cores L_1 and L_2 are expressed, after normalization, by

$$v_1^3 = u_0 + u_1 + u_2, \quad v_2^3 = u_0 + u_1 - u_2, \tag{5.27}$$

where $i_0 = I_n u_0$. By virtue of (5.27), Eqs. (5.26) lead to

$$\left.\begin{aligned} \dot{a} + \tfrac{1}{8}k_1[(a^2+3b^2)a - 8u_0] &= B\sin 2\tau, \\ \ddot{b} + k_2\dot{b} + \tfrac{1}{8}(3a^2+b^2)b &= 0. \end{aligned}\right\} \tag{5.28}$$

We consider the case in which k_1 is small. The first equation of (5.28) then has an approximate solution

$$a = -\frac{B}{2}\cos 2\tau + a_0, \tag{5.29}$$

a_0 being an integrating constant. The second equation of (5.28), upon substitution of (5.29), leads to a form of Hill's equation with terms for damping and nonlinearity. The solution may have the fundamental period 2π, i.e., twice the period of the applied force. Hence, an approximate solution for (5.28) may be expected to have the form

$$\left.\begin{aligned} a &= -w\cos 2\tau + z(\tau), \qquad w = \frac{B}{2}, \\ b &= x(\tau)\sin\tau + y(\tau)\cos\tau, \end{aligned}\right\} \tag{5.30}$$

where $x(\tau)$, $y(\tau)$, and $z(\tau)$ are slowly varying functions of time τ. Substituting (5.30) into (5.28) and equating the coefficients of the terms containing $\cos\tau$ and $\sin\tau$ and the nonoscillatory terms separately to zero, we obtain

$$\left.\begin{aligned} \dot{x} &= \frac{1}{2}\left[-k_2 x + Ay + \frac{3}{8}wyz\right] \equiv X(x,y,z), \\ \dot{y} &= \frac{1}{2}\left[-Ax - k_2 y + \frac{3}{8}wxz\right] \equiv Y(x,y,z), \\ \dot{z} &= -\frac{1}{8}k_1\left[\left(\frac{3}{2}r^2 + \frac{3}{2}w^2 + z^2\right)z + \frac{3}{4}(x^2 - y^2)w - 8u_0\right] \equiv Z(x,y,z), \\ &\text{where} \\ A &= 1 - \frac{3}{32}(r^2 + 2w^2 + 4z^2), \qquad r^2 = x^2 + y^2. \end{aligned}\right\} \tag{5.31}$$

It should, however, be remembered that the same assumptions as those mentioned in Section 5.2.1 must be made for the derivation of (5.31).

5.3.2 Periodic Solutions and Conditions for Stability

The periodic solution for which the components $X(\tau)$, $y(\tau)$, and $Z(\tau)$ are constant is determined by

$$\dot{x} = 0, \quad \dot{y} = 0, \quad \text{and} \quad \dot{z} = 0.$$

Substituting these conditions in (5.31), the components $r_0 (= \sqrt{x_0^2 + y_0^2})$ and z_0 of the periodic solution are given by

$$\left.\begin{aligned} A^2 + k_2^2 &= \left(\frac{3}{8} w z_0\right)^2, \\ \left(\frac{3}{2} r_0^2 + \frac{3}{2} w^2 + z_0^2\right) z_0 + \frac{2 A r_0^2}{z_0} &= 8 u_0. \end{aligned}\right\} \tag{5.32}$$

The components x_0, y_0 , of the amplitude r_0 are found to be

$$\left.\begin{aligned} x_0 &= r_0 \cos\theta, \quad r_0 \cos(\theta + \pi), \\ y_0 &= r_0 \sin\theta, \quad r_0 \sin(\theta + \pi), \end{aligned}\right. $$

where

$$\cos 2\theta = \frac{8A}{3 w z_0}, \quad \sin 2\theta = \frac{8 k_2}{3 w z_0}. \tag{5.33}$$

We see from (5.33) that there are usually two 1/2-harmonic periodic solutions differing in phase by π radians with the same amplitude, if determined. Such two solutions will be called a pair of the 1/2-harmonic solutions.

Proceeding analogously to Section 5.2.2, the stability conditions for the periodic solution are given by

$$\begin{aligned} - k_2 A_0 r_0^2 + k_1 \Big\{ k_2 \Big[\frac{3}{8} k_1 (r_0^2 + w^2 + 2 z_0^2) + 2 k_2\Big] (r_0^2 + w^2 + 2 z_0^2) \\ - \frac{1}{16} (32 - 3 r_0^2 + 12 z_0^2) A_0 r_0^2 - \frac{9}{64} (2 r_0^2 z_0^2 - x_0^2 y_0^2) w^2 \Big\} > 0, \end{aligned}$$

and

$$\left(1 - \frac{3}{32} r_0^2 - \frac{3}{8} z_0^2\right) z_0 \frac{d u_0}{d r_0^2} = \frac{1}{4} \left(1 - \frac{3}{32} r_0^2 - \frac{3}{16} w^2 - \frac{3}{8} z_0^2\right) z_0 \frac{d u_0}{d z_0^2} > 0. \tag{5.34}$$

Numerical analysis of the periodic solutions shows that various types of the oscillations exist according to the different values of the system parameters. They are as follows:

Case 1 - There are two unstable states of the 1/2-harmonic periodic solutions, differing in phase by π radians. The periodic solution without 1/2-harmonic (i.e. $r_0 = 0$) is readily found to be unstable.

Case 2 - There are two pairs of the unstable states of the 1/2-harmonic periodic solutions with different amplitudes. The periodic solution with $r_0 = 0$ is stable.

Case 3 - There are two pairs of the 1/2-harmonic periodic solutions with different amplitudes; among them only one pair is stable. The periodic solution with $r_0 = 0$ is stable.

Case 4 - There are three pairs of the 1/2-harmonic periodic solutions with different amplitudes; among them only one pair is stable. The periodic solution with $r_0 = 0$ is unstable.

Case 5 - There are four pairs of the 1/2-harmonic periodic solutions with different amplitudes; among them only one pair is stable. The periodic solution with $r_0 = 0$ is stable.

5.3.3 Quasi-Periodic Oscillations

A similar procedure to that mentioned in Section 5.2.3 is also applicable to the present investigation. We see from (5.31) that $\dot{z} \ll \dot{x}$ and $\dot{z} \ll \dot{y}$ for a sufficiently small value of k_1. The representative point of the system (5.31) approaches the characteristic curve defined by $\dot{x} = 0$ and $\dot{y} = 0$, or

$$A^2 + k_2^2 = \left(\frac{3}{8} w z\right)^2, \qquad (5.35)$$

and then moves in its neighborhood. Figure 5.8 shows the characteristic curve (5.35) for $k_2 = 0.20$ and $B = 1.00$. The points P_1 and P_2 represent the equilibrium states which are satisfied by (5.32). Both of these states, referring to the stability conditions (5.34), are unstable. Investigating the sign of $\dot{z}$ along the characteristic curve, the representative point gradually moves in the direction of the arrows with increasing τ. Hence, discontinuous jumps occur at the limiting points Q and R, and the representative point keeps on moving near the limit cycle represented by the thick line in the figure.

5.3.4 Numerical Examples

(a) When the system parameters are given by

$$k_1 = 0.20, \quad k_2 = 0.20, \quad B = 1.00, \quad \text{and} \quad u_0 = 0.80. \tag{5.36}$$

A numerical analysis was carried out for the system (5.31) by using these values of the parameters. The representative point keeps on moving along one of the two limit cycles of Fig. 5.9(a) or Fig. 5.10(a). Figure 5.9 shows the projections of the limit cycles on the x, y and x, z planes, while Fig. 5.10 shows the limit cycles in the x, y, z space. The time intervals between two successive points on the limit cycles are 2π or equal to one cycle of the 1/2-harmonic oscillation. The time required for the representative point to complete one revolution along the limit cycle is $\pi \times 14.8 \ldots$.

(b) When the system parameters are given by

$$k_1 = 0.10, \quad k_2 = 0.20, \quad B = 1.00, \quad \text{and} \quad u_0 = 0.80. \tag{5.37}$$

The limit cycle caluculated with these values of the parameters is shown in Fig. 5.9(b) or Fig. 5.10(b). The period of one revolution along the limit cycle is $\pi \times 54.2 \ldots$

(c) Comparison of the Two Examples

There are two distinctive types of the quasi-periodic oscillation as illustrated in Fig. 5.9(a) and (b) or 5.10(a) and (b). The type (a) has two separatelimit cycles which are symmetrically located about the z axis. The projections of these limit cycles on the x, y plane do not contain the origin in their interiors. In this case the quasi-periodic oscillation is synchronized with the applied force, even though the waveform is affected by amplitude and phase modulation. In Fig. 5.9(b) two limit cycles are jointed, resulting in a single loop; the projection on the x, y plane contains the origin in its interior. The quasi-periodic oscillation in this case is not synchronized with the applied force, since one revolution along the limit cycle results in the phase shift by 2π radians or two cycles of the applied force.

5.3.5 Analog-Computer Analysis

The waveforms of $b\,(= v_1 - v_2)$ are shown in Fig. 5.11. The successive points on the curves indicate the instants when $\tau = 2n\pi$, n being 1, 2, 3, ... Figure 5.11(a) is obtained for the system parameters as given by (5.36); the time marks on the curve appear only on the negative side of b. In Fig. 5.11(b) the system parameters are given by (5.37); the time marks appear alternately on both sides of b. The quantities $x(\tau)$, $y(\tau)$, and $z(\tau)$ in (5.30) are evaluated from these waveforms and shown in Fig. 5.12. These limit cycles agree well with those obtained in the preceding section.

6. Conclusion

The two representative cases of the quasi-periodic oscillations have been studied in this chapter. The first is the case in which a harmonic oscillation in a resonant nonlinear circuit becomes unstable and changes into a quasi-periodic oscillation. The second case deals with the quasi-periodic oscillation which develops from a subharmonic oscillation of order 1/2 in a parametric excitation circuit. In short, quasi-periodic oscillations are considered to occur due to the interference between oscillations in a circuit with an applied force and oscillations in a circuit with low impedance elements.

The phase-space analysis has been used for the investigation. A periodic oscillation is correlated with a singular point in the phase space, while a quasi-periodic oscillation is represented by a limit cycle. The occurence of the quasi-periodic oscillation has been explained qualitatively with limiting values of the system parameters. The period required for the representative point to complete one revolution along the limit cycle has been calculated for several numerical examples. It is very difficult in general to distinguish with mathematical rigor between a quasi-periodic oscillation and a periodic oscillation with large period. However it might be reasonable to expect a quasi-periodic oscillation provided the period of the amplitude variation varies continuously with change in the system parameters while the period of the applied force is kept constant.

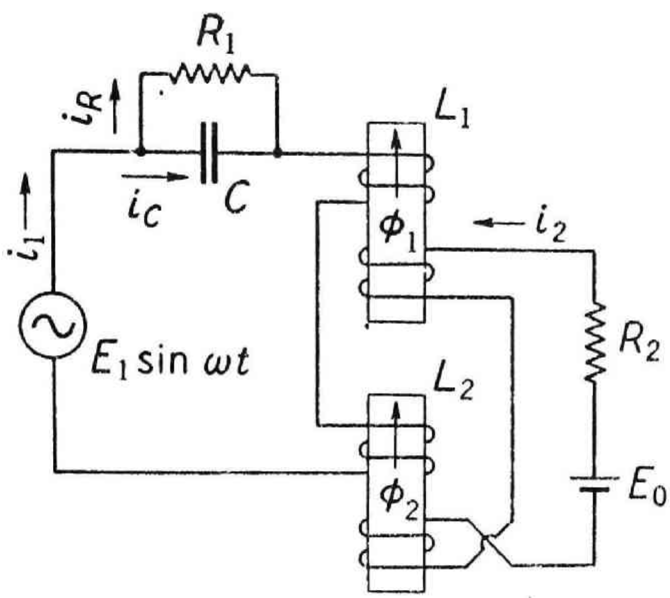

Fig. 5.1 Resonant circuit containing saturable core reactors with secondary d-c windings.

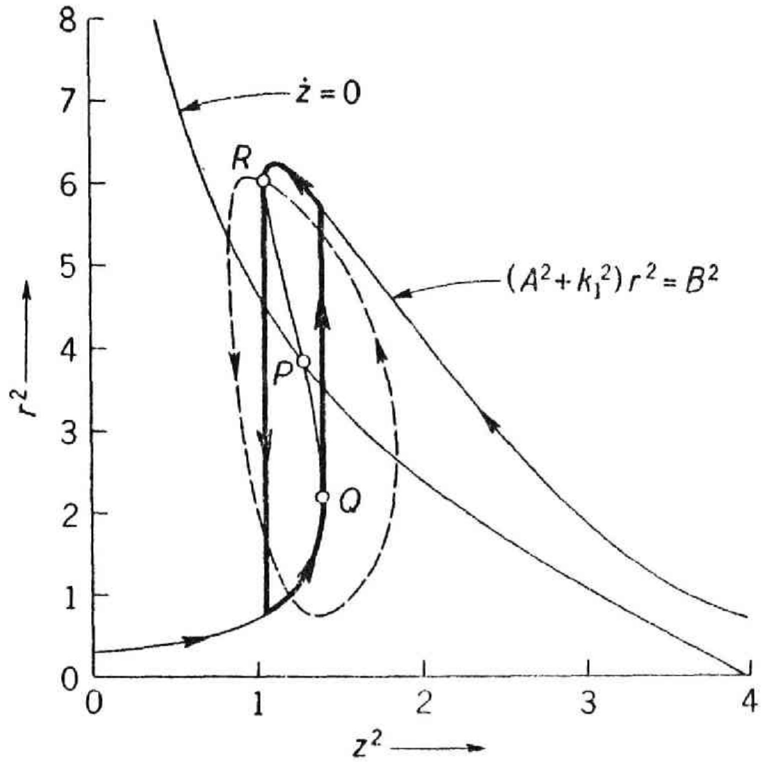

Fig. 5.2 Limit cycle with discontinuities for $k_2 \rightarrow 0$.

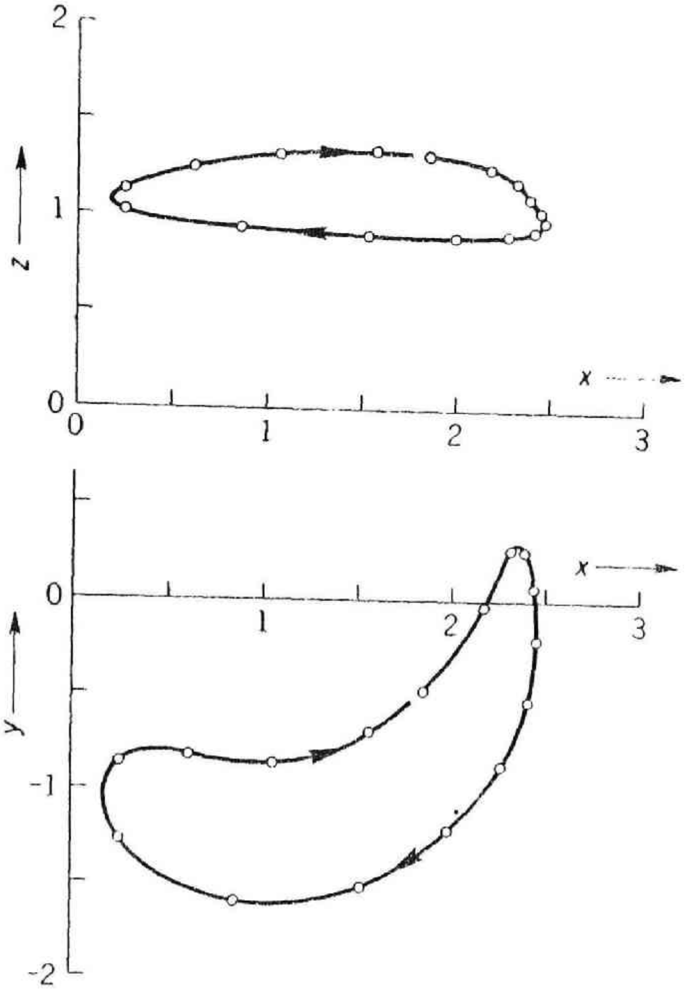

Fig. 5.3 Projections of the limit cycle on the x, y and x, z phase planes. The system parameters are given by Eqs. (5.24).

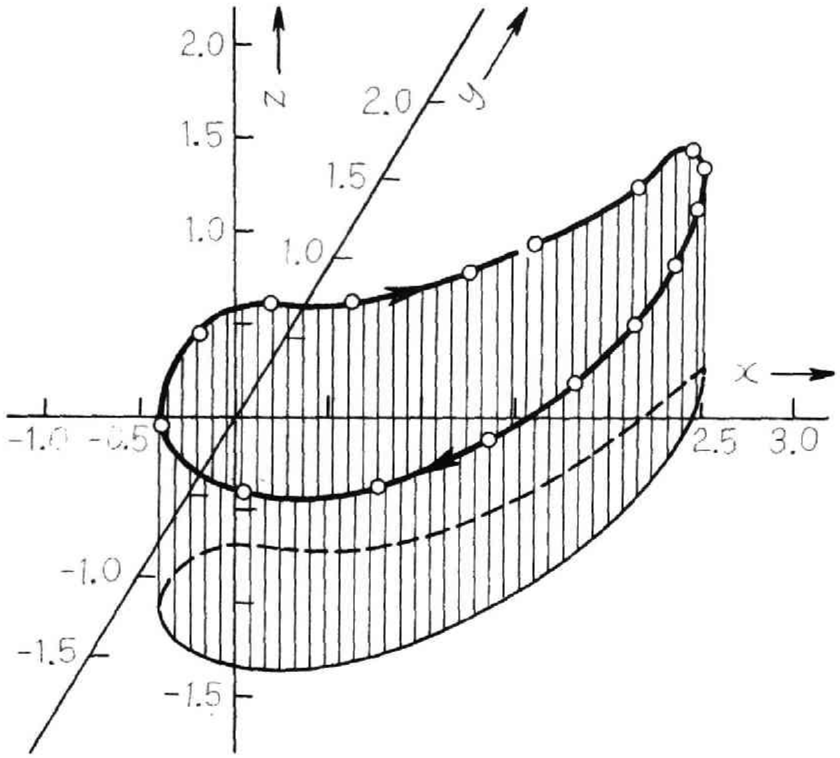

Fig. 5.4 Limit cycle in the x, y, z phase space. The system parameters are given by Eqs. (5.24).

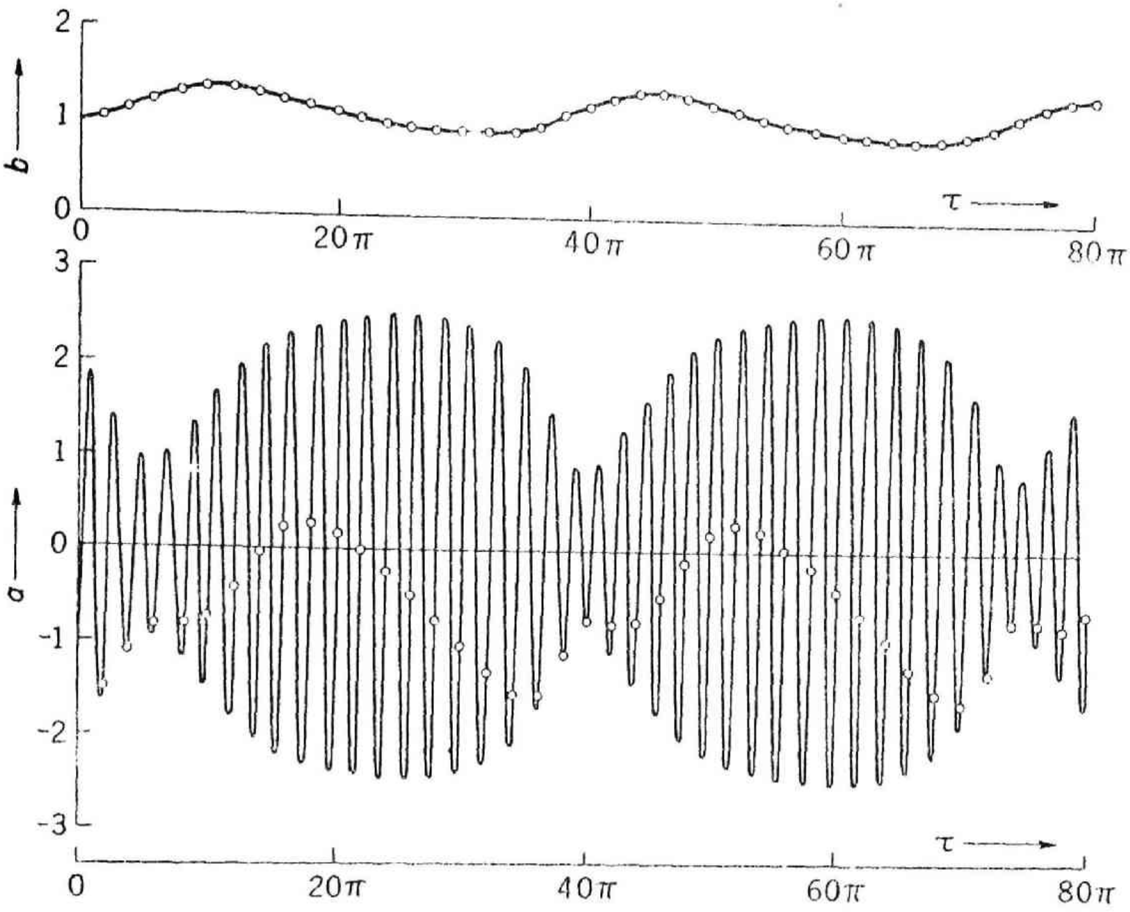

Fig. 5.5 Waveforms of the quasi-periodic oscillation obtained by analog-computer analysis. The system parameters are the same as in the case of Fig. 5.3.

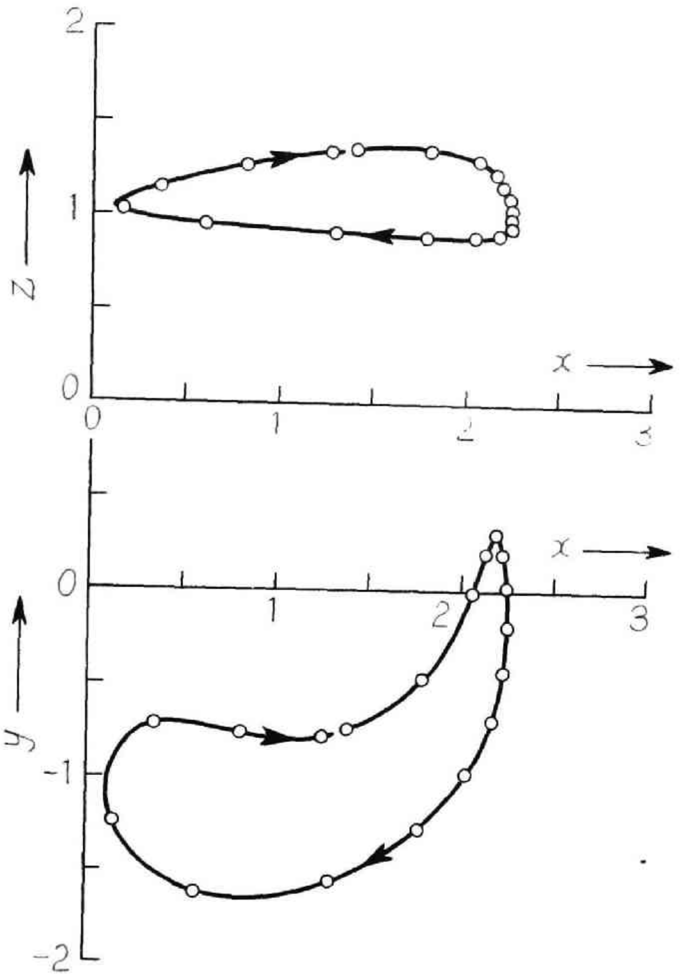

Fig. 5.6 Limit cycle reproduced from the waveforms of Fig. 5.5.

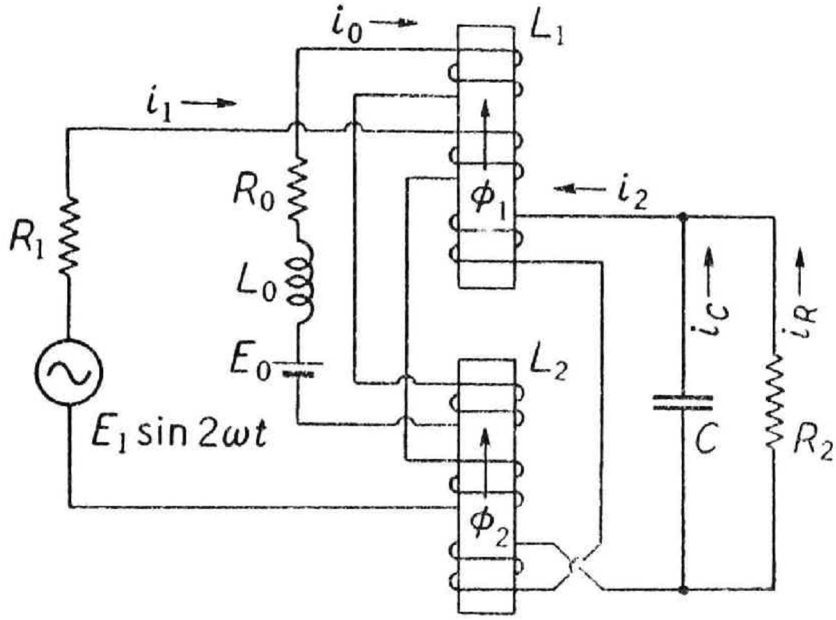

Fig. 5.7 Parametric excitation circuit in which the subharmonic oscillation of order 1/2 occurs.

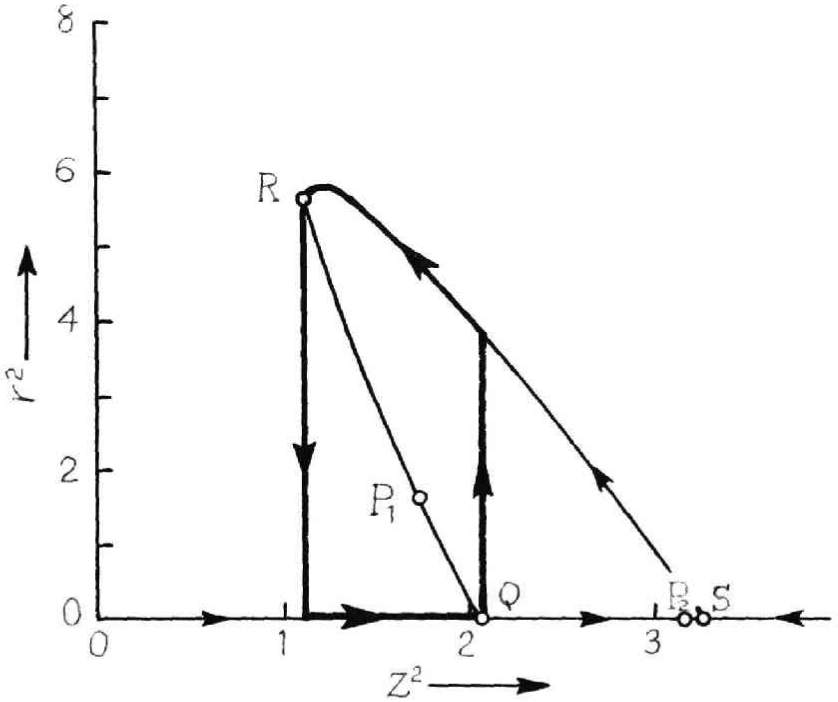

Fig. 5.8 Limit cycle with discontinuities for $k_1 \rightarrow 0$.

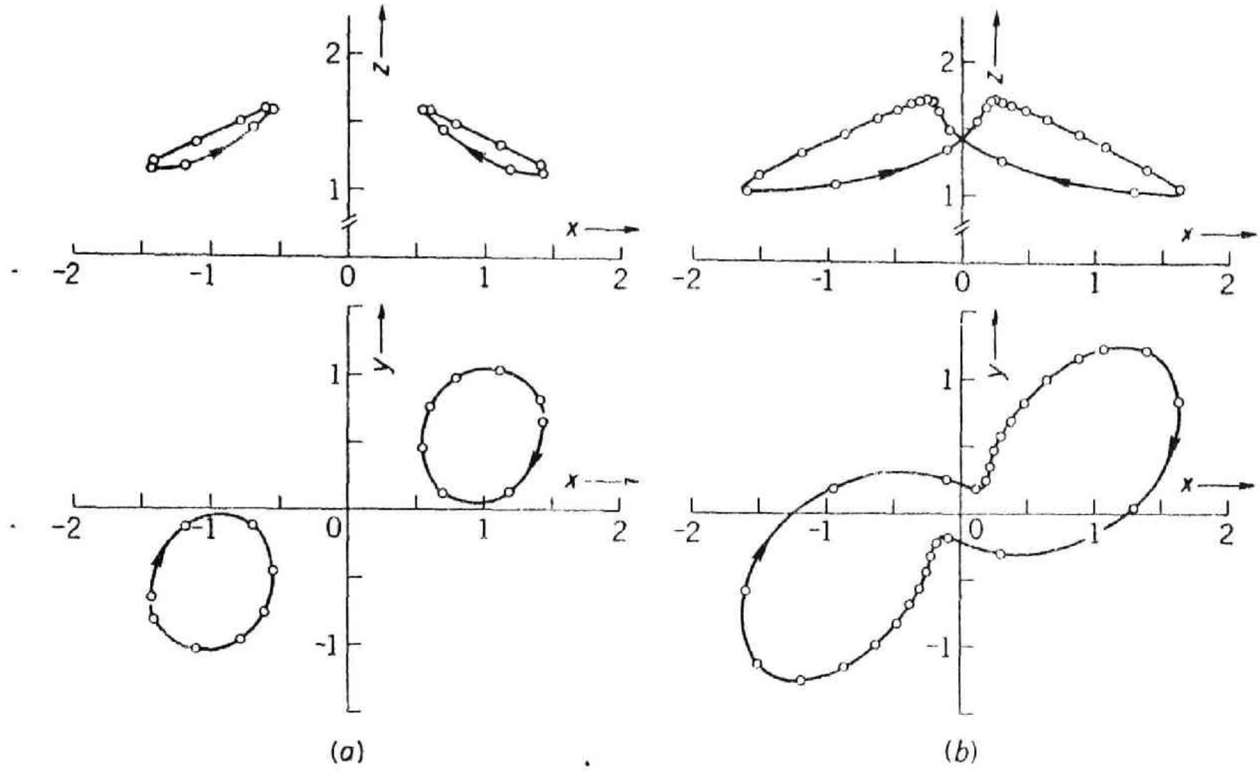

Fig. 5.9 Projections of the limit cycles on the x, y and x, z phase planes. (a) The system parameters are given by Eqs. (5.36). (b) The system parameters are given by Eqs. (5.37).

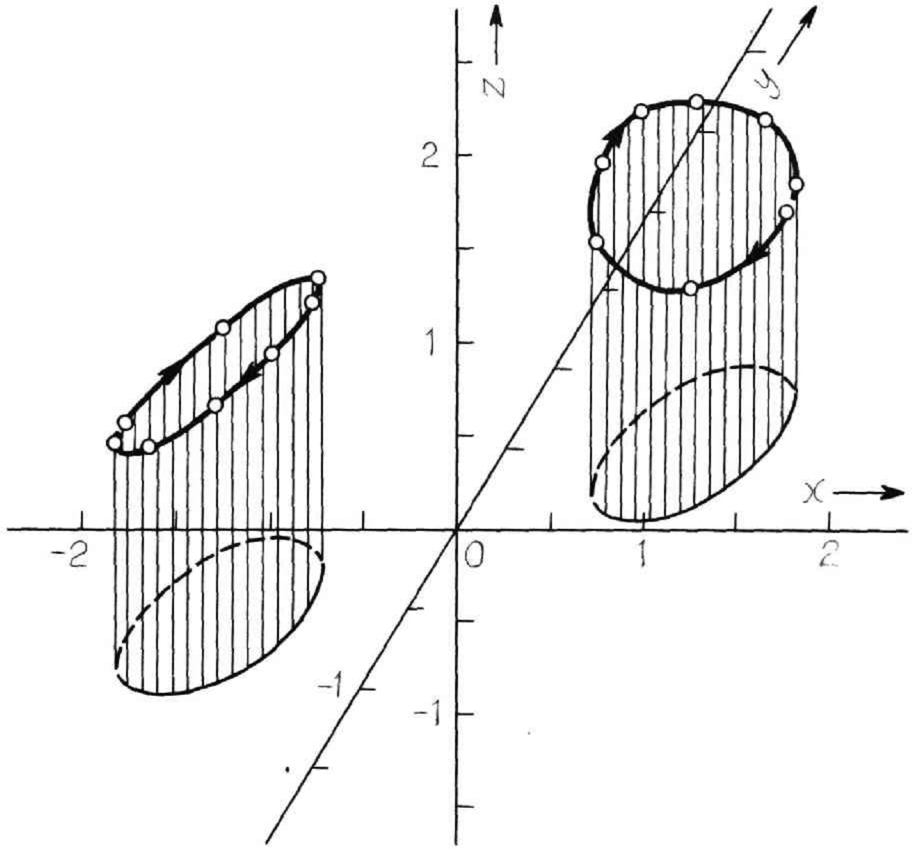

Fig. 5.10(a) Limit cycles in the x, y, z phase space. The system parameters are given by Eqs. (5.36).

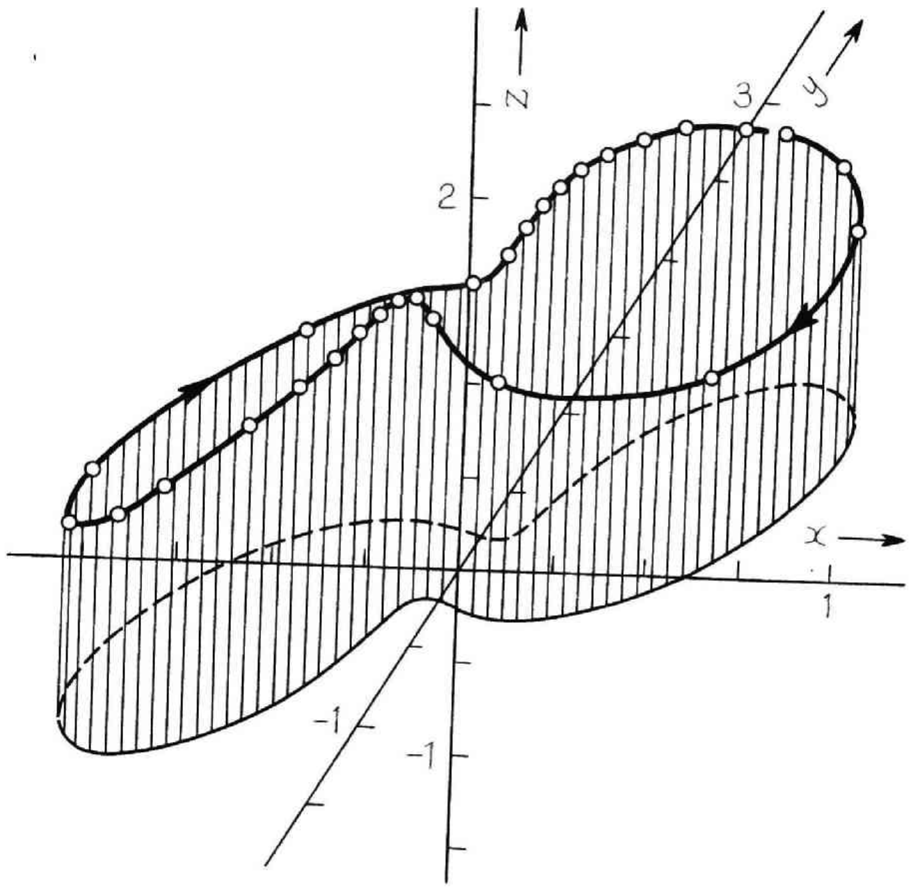

Fig. 5.10(b) Limit cycle in the x, y, z phase space. The system parameters are given by Eqs. (5.37).

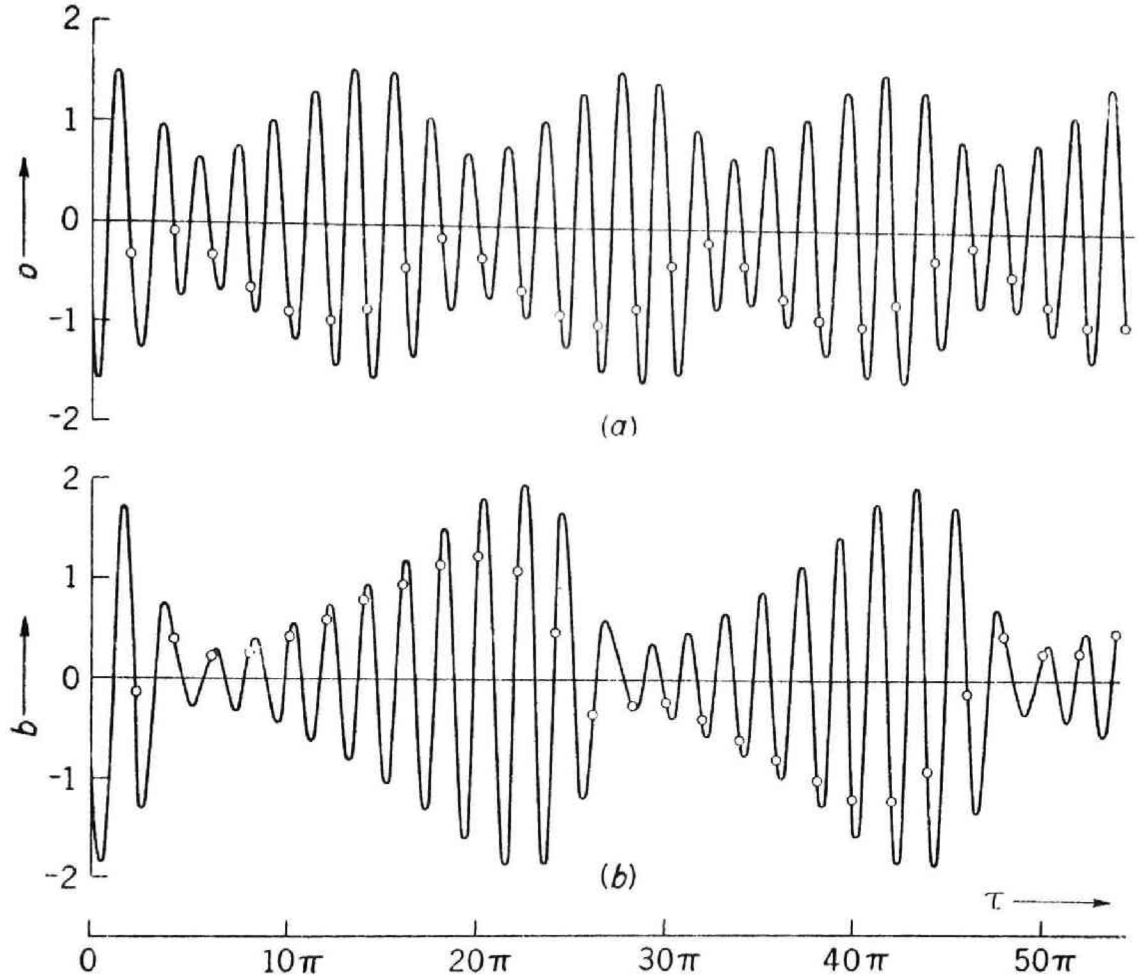

Fig. 5.11 Waveforms of the quasi-periodic oscillations obtained by analog-computer analysis. (a) The system parameters are the same as in the case of Fig. 5.9(a). (b) The system paramctors are the same as in the case of Fig. 5.9(b).

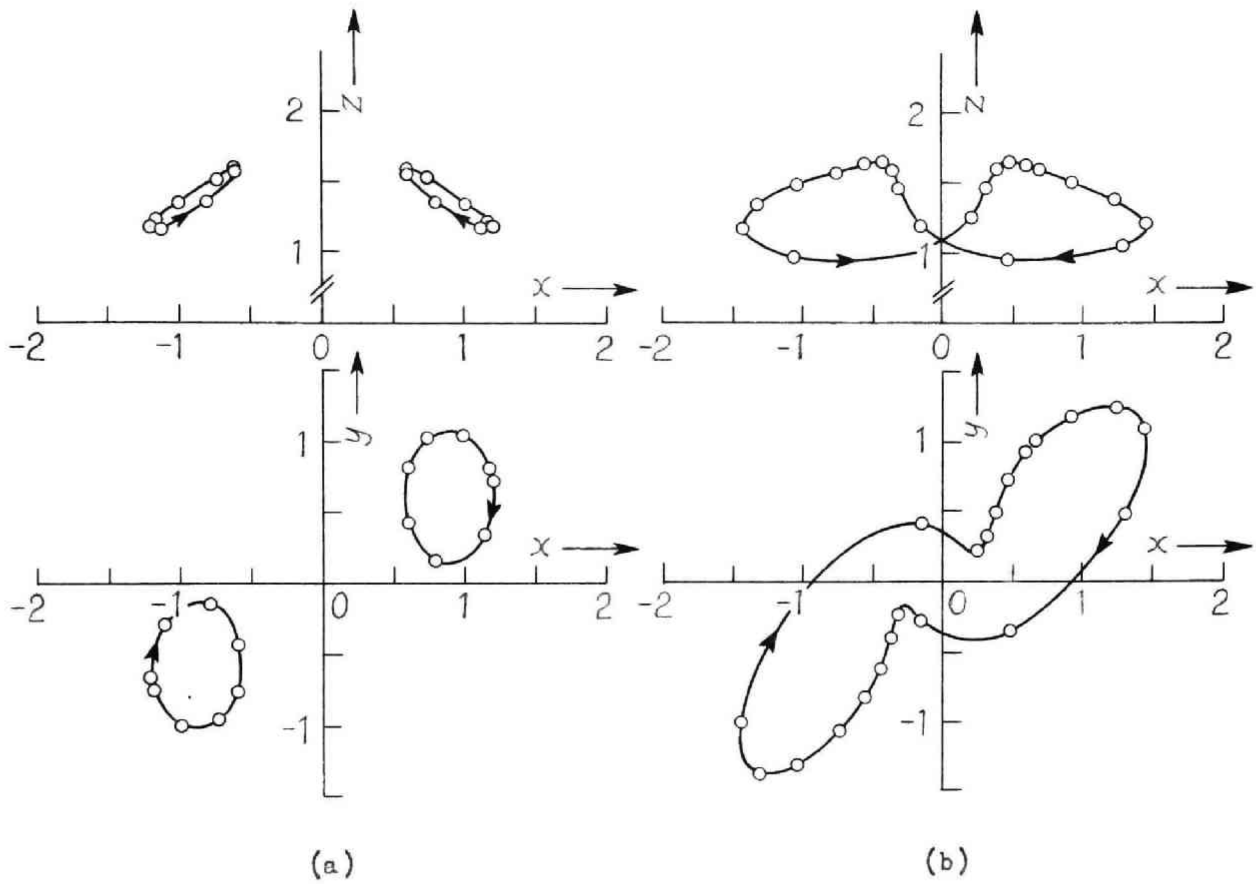

Fig. 5.12 Limit cycles reproduced from the waveforms of Fig. 5.11.

APPENDIX I

COMPLEMENTARY REMARKS TO ITERATION METHOD

There may be a number of ways of the iteration procedure for obtaining a periodic solution of a differential equation. One of them were explained in Section 1.3. Here we describe another way which is somewhat different from that of Section 1.3. Let us consider again, as an example, the harmonic solution for Duffing's equation

$$\frac{d^2x}{dt^2} + (1+\mu\alpha)x + \mu\beta x^3 = \mu F\cos t, \tag{I.1}$$

where μ is a small parameter. Equation (I.1) is rewritten in the form

$$\frac{d^2x}{dt^2} + x = -\mu(\alpha x + \beta x^3 - F\cos t). \tag{I.2}$$

We start with the solution*

$$x_0(t) = A_1\cos t. \tag{I.3}$$

as a first approximation. Since this solution is obtained by ignoring the right-hand side of (I.2), the difference between $x_0(t)$ and the exact solution $x(t)$ would be of order μ.

Inserting $x_0(t)$ into the right-hand side of (I.2) we obtain the differential equation to find the second approximation $x_1(t)$; namely,

---

* A term $B_1\sin t$ could be added, but B would turn out to be zero in the next step of the iteration process. One could, in fact, show that only terms $A_n\cos nt$ with n odd would appear in the solution. We shall therefore ignore all the sine terms in what follows.

$$\frac{d^2x_1}{dt^2}+x_1=-\mu(\alpha A_0+\frac{3}{4}\beta A_0^3-F)\cos t-\frac{1}{4}\mu\beta A_0^3\cos 3t. \tag{I.4}$$

Since the right-hand side of this equation may differ from that of (I.2) by the amount of order μ^2, one may expect a second approximation $x_1(t)$ that must be correct up to the order of μ. The periodicity condition for $x_1(t)$ requires that no secular terms should appear in the solution $x_1(t)$; hence,

$$\alpha A_0+\frac{3}{4}\beta A_0^3-F=0, \tag{I.5}$$

which determines the amplitude A_0. Once the relation (I.5) has been satisfied, the general solution of (I.4) is found to be

$$x_1=A_1\cos t+\frac{1}{32}\mu\beta A_0^3\cos 3t. \tag{I.6}$$

where the amplitude A_1 may be expected to differ from A_0 only by the amount of order μ.

Inserting (I.6) into the right-hand side of (I.2) gives

$$\frac{d^2x_2}{dt^2}+x_2=-\mu[(\alpha A_1+\frac{3}{4}\beta A_1^3-F)+\frac{3}{128}\mu\beta^2A_0^3A_1^2]\cos t$$

$$-\frac{1}{4}\mu\beta[A_1^3+\frac{1}{16}\mu(2\alpha+3\beta A_1^2)A_0^3]\cos 3t$$

$$-\frac{3}{128}\mu^2\beta^2A_0^3A_1^2\cos 5t. \tag{I.7}$$

Terms of order higher than μ^2 are omitted in the right-hand side of this equation. Since the right-hand side of (I.7) may differ from that of (I.2) by the amount of order μ^3, the third approximation $x_2(t)$ must be a correct solution up to the order of μ^2. The periodicity condition for $x_2(t)$ requires that

$$\alpha A_1 + \frac{3}{4}\beta A_1^3 - F + \frac{3}{128}\mu\beta^2 A_0^3 A_1^2 = 0 \tag{I.8}$$

Bearing in mind that the difference between A_0 and A_1 is of order μ, we solve (I.8) for A_1 and obtain

$$A_1 = A_0 - \frac{3\mu\beta^2 A_0^5}{128(\alpha + \frac{9}{4}\beta A_0^2)} . \tag{I.9}$$

Therefore we write

$$x_1(t) = \left[A_0 - \frac{3\mu\beta^2 A_0^5}{128(\alpha + \frac{9}{4}\beta A_0^2)}\right]\cos t + \frac{1}{32}\mu\beta A_0^3 \cos 3t. \tag{I.10}$$

The results obtained by the above procedure agree with the solutions obtained by the perturbation method. Refer to Section 1.2.

APPENDIX II

ANALYSIS OF ERRORS OF GRAPHICAL INTEGRATION METHODS

Leaving aside incidental mistakes on the part of the constructor, there are essentially several sources of errors in the graphical methods themselves. Here we consider the local truncation error, i.e., the error committed at each step by use of the approximation, of the methods described in Chapter II.

II.1 Errors of the Slopeline Method

In the first place, let us consider the graphical process for the first-order equation described in Section 2.2.1. The change Δx for the time interval Δt may be expanded in Taylor's series

$$\Delta x = x'(t_0)\Delta t + \frac{1}{2}x''(t_0)(\Delta t)^2 + \frac{1}{6}x'''(t_0)(\Delta t)^3 + O_4(\Delta t). \tag{II.1}$$

Substitution of Eq. (2.1) into (II.1) leads to

$$\Delta x = f_0 \cdot \Delta t + \frac{1}{2} f_0' \cdot (\Delta t)^2 + \frac{1}{6} f_0'' \cdot (\Delta t)^3 + O_4(\Delta t). \tag{II.2}$$

On one hand, the approximate increment Δx_s , which is graphically obtained, is written as

$$\begin{aligned} \Delta x_s &= \frac{1}{2}(f_0 + f_1)\Delta t \\ &= f_0 \cdot \Delta t + \frac{1}{2} f_0' \cdot (\Delta t)^2 + \frac{1}{4} f_0'' \cdot (\Delta t)^3 + O_4(\Delta t). \end{aligned} \tag{II.3}$$

Then we obtain the general expression for the local error

$$\varepsilon_s = \Delta x_s - \Delta x = \frac{1}{12} f_0''(\Delta t)^3 + O_4(\Delta t). \tag{II.4}$$

Next we consider the graphical method for the second-order differential equation described in Section 2.2.2. By maing use of Taylor's expansion for the increments, we have

$$
\left.
\begin{aligned}
\varepsilon_x &= \Delta x_s - \Delta x \\
&= (S_m - \tfrac{1}{2})(\tfrac{dg}{dx})_{x=x_0}[g(x_0) - y_0](\Delta t)^2 + \tfrac{1}{2}\{\tfrac{1}{6}[g(x_0) - y_0] + (S_n - \tfrac{1}{3})\cdot \\
&\quad (\tfrac{dh}{dy})_{y=y_0}[x_0 + h(y_0)] - (S_m^2 - \tfrac{1}{3})(\tfrac{d^2g}{dx^2})_{x=x_0}[g(x_0) - y_0]^2 - (S_m^2 - \tfrac{1}{3})(\tfrac{dg}{dx})_{x=x_0}\cdot \\
&\quad [-h(y_0) - x_0 - (\tfrac{dg}{dx})_{x=x_0} y_0 + (\tfrac{dg}{dx})_{x=x_0} g(x_0)]\}(\Delta t)^3 + O_4(\Delta t), \\
\varepsilon_y &= \Delta y_s - \Delta y \\
&= (S_n - \tfrac{1}{2})(\tfrac{dh}{dy})_{y=y_0}[h(y_0) + x_0](\Delta t)^2 + \tfrac{1}{2}\{\tfrac{1}{6}[h(y_0) + x_0] - (S_m - \tfrac{1}{3})\cdot \\
&\quad (\tfrac{dg}{dx})_{x=x_0}[g(x_0) - y_0] - (S_n^2 - \tfrac{1}{3})(\tfrac{d^2h}{dy^2})_{y=y_0}[h(y_0) + x_0]^2 - (S_n^2 - \tfrac{1}{3})(\tfrac{dh}{dy})_{y=y_0}\cdot \\
&\quad [g(x_0) - y_0 + (\tfrac{dh}{dy})_{y=y_0} x_0 + (\tfrac{dh}{dy})_{y=y_0} h(y_0)]\}(\Delta t)^3 + O_4(\Delta t),
\end{aligned}
\right\} \quad \text{(II.5)}
$$

with

$$
x_m = x(t_0 + \Delta t_m), \qquad \Delta t_m = S_m \Delta t,
$$

$$
y_n = y(t_0 + \Delta t_n), \qquad \Delta t_n = S_n \Delta t.
$$

The coefficients S_m and S_n are found to be

$$
\left.
\begin{aligned}
S_m &= \frac{1}{2} - \frac{1}{8}\,\frac{x_0 + h(y_0) + (\frac{dg}{dx})_{x=x_0}[g(x_0) - y_0]}{g(x_0) - y_0}\,\Delta t + O_2(\Delta t), \\
S_n &= \frac{1}{2} + \frac{1}{8}\,\frac{-y_0 + g(x_0) - (\frac{dh}{dy})_{y=y_0}[h(y_0) + x_0]}{h(y_0) + x_0}\,\Delta t + O_2(\Delta t).
\end{aligned}
\right\} \quad \text{(II.6)}
$$

Substitution of Eq. (II.6) into (II.5) leads to the expression of (2.14).

Errors of the graphical process in Section 2.2.3 are estimated similarly.

II.2 Errors of the Delta Method

We consider the graphical construction procedure illustrated in Section 2.3.1. The exact increments Δx and Δv may be written in Taylor's series

$$\left.\begin{aligned}\Delta x &= v_0(\Delta\tau) - \frac{1}{2}(x_0+\delta_0)(\Delta\tau)^2 - \frac{1}{6}\left[v_0 + \left(\frac{d\delta}{d\tau}\right)_0\right](\Delta\tau)^3 \\ &\quad + O_4(\Delta\tau), \\ \Delta v &= -(x_0+\delta_0)(\Delta\tau) - \frac{1}{2}\left[v_0 + \left(\frac{d\delta}{d\tau}\right)_0\right](\Delta\tau)^2 + \frac{1}{6}\cdot \\ &\quad \left[x_0 + \delta_0 - \left(\frac{d^2\delta}{d\tau^2}\right)_0\right](\Delta\tau)^3 + O_4(\Delta\tau).\end{aligned}\right\} \qquad (II.7)$$

Construction of Fig. 2.10 makes the approximate increments Δx_δ and Δv_δ as

$$\left.\begin{aligned}\Delta x_\delta &= v_0(\Delta\theta) - \frac{1}{2}(x_0+\delta_0)(\Delta\theta)^2 - \frac{1}{6}v_0(\Delta\theta)^3 + O_4(\Delta\theta), \\ \Delta v_\delta &= -(x_0+\delta_0)(\Delta\theta) - \frac{1}{2}v_0(\Delta\theta)^2 + \frac{1}{6}(x_0+\delta_0)(\Delta\theta)^3 + (\Delta\theta).\end{aligned}\right\} \qquad (II.8)$$

By virtue of the relation (2.31), which shows the equivalence of $\Delta\tau$ and $\Delta\theta$, the local errors are expressed in the forms of (2.30).

In the modified method of Section 2.3.2, the constructed increments are found to be

$$\left.\begin{aligned}\Delta x_\delta &= v_0(\Delta\tau) - \frac{1}{2}(x_0+\delta_0)(\Delta\tau)^2 - \frac{1}{6}\left[v_0 + \frac{1}{4}\left(\frac{d\delta}{d\tau}\right)_0\right](\Delta\tau)^3 + O_4(\Delta\tau), \\ \Delta v_\delta &= -(x_0+\delta_0)(\Delta\tau) - \frac{1}{2}\left[v_0 + \left(\frac{d\delta}{d\tau}\right)_0\right](\Delta\tau)^2 \\ &\qquad + \left[\frac{1}{6}(x_0+\delta_0) - \frac{1}{8}\left(\frac{d^2\delta}{d\tau^2}\right)_0\right](\Delta\tau)^3 + O_4(\Delta\tau).\end{aligned}\right\} \qquad (II.9)$$

Thus we obtain Eqs.(2.32).

APPENDIX III

REGIONS OF PARAMETERS OF DUFFING'S EQUATION IN WHICH THE OSCILLATIONS OF DIFFERENT TYPES ARE SUSTAINED

It might be worth-while illustrating the regions of the parameters of Duffing's equation in which harmonic and subharmonic oscillations are obtained for the particular examples described in Chapter IV.

As mentioned in Section 4.2, the periodic solutions (4.5) and (4.6) are to be expected for Duffing's equation (4.4). Figure III.1 shows the regions of the system parameters, B and k, in which harmonic and subharmonic oscillations are obtained. In the area hatched by full lines, one obtains two different types of harmonic oscillations, resonant and nonresonant oscillations,* which one will occur depending on the initial conditions. Outside this region the harmonic oscillation is uniquely obtained. The dotted area is the region of 1/3-harmonic oscillation. The location of the system parameters in Eq. (4.22) is indicated by point P in the figure.

Figure III.2 shows the region of 1/2-harmonic oscillation for Eq. (4.4). In this narrow region 1/2-harmonic response is obtained in spite of the symmetrical characteristic of the system.

Figures III.3 and III.4 show the regions of harmonic and subharmonic solutions for Eq. (4.23) respectively. The variable parameters are B and B_o,

---

* Both of the oscillations have the same frequency as the driving frequency; for convenience' sake, we distinguish between them by the terms resonant and nonresonant oscillations according as the amplitude of the oscillation is larger or smaller.

while k is kept constant. It will be obvious from the form of Eq. (4.23) that the regions of those periodic solutions also appear for negative values of B_0 symmetrically about the B-axis. Point Q in these figures shows the location of the parameters as given in Eq. (4.36).

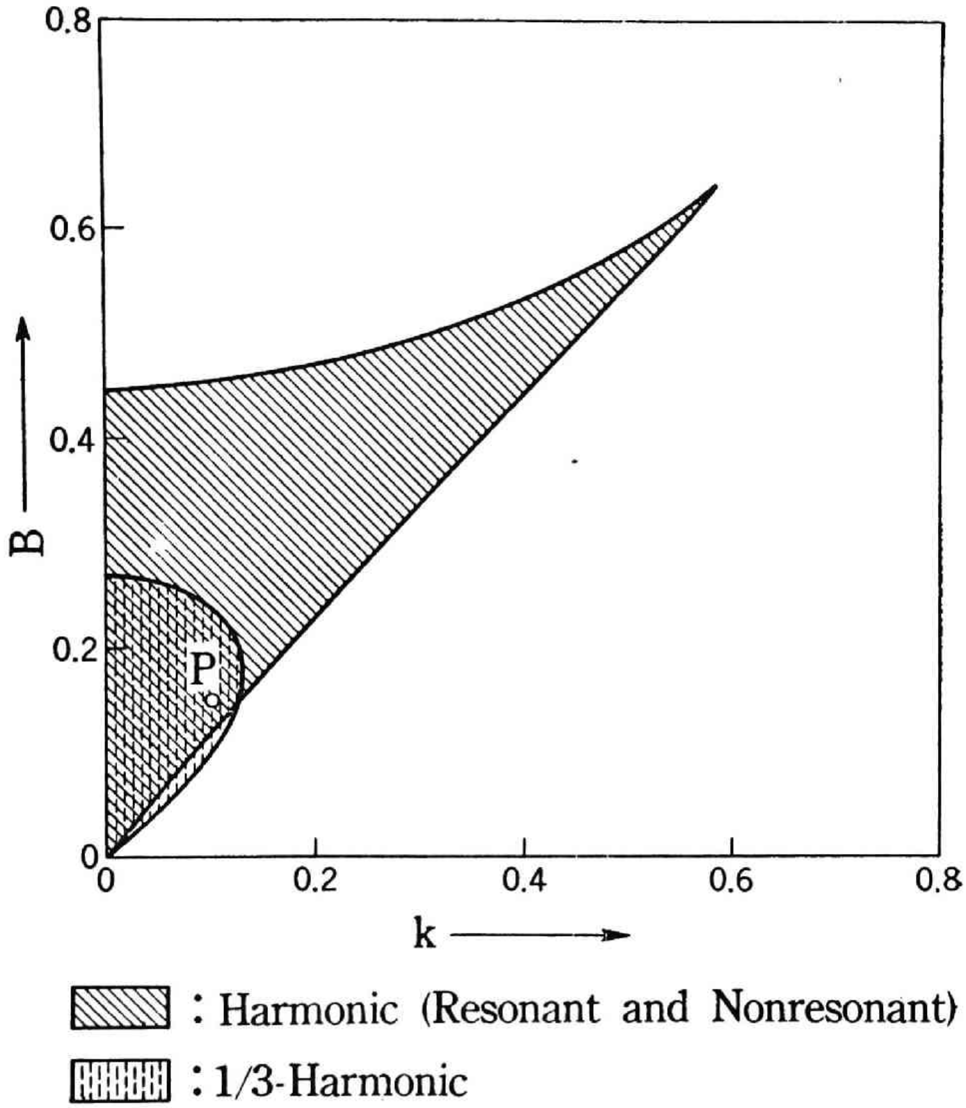

Fig. III.1 Regions in which the oscillations of different types are sustained.

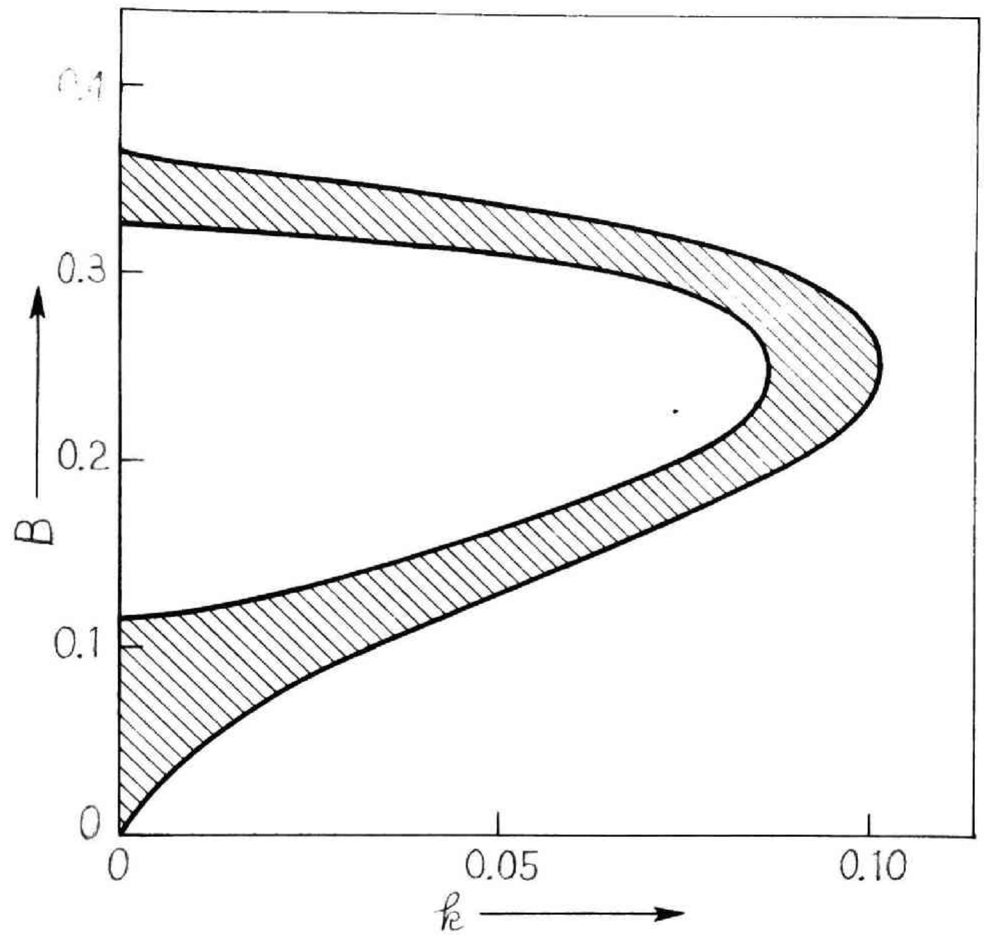

Fig. III.2 Region in which the 1/2-harmonic oscillations are sustained.

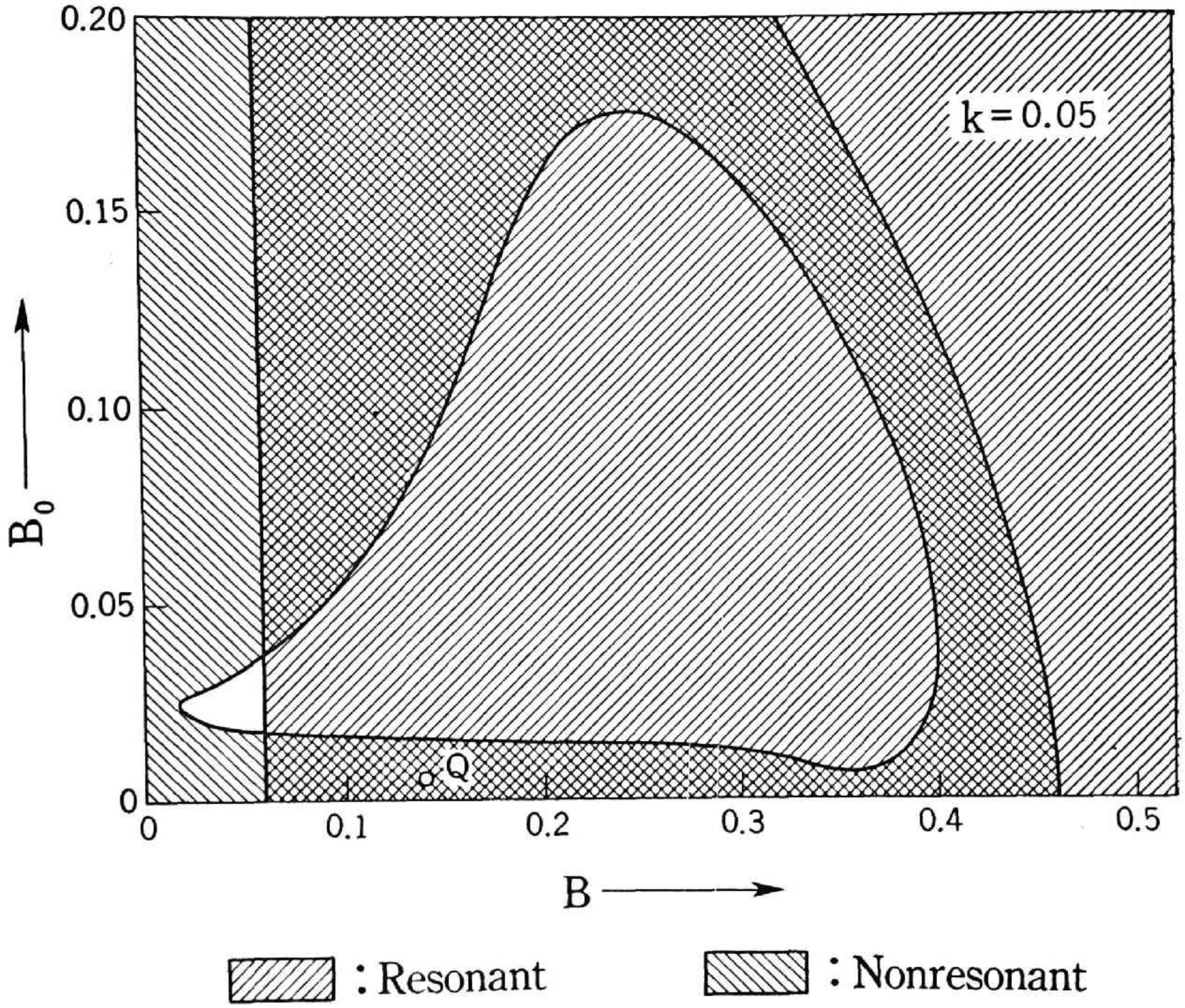

Fig. III.3 Regions in which the harmonic oscillations are sustained.

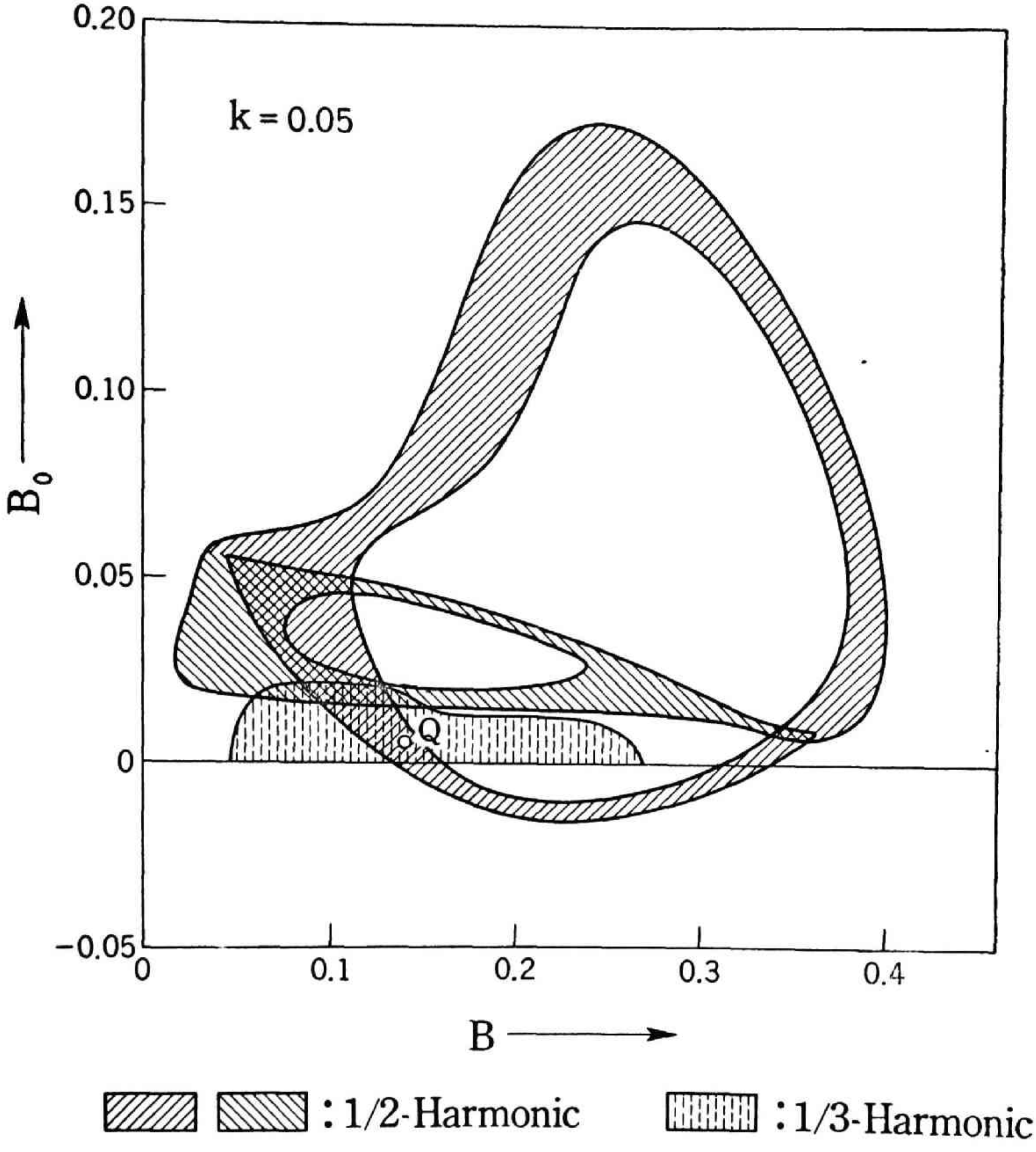

Fig. III.4 Regions in which the subharmonic oscillations are sustained.

APPENDIX IV

SOLUTIONS OF THE VARIATIONAL EQUATIIONS ASSOCIATED WITH THE UNSTABLE FIXED POINTS

As mentioned in Chapter IV, the boundary between the domains of attraction is the locus of the images that approach the directly unstable fixed point with increasing time. The locus may be obtained by integrating Duffing's equation for decreasing time. The initial points of integration should be on the line segment which passes through the unstable fixed point with slope α of (4.21). In order to compute the direction α of the boundary curve, one must determine the characteristic exponent μ and the periodic function $\psi(\tau)$ of the solution (4.15). These quantities, μ and $\psi(\tau)$, were calculated by making use of the formulas in Reference 30, pp. 127-137. The results of the computation are shown in what follows.

(1) For the unstable fixed point 3 in Table 4.1:

The periodic solution is given by

$$v_{o3} = 0.806 \sin\tau - 0.716 \cos\tau + 0.023 \sin 3\tau + 0.037 \cos 3\tau.$$

The variational equation leads to a Hill's equation of the form

$$\left.\begin{aligned} &\frac{d^2\eta}{d\tau^2} + \left[\theta_0 + 2\sum_{n=1}^{3} \theta_n \cos(2n\tau - \varepsilon_n)\right]\eta = 0, \\ &\text{where} \quad \theta_0 = 1.745, \\ &\theta_1 = 0.943, \qquad \varepsilon_1 = -1.692,^* \\ &\theta_2 = 0.071, \qquad \varepsilon_2 = 2.861, \\ &\theta_3 = 0.001, \qquad \varepsilon_3 = 1.123. \end{aligned}\right\} \qquad \text{(IV.1)}$$

A particular solution of (IV.1) is given by

$$\left.\begin{aligned} &\eta(\tau) = e^{-\mu\tau}\cdot\psi_3(\tau), \\ &\text{where} \\ &\mu = 0.181, \\ &\psi_3(\tau) = \sin(\tau + 1.040) - 0.121\sin(3\tau - 0.307) \\ &\qquad -0.005\sin(5\tau + 1.494) + 0.003\sin(7\tau - 0.123). \end{aligned}\right\} \quad (IV.2)$$

Substituting μ, $\psi_3(0)$, and $\dot{\psi}_3(0)$ as given by (IV.2) into (4.21) we may readily find the direction α of the boundary curve at the unstable fixed point 3; thus we have

$$\alpha = -0.020.$$

(2) For the unstable fixed point 7 in Table 4.1:

The periodic solution is given by

$$v_{07} = 0.149\sin\tfrac{1}{3}\tau + 0.226\cos\tfrac{1}{3}\tau + 0.025\sin\tau - 0.171\cos\tau.$$

The variational equation leads to a Hill's equation of the form

$$\left.\begin{aligned} &\frac{d^2\eta}{d\tau^2} + [\theta_0 + 2\sum_{n=1}^{3}\theta_n\cos(2n\tfrac{\tau}{3} - \varepsilon_n)]\eta = 0, \\ &\text{where} \quad \theta_0 = 0.153, \\ &\theta_1 = 0.102, \qquad \varepsilon_1 = 1.875, \\ &\theta_2 = 0.070, \qquad \varepsilon_2 = -2.707, \\ &\theta_3 = 0.022, \qquad \varepsilon_3 = -0.295. \end{aligned}\right\} \quad (IV.3)$$

---

* The arguments ε's are measured in radians.

A particular solution of (IV.3) is given by

$$\left.\begin{aligned} &\eta(\tau) = e^{-\mu\tau}\cdot \psi_7(\tau), \\ &\text{where} \\ &\mu = 0.139, \\ &\psi_7(\tau) = \sin\left(\tfrac{1}{3}\tau - 0.485\right) - 0.102\sin(\tau + 1.417) \\ &\qquad + 0.033\sin\left(\tfrac{5}{3}\tau + 0.618\right) + 0.004\sin\left(\tfrac{7}{3}\tau + 0.617\right). \end{aligned}\right\} \quad \text{(IV.4)}$$

Substituting (IV.4) into (4.21) we obtain finally

$$\alpha = -0.644.$$

(3) For the unstable fixed point 8 in Table 4.1:

Since

$$v_{08}(\tau) = v_{07}(\tau + 2\pi),$$

a particular solution of the Hill's equation associated with $v_{08}(\tau)$ is given by

$$\eta(\tau) = e^{-\mu\tau}\cdot \psi_8(\tau).$$

where

$$\mu = 0.139,$$

$$\psi_8(\tau) = \psi_7(\tau + 2\pi).$$

Hence

$$\alpha = -0.164.$$

(4) For the unstable fixed point 9 in Table 4.1:

Since

$$v_{09}(\tau) = v_{07}(\tau + 4\pi),$$

a particular solution of the Hill's equation associated with $v_{09}(\tau)$ is given by

$$\eta(\tau) = e^{-\mu\tau} \cdot \varphi_9(\tau),$$

where

$$\mu = 0.139,$$

$$\varphi_9(\tau) = \varphi_9(\tau + 4\pi).$$

Hence

$$\alpha = 0.263.$$

(5) For the unstable fixed point 3 in Table 4.2:

The periodic solution is given by

$$v_{03} = 0.003 + 0.399 \sin\tau - 0.983 \cos\tau + 0.038 \sin 3\tau - 0.016 \cos 3\tau.$$

The variational equation leads to a Hill's equation of the form

$$\left.\begin{aligned}
&\frac{d^2\eta}{d\tau^2} + \left[\theta_0 + 2\sum_{n=1}^{6}\theta_n \cos\left(2n\frac{\tau}{2} - \varepsilon_n\right)\right]\eta = 0, \\
&\text{where} \\
&\theta_0 = 1.687, \\
&\theta_1 = 0.009, \qquad \varepsilon_1 = 2.756, \\
&\theta_2 = 0.923, \qquad \varepsilon_2 = -0.757, \\
&\theta_3 = 0.0004, \qquad \varepsilon_3 = 1.966, \\
&\theta_4 = 0.066, \qquad \varepsilon_4 = -1.560, \\
&\theta_5 = 0, \\
&\theta_6 = 0.001, \qquad \varepsilon_6 = -2.349,
\end{aligned}\right\} \qquad (IV.5)$$

A particular solution of (IV.5) is given by

$$\eta(\tau) = e^{-\mu\tau} \cdot \varphi_3(\tau),$$

where

$$\left.\begin{aligned} \mu &= 0.208, \\ \psi_3(\tau) &= 0.006 + \sin(\tau + 0.634) - 0.004 \sin(2\tau + 0.512) \\ &\quad + 0.120 \sin(3\tau + 1.259) - 0.004 \sin(5\tau - 0.988). \end{aligned}\right\} \qquad (IV.6)$$

Substituting (IV.6) into (4.21) we obtain finally

$$\alpha = 1.054.$$

(6) For the unstable fixed point 6 in Table 4.2:

The periodic solution is given by

$$v_{06} = 0.059 + 0.255 \sin \tfrac{1}{2}\tau + 0.416 \cos \tfrac{1}{2}\tau + 0.039 \sin \tau - 0.220 \cos \tau.$$

The variational equation leads to a Hill's equation of the form

$$\left.\begin{aligned} &\frac{d^2\eta}{d\tau^2} + \Big[\theta_0 + 2\sum_{n=1}^{4} \theta_n \cos\Big(2n\frac{\tau}{4} - \varepsilon_n\Big)\Big]\eta = 0, \\ &\text{where} \\ &\theta_0 = 0.436, \\ &\theta_1 = 0.126, \qquad \varepsilon_1 = 2.748, \\ &\theta_2 = 0.132, \qquad \varepsilon_2 = 1.332, \\ &\theta_3 = 0.164, \qquad \varepsilon_3 = -2.768, \\ &\theta_4 = 0.037, \qquad \varepsilon_4 = 0.312. \end{aligned}\right\} \qquad (IV.7)$$

A particular solution of (IV.7) is given by

$$\eta(\tau) = e^{-\mu\tau}\, \psi_6(\tau),$$

where

$$\mu = 0.196,$$

$$\left.\begin{aligned}\psi_6(\tau) = -0.245 + \sin(\tfrac{1}{2}\tau - 0.227) - 0.294\sin(\tau + 1.074)\\ + 0.034\sin(\tfrac{3}{2}\tau - 1.134) - 0.047\sin(2\tau - 0.401)\\ + 0.003\sin(\tfrac{5}{2}\tau - 0.326) + 0.002\sin(3\tau + 1.168)\\ + 0.001\sin(\tfrac{7}{2}\tau - 1.203).\end{aligned}\right\} \qquad \text{(IV.8)}$$

Substituting (IV.8) into (4.21) we obtain finally

$$\alpha = -0.601.$$

(7) For the unstable fixed point 7 in Table 4.2:

Since

$$v_{07}(\tau) = v_{06}(\tau + 2\pi),$$

a particular solution of the Hill's equation associated with $v_{07}(\tau)$ is given by

$$\eta(\tau) = e^{-\mu\tau}\cdot\psi_7(\tau),$$

where

$$\mu = 0.196,$$

$$\psi_7(\tau) = \psi_6(\tau + 2\pi).$$

Hence

$$\alpha = 2.994.$$

(8) For the unstable fixed point 11 in Table 4.2:

The periodic solution is given by

$$v_{011} = 0.039 + 0.177\sin\tfrac{1}{3}\tau + 0.165\cos\tfrac{1}{3}\tau + 0.012\sin\tau - 0.160\cos\tau.$$

The variational equation leads to a Hill's equation of the form

$$\frac{d^2\eta}{d\tau^2} + [\theta_0 + 2\sum_{n=1}^{6}\theta_n\cos(2n\tfrac{\tau}{6} - \varepsilon_n)]\eta = 0,$$

where

$$
\left.
\begin{aligned}
\theta_0 &= 0.131, & & \\
\theta_1 &= 0.026, & \varepsilon_1 &= 0.[illegible]20, \\
\theta_2 &= 0.098, & \varepsilon_2 &= 1.[illegible], \\
\theta_3 &= 0.019, & \varepsilon_3 &= 3.070, \\
\theta_4 &= 0.058, & \varepsilon_4 &= -2.[illegible], \\
\theta_5 &= 0, & & \\
\theta_6 &= 0.021, & \varepsilon_6 &= -0.192.
\end{aligned}
\right\}
\tag{IV.9}
$$

A particular solution of (IV.9) is given by

$$
\left.
\begin{aligned}
&\eta(\tau) = e^{-\mu\tau}\cdot\psi_{11}(\tau), \\
&\text{where} \\
&\mu = 0.140, \\
&\psi_{11}(\tau) = -0.119 + \sin\left(\tfrac{1}{3}\tau - 0.459\right) + 0.045\sin\left(\tfrac{2}{3}\tau - 0.774\right) \\
&\qquad - 0.070\sin(\tau + 1.426) - 0.015\sin\left(\tfrac{4}{3}\tau - 0.653\right) \\
&\qquad - 0.025\sin\left(\tfrac{5}{3}\tau - 1.021\right) + 0.002\sin(2\tau + 1.547) \\
&\qquad + 0.001\sin\left(\tfrac{7}{3}\tau + 0.410\right).
\end{aligned}
\right\}
\tag{IV.10}
$$

Substituting (IV.10) into (4.21) we obtain finally

$$\lambda = -0.674.$$

(9) For the unstable fixed point 12 in Table 4.2:

Since

$$v_{012}(\tau) \quad v_{011}(\tau + 2\pi),$$

a particular solution of the Hill's equation associated with $v_{012}(\tau)$ is given by

$$\eta(\tau) = e^{-\mu\tau} \cdot \psi_{12}(\tau),$$

where

$$\mu = 0.140,$$

$$\psi_{12}(\tau) = \psi_{11}(\tau + 2\pi).$$

Hence

$$\alpha = -0.114.$$

(10) For the unstable fixed point 1^3 in Table 4.2:

Since

$$v_{013}(\tau) = v_{011}(\tau + 4\pi),$$

a particular solution of the Hill's equation associated with $v_{013}(\tau)$ is given by

$$\eta(\tau) = e^{-\mu\tau} \cdot \psi_{13}(\tau),$$

where

$$\mu = 0.140,$$

$$\psi_{13}(\tau) = \psi_{11}(\tau + 4\pi).$$

Hence

$$\alpha = 0.141.$$

REFERENCES

A. SCIENTIFIC PAPERS

1. Angus, R. W.: Waterhammer in pipes, Inst. of Mech. Eng. Proc., Vol. 136, p. 245 (1937).
2. Bergeron, L.: Du coup de belier en hydraulique au coup de foudre en electricité, Dunod, Paris (1950).
3. Bessonov, L. A.: Auto-oscillations in electric circuits containing iron cores, Gosenergoizdat, Moscow (1958, in Russian).
4. Blair, K. W., and W. S. Loud: Periodic solutions of $x'' + cx' + g(x) = Ef(t)$ under variation of certain parameters, J. Soc. Indust. Appl. Math., Vol. 8, pp. 74-101 (1960).
5. Buland, R. N.: Analysis of nonlinear servos by phase-plane-delta method, J. Franklin Inst., Vol. 257, pp. 37-48 (1954).
6. Hámos, L. V.: Beitrag zur Frequenzanalyse von nichtlinearen Systemen, Fachtagung Regelungstechnik, Beitrag Nr. 65, Heidelberg (1956).
7. Hayashi, C., and Y. Nishikawa: Graphical solution of nonlinear differential equations by slopeline method, Reports of Soc. for the study of Elec. Machines for Automatic Control (1950, in Japanese).
8. Hayashi, C., Y. Nishikawa, and M. Abe: Subharmonic oscillations of order one half, IRE Trans. of the Professional Group on Circuit Theory, Vol. CT-7, pp. 102-111 (1960).
9. Hayashi, C., Y. Nishikawa, and M. Abe: Subharmonic oscillations of order one half, Reports of the Annual Meeting of JIEE, No. 48 (1958, in Japanese).

10. Hayashi, C., Y. Nishikawa, and M. Abe: Subharmonic oscillations of order one half, JIECE Reports of the Professional Group on Nonlinear Theory (1958, in Japanese).

11. Hayashi, C.: Initial conditions for certain types of nonlinear oscillations Symposium on Nonlinear Circuit Analysis, Polytechnic Institute of Brooklyn, Brooklyn, N. Y., Vol. 6, pp. 63-92 (1956).

12. Hayashi, C., and Y. Nishikawa: Initial conditions leading to different types of periodic solutions for Duffing's equation, International Symp. on Nonlinear Vibrations, Academy of Ukrainian SSR, Kiev (1961).

13. Hayashi, C., and Y. Nishikawa: Initial value problem of Duffing's equation I, Reports of the Annual Meeting of JIEE, No. 30 (1960, in Japanese).

14. Hayashi, C., and Y. Nishikawa: Initial value problem of Duffing's equation II (unsymmetrical system), Reports of the Annual Meeting of JIEE, No. 31 (1961, in Japanese).

15. Hayashi, C., and Y. Nishikawa: Initial value problem of Duffing's equation III (mapping method), Reports of the Annual Meeting of JIEE (1962, in Japanese).

16. Hayashi, C., and Y. Nishikawa: Initial conditions leading to different types of periodic solutions for Duffing's equation, JIECE Reports of the Professional Group on Nonlinear Theory (1960, in Japanese).

17. Hayashi, C.: Stability investigation of the nonlinear periodic oscillations J. Appl. Phys., Vol. 24, pp. 344-348 (1953).

18. Hayashi, C.: Quasi-periodic oscillations in non-linear control systems, International Federation of Automatic Control Congress, pp. 12-16, Moscow, (1960).

19. Hayashi, C., and Y. Nishikawa: Quasi-periodic oscillations in nonlinear circuits, Reports of the Annual Meeting of JIEE, No. 6 (1959, in Japanese).

20. Hayashi, C., and Y. Nishikawa: Quasi-periodic oscillations in nonlinear circuits, JIECE Reports of the Professional Group on Nonlinear Theory (1959, in Japanese).

21. Jacobsen, L. S.: On a general method of solving second-order ordinary differential equations by phase-plane-delta displacements, J. Appl. Mech, Vol. 19, pp. 543-553 (1952).

22. Ludeke, C. A.: Nonlinear phenomena, Trans. ASME, Vol. 79, pp. 439-444 (1957).

23. Paynter, H. M.: Methods and results from M. I. T. studies in unsteady flow, J. of the Boston Soc. of Civil Engineers, Vol. 39, pp. 120-165 (1952).

24. Rjasin, P.: Einstellungs- und Schwebungsprozesse bei der Mitnahme, J. Technical Physics, USSR, Vol. 5 (1935, in Russian).

25. Schnyder, O.: Druckstösse in Pumpensteigleitungen, Schweizerische Bauzeitung, Vol. 94, No. 22 and 23 (1929).

26. Sorensen, K. E.: Graphical solution of hydraulic problems, ASCE Proc., Vol. 78, Separate No. 116 (1952).

27. Thomson. W. T.: Resonant non-linear control circuits, Trans. Amer. Inst. Elec. Engrs., Vol. 57, pp. 469-476 (1938).

28. Urabe, M.: Periodic solutions of van der Pol's equation with damping coefficient $\lambda = 0 - 10$, IRE Trans. of the Professional Group on Circuit Theory, Vol. CT-7, pp. 382-386 (1960).

B. BOOKS

29. Cunningham, W. J.: Introduction to nonlinear analysis, McGraw-Hill Book Co., New York (1958).

30. Hayashi, C.: Forced oscillations in nonlinear systems, Nippon Printing and Publishing Co., Osaka, Japan (1953).

31. Minorsky, N.: Introduction to nonlinear mechanics, J. W. Edwards, Ann Arbor (1947).

32. Stoker, J. J.: Nonlinear Vibrations, Interscience Publishers, New York (1950).

33. Duffing, G.: Erzwungene Schwingungen bei veränderlicher Eigenfrequenz und ihre technische Bedeutung, Sammlung Vieweg, Braunschweig (1918).